Bulk geochemical, biomarker and leaf wax isotope records of Mfabeni peatland, KwaZulu Natal, South Africa since the late Pleistocene

by

Andrea Baker

Dissertation presented for the degree of Doctor of Earth Sciences in the

Faculty of Science at

Stellenbosch University

Supervisor: Dr Joyanto Routh

Co-supervisor: Prof. Alakendra N. Roychoudhury

March 2016

DECLARATION

By submitting this thesis electronically, I declare that the entirety of the work contained therein is my own, original work, that I am the sole author thereof (save to the extent explicitly otherwise stated), that reproduction and publication thereof by Stellenbosch University will not infringe any third party rights and that I have not previously in its entirety or in part submitted it for obtaining any qualification.

Signed:
Andrea Baker
Date: March 2016

ABSTRACT

Southern Africa is a topographically diverse region that is influenced by temperate, sub-tropical and tropical climates encompassing varying rainfall zones. The core regional contemporary climatic drivers are the large sea surface temperature (SST) gradients between the Atlantic and Indian Oceans, and seasonal fluctuations in the Inter Tropical Convergence Zone (ITCZ). Our understanding of how these two mechanisms interacted in the past and how ecosystems responded to these climate drivers is ambiguous, mainly due to a lack of continuous archives as a consequence of the region's semi-arid climate. The Mfabeni peatland is a 11 m thick continuous peat sequence that has been dated to ca. 47 kcal yr BP. It is the only known coastal peatland record in the summer rainfall zone of Southern Africa to transcend the Last Glacial Maximum (LGM), and gives us the opportunity to reconstruct high-resolution palaeoenvironment records under both glacial and interglacial conditions on the south eastern coastline of the African continent.

A diverse set of geochemical techniques and analysis (bulk C and N elemental and stable isotopes; different biomarkers and leaf wax $\delta^{13}C$ isotope) was undertaken on a 810 cm long core to reconstruct primary productivity, organic matter (OM) sources, rates of OM remineralisation, peatland hydrology and relative contributions of C3 and C4 plant matter into the peat deposit. These geochemical climatic indicators were used to infer precipitation intensities and relative temperatures at time of sedimentation and, in conjunction with other regional archives, the dominant mechanisms (Indian Ocean SST changes versus changes in the position of ITCZ) driving climatic fluctuations since the late Pleistocene were explored.

We established the Mfabeni peatland to be a well-preserved and unique palaeoecological archive that recorded both environmental and climatic signals throughout the depositional history of the peatland. Even though the dominant OM source of the peat was terrestrial and emergent plants, there were definitive periods of predominant submerged macrophyte input, suggesting elevated water levels. A general positive trend was observed between the temperature and moisture proxies, however the local plant physiology (*n*-alkane chain lengths; ACL_{alk}) and plant types

(terrestrial vs aquatic and their influence on OM lability; CPI_{alk}) was dominated by moisture availability as opposed to temperature variations, arguably due to the relatively moderate cooling experience in the sub-tropics during the LGM. The leaf wax C isotope data set established variability in the proportional balance of C3 and C4 plants, with interchanges between plant clades and inter family C3 and C4 switches in response to changes in environmental conditions. However, plant assemblage shifts were absent during some of the more ephemeral climatic events which we concluded was due to local hydrological overprinting.

The Mfabeni archive correlates strongly with Mozambique Channel SST records, suggesting the dominant climate forcing factor in south eastern Africa to be the evaporation potential and advection of moisture from the adjacent Indian Ocean since the late Pleistocene. It was also noted that the Mfabeni record exhibited overall opposite environmental responses to Northern Hemisphere climatic events, suggesting an anti-phase coupling between the two hemispheres.

OPSOMMING

Suidelike Afrika is a topografies diverse streek wat beïnvloed word deur gematigde, sub-tropiese en tropiese climate omvattende wisselende groeiseisoen reënval sones. Die kern streeks kontemporêre klimaatsdrywers is die groot see-oppervlak temperatuur (SST) gradiënte tussen die Atlantiese en Indiese Oseane, asook seisoenale skommelinge in die Intertropiese Konvergensiesone (ITCZ). Ons begrip van hoe die interaksie tussen die twee meganismes in die verlede was en hoe ekostelsels reageer het teenoor hierdie klimaatsdrywers is dubbelsinnig grootliks as gevolg van ‘n tekort aan deurlopende argiewe as ‘n gevolg van die streek se semi-droë klimaat. Die Mfabeni veenland is ‘n 11 meter dik aaneenlopende veen reeks gedateer ongeveer 47 kcal jaar BP. Dit is die enigste bekende kus veenland rekord in die somerreënval sone van Suider-Afrika wat die Laaste Ystydperk Maksimum (LGM) oortref het en gee ons die geleentheid om hoë resolusie paleo-omgewings rekords te rekonstrueer onder beide ystydperk en tussen-ystydperk toestande op die suid-oostelike kuslynvan die Afrika continent.

‘n Diverse stel geochemiese tegnieke en analise was (grootmaat C en N elementele en stabiele isotope; biomerkers en blaarwas $\delta^{13}C$ isotoop) onderneem op ‘n 810 cm lang kern om primêre produktiwiteit , organiese material (OM) bronne, tempo van OM hermineralisasie, veenland hidrologie en relatiewe bydraes van C3 en C4 plantmateriaal tot die veen afsetting te rekonstrueer. Ek het toe hierdie geochemiese klimaat aanwysers gebruik om neerslag intensiteite en relatiewe temperature gedurende sedimentasie af te lei en, in samewerking met ander streeksargiewe, het ek die dominante meganisme (Indiese Oseaan SST veranderinge vs. veranderinge in die posisie van ITCZ) wat die klimaatskommelinge vanaf die laat Pleistocene tydperk dryf afgelei.

Ons het vasgestel dat die Mfabeni veenland ‘n goed gepreserveerde/bewaarde en unieke paleo-ekologiese argief is wat beide omgewings- en klimaatsseine deurlopende die afsettings geskiedenis van die veenland opneem. Alhoewel die dominante OM bron van die veen land- en ontluikende plante was, was daar definitiewe periodes van oorheersende onderwater makrofiet insette wat verhoogde watervlakke voorstel. ‘n Algemene positiewe tendens was opgemerk tussen die temperature en vog gevolgmatigdes. Die plaaslike plantfisiologie (n-alkaan ketting lengtes;

ACLalk) en plantsoorte (land vs. akwaties en hulle invloed op OM labiliteit) was egter gedomineer deur vogbeskikbaarheid daarteenoor temperatuur variasies, waarskynlik as gevolg van die relatiewe matige afkoeling wat ervaar was in die subtropiese areas gedurende die LGM. Die blaarwas C isotoop datastel het vasgestel dat variasie in die proporsionele balans van C3 en C4 plante plaasvind, met verwisseling tussen plant klades en interfamilie C3 en C4 skakelaars in reaksie tot veranderinge in omgewings toestande. Die plantsamestelling-skuif was egter afwesig gedurende sommige van die meer efemere klimaatstoestand gebeurtenisse en ons het vasgestel dat dit ‘n nagevolg van plasslike hidrologiese oordrukking is.

Die Mfabeni argief korreleer sterk met Mozambiek Kanaal SST rekords en stel voor dat die dominante klimaat dwingende faktor in suid-oostelike Afrika die verdampingspotensiaal en adveksie van vog is van die aangrensende Indiese Oseaan vanaf die laat Pleistocene tydperk. Dit was ook opgemerk dat die Mfabeni rekord algeheel teenoorgestelde omgewings reaksies toon teenoor die Noordelike Halfrond klimaatsgebeurtenisse, wat daarop dui dat daar ‘n anti-fase koppeling is tussen die twee Halfronde.

ACKNOWLEDGEMENTS

This thesis would not have been possible if it wasn't for the excellent working relationship fostered by my two supervisors, Dr Joyanto Routh (Joy) and Prof AN Roychoudhury (Roy). Even though Joy was based in India and subsequently Sweden during the project, he was always available to me via Skype and email, and engaged me no matter what time of the day or night. Joy provided me the opportunity to learn and work in his specialised organic geochemistry labs in India and Sweden, and under his guidance I acquired invaluable experience with biomarker techniques and analysis. Our writing collaboration was a very fruitful one, allowing me to improve my scientific writing and concept design. Roy used his charm to convince me to undertake a PhD, by instilled in me the confidence to attempt such a huge undertaking and for that I'm eternally grateful. His open door policy made it easy to approach him with challenges, uncertainties, frustrations and even when I just needed to vent. His sense of humour and quite supportive nature instilled calm and confidence in me to continue when I felt like throwing in the towel after a few mishaps in the lab. Both Joy and Roy helped me become a better scientist by nurturing my critical thinking and giving me opportunities to develop my research career through invaluable opportunities and experiences.

Both my co-authors contributed specialist knowledge, insights and provided rewarding collaborations. Dr Blaauw developed a robust age-depth model that my entire thesis was underpinned on. His expertise in age-depth modelling gave me the confidence to reconstruct the peatland archive and compare my findings to supplementary regional records. Dr Pedentchouk's specialist leaf wax C isotope analysis and knowledge helped me to tease out the C3 and C4 plant reconstruction in the Mfabeni core. His hands-on approach to collaborating was very helpful and his guidance in applying this specialised proxy to the peatland archive assisted me in understanding this powerful analytical tool.

I'd like to thank Alistair Clulow who arranged site access, introduction to the iSimangaliso park management staff and assisting in identifying the sampling site within the peatland. I will be eternally grateful to Piet-Louis Grundling for making available, at the last minute, his specialist Russian peat corer that allowed for us to successfully extract the 810 cm long core. Much

gratitude goes to the iSimangaliso Authority and Ezemvelo KZN Wildlife for granting sampling permission and park access.

Thanks goes to Esmé Spicer, Cynthia Sanchez-Garrido, Renata Smit, Ian Newton, Lena Lundman, Tomaz Gozlar, Eric Ward and Megan Hill for assisting with core processing and analytical preparations, lab consumable procurements, design and development of specialist lab equipment, and various geochemical analysis.

The project was supported through a bilateral funding agreement by the Swedish Research Link-South Africa program (Grant 348-2009-6500). Student support was supplied by the Department of Science and Technology, National Research Foundation and InKaba yeAfrica (AEON).

Last but not least I'd like to say a special thank you to my friends and family. To my Earth Science friends, I owe you all a huge heap of gratitude for helping to make my time as a postgraduate so special. I will never forget the wonderful science and social times we shared and I'm sure we will all hold our friendships dear even if we scatter to different parts of the world. Stay true to yourselves and follow your passions where ever they may take you.

To my ever supportive and loving family, Mom, Dad and Lollie, I want to say a heartfelt thank you for always being so supportive and encouraging my PhD journey. Even though most of the scientific content was unfamiliar to you, you always allowed me to discuss the three things I'm most passionate about – Geology, Chemistry and the Environment – and enthusiastically listened and encouraged my passions.

To my partner in life and science, Arnie, I want you to know that I love and cherish you and have enjoyed every minute that has been this PhD journey together. With the arrival of our son, we have now embarked on a different journey, one which has and will bring us much joy and spurs us on to achieve even more in life together.

TABLE OF CONTENTS

LIST OF FIGURES

Chapter 1: Introduction

Chapter 2: ***Geochemical records of palaeoenvironmental controls on peat forming processes in the Mfabeni peatland, KwaZulu Natal, South Africa since the Late Pleistocene***

Chapter 3: ***Biomarker records of palaeoenvironmental variations in subtropical southern Africa since the late Pleistocene: evidences from a coastal peatland***

Chapter 4: Carbon isotope records of climatic variability in Mfabeni peatlands (South Africa) since the late Pleistocene

Chapter 5: Synopsis

LIST OF TABLES

CHAPTER 1: Introduction

1.1. Background

Peatlands play an important role in the global carbon (C) cycle as they can be either net sinks or sources of atmospheric CO_2, one of the largest suppliers of atmospheric methane (CH_4) and dissolved organic carbon (DOC; Strack, 2008) to downstream ecosystems. The amount of C sequestered in peatlands is a measure of the difference between net primary production (NPP) and ecosystem respiration (Chimner and Ewel, 2005). NPP is controlled primarily by growing season insolation, and water availability, with warmer temperatures and high precipitation usually resulting in enhanced primary production. Ecosystem respiration is mainly dependent on the lability of organic matter (OM) undergoing remineralisation and autotrophic respiration (Moore and Basiliko, 2006), and since respiration is enzymatically controlled, it is also positively related to temperature. However, microbial decomposition tends to slow down under anaerobic conditions and therefore, water table position and the extent of waterlogging events within a tropical peatland is the dominant factor influencing respiration rates (Moore and Delva, 1993). This results in peat accumulating under elevated temperatures, as opposed to boreal peatlands where peat accumulates due to permafrost developing under sub-zero temperatures. At the same time, methane, another greenhouse gas (GHG), is generated under highly reducing, anaerobic conditions by methanogenic bacteria, and is produced in the water saturated peat horizons and transferred to the atmosphere via diffusion, ebullition and vascular systems in plants.

The majority of contemporary peatlands are found in the northern hemisphere (constituting ~90% of the global peatlands; Strack et al., 2008) and cover large areas of boreal and temperate zones in North America, Asia and Europe (Figure 1). They normally occur in low-relief, poorly drained areas which are subject to high precipitation and low temperatures (Immirzi et al., 1992). In boreal peatlands, the relatively short, but warm and wet summers, results in high primary production, while permafrost in the top soil during the long cold winters restricts bacterial decomposition of OM. On the other hand, the relatively fewer contemporary tropical and sub-tropical peatlands occur

mainly in low altitude, coastal and sub-coastal areas dominated by swamp forests, mangroves or marshes (Rieley et al., 1996) in SE Asia, Central America and Southern Africa (Figure 1; ~11%; Strack et al., 2008; Page et al., 2011). They develop mainly due to regional environmental and topographic conditions which allow peat to accumulate under high precipitation and high temperature conditions (Page et al., 2011).

Although contemporary northern boreal and temperate peatlands cover an estimated 350 million ha, equal to only about 3% of the earth's surface, they store more than ~450 Petagrams (1 Pg = 10^{15}g) of C, equivalent to approximately one third of the global soil C storage capacity and up to 75% of pre-industrial atmospheric CO_2 levels (Strack, 2008). Contemporary peatlands situated in the tropics constitute approximately ~60 Petagrams stored C (Strack, 2008). Due to the generally higher C accumulation rates in tropical peat deposits (Chimner and Ewel, 2005; Strack, 2008), they represent over a third of the potential global peatland C sink, while only constituting ~11% areal coverage of total global peatlands (Strack, 2008; Page et al., 2011). Tropical peat deposits typically form when plant material is deposited under acidic and anaerobic conditions, inhibiting decay due to combination of permanent water saturation, low oxygen levels and high levels of acidity. Therefore, climate (temperature and precipitation) and waterlogging (geomorphology) are the main controlling factors which facilitate accumulation of peat deposits in the tropics. However, due to their close proximity to densely populated areas, tropical peatlands are under greater threat from human development / utilisation (drainage and/or burning for agriculture and industry) and therefore more sensitive to climate change as they are often disturbed (Rieley et al., 1996).

Peatlands are superior archives for palaeoclimatic and palaeoenvironmental studies because they are subject to mainly autochthonous depositional regimes that are climate controlled (Blackford, 2000), and the geochemical signals of these parameters are well preserved in the sediments. Due to their high OC content, peatlands are suitable for ^{14}C dating and palaeoreconstructions using multi-proxy investigations, namely elemental, stable C and N isotopes, biomarker and compound specific isotope analysis. Additionally, fluctuations in the peatland physical C accumulation rates preserve varying degrees of positive precipitation-evaporation balance, especially in ombrotrophic

peatlands, which are solely regulated by climate (Charman et al., 2004) and serve as excellent records of prevailing climate at time of sedimentation.

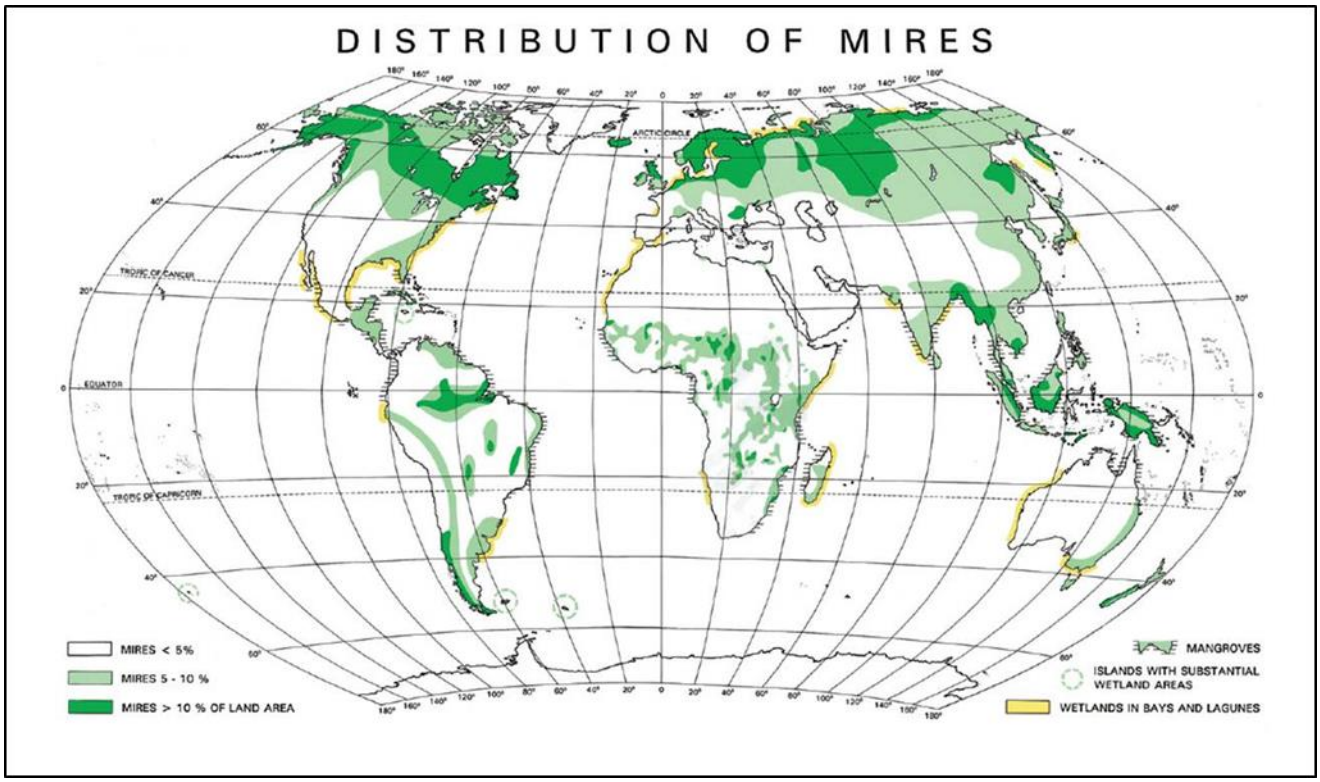

Figure 1: Global distribution of different types of peatlands (from Strack, 2008, Available via International Peat Society, www.peatsociety.fi)

Southern Africa is situated at a dynamic junction between tropical, sub-tropical and temperate climate systems. The region is dominated by large seasonal fluctuations in the Inter Tropical Convergence Zone (ITCZ; Stokes et al., 1997), and high sea surface temperature (SST) gradients between the warm Agulhas and cold Benguela oceanic currents fringing the region (Preston-Whyte and Tyson, 1998; Tyson and Preston-Whyte, 2000). Uncertainty, however, still surrounds the mechanism of interaction between these different climate drivers and whether terrestrial ecosystems in the region responded abruptly or gradually to the ensuing climatic shifts, most notably during the transition from the last glacial maximum (LGM) to the Holocene. The biggest hindrance to understanding Southern Africa palaeoclimate variations (and the environmental responses to climate fluctuations) is the general lack of continuous terrestrial archives (Nash and Meadows, 2012; Scott et al., 2008). This is mainly due to the regional topography and a semi-arid climate not being conducive for preservation of climate archives (Chase and Meadows, 2007).

Regional terrestrial archives in Southern Africa that have been explored vary from speleothems (Holmgren et al., 2003; Holzkämper et al., 2009; Lee-Thorp et al., 2001; Talma and Vogel, 1992), coastal or inland lake sediments (Kristen et al., 2010; Meadows et al., 1996; Neumann et al., 2008, 2010;Partridge, 2002; Walther and Neumann, 2011) and regional peatlands (Finch and Hill, 2008; Norström et al., 2009; Quick et al., 2015 a,b) to the less orthodox *Hyrax* midden deposits (Chase et al., 2010, 2011, 2012; Valsecchi et al., 2013) and multi-archive studies (Chase and Meadows, 2007; Chase and Thomas, 2007; Meadows, 2001; Meadows and Baxter, 1999; Scott et al., 2008).

The most pertinent palaeoclimate reconstruction was one undertaken by Holmgren et al. (2003) on stalagmites recovered from the Cold Air Cave in the summer rainfall zone (SRZ) of South Africa. They used oxygen and carbon stable isotope data to establish a detailed high-resolution climate record for the region from 24.4 ka to present day, with an exception of a hiatus extending from 12.7 to 10.2 ka, coinciding with the Younger Dryas (YD). Neumann et al., (2008, 2010) undertook palynological and sedimentological studies on proximal Lake Sibaya and Eteza to reconstruct the Holocene climate on the north eastern KwaZulu Natal coast. These two archives presented a high-resolution record of climate driven vegetation changes on the same coastline that the Mfabeni peatland is located; however both records only cover the Holocene. To the author's knowledge, the only other geochemical climate study undertaken on a peatland in the SRZ of Southern Africa was done by Norström et al. (2009). They employed pollen, carbon and nitrogen elemental ratio and stable isotope compositions, as well as microscopic charcoal concentrations to reconstruct the palaeoenvironment around the Drakensberg escarpment. They produced a high resolution record from the late Pleistocene to the early Holocene (16 – 7.5 ka), however the mid- and late-Holocene record was blurred due to slow peat accumulation and low data resolution.

Nonetheless, terrestrial archives in Southern Africa tend to record site specific palaeoenvironmental conditions over varying time intervals, with only a few archives extending as far back as the LGM. Many records are temporally discontinuous (speleothems), suffer from dating inconsistencies (ka vs kcal yr BP vs years before 2000 AD) and tend to be geographically clustered resulting in lack of ubiquitous distribution of climate change records across the region. In addition, conclusions derived from different proxies often yield different results and magnitudes

in response to the perceived climate variability in the region. Therefore, additional high-resolution multi-proxy and multi-archive regional studies are required to elucidate terrestrial environmental responses to past climatic shifts in Southern Africa.

1.1.1. Study site

The iSimangaliso Wetland park (formerly known as the Greater St Lucia Wetland park) is an important, internationally recognized wetland ecosystem, which was granted UNESCO World Heritage status in 1999 (Vrdoljak and Hart, 2007). It is located on the north-eastern coast of KwaZulu-Natal, South Africa and forms the southern end of the Maputaland coastal plain (Figure 2). Lake St Lucia dominates the park and has a north-south orientation parallel to the coast and covers an area of 350 km^2, with an average depth of 90 cm (Orme, 1990). At the southern end, a narrow 22 km long channel connects the main water-body to the Indian Ocean, while the main rivers of Mkhuze, Nyalazi, Mzinene and Hluhluwe, with a combined catchment area of 6085 km^2, flows into the northern end of lake St Lucia (Taylor et al., 2006). The hydrology in the park is dominated by regional and local rainfall, riverine runoff, groundwater recharge and the inward/outward movement of seawater from the Indian Ocean. The large eastern unconfined Maputaland aquifer is structurally controlled by 1 km wide and up to 180 m high coastal dune barrier that separates the lake from the Indian Ocean (Taylor et al., 2006). The barrier is made up of marine, alluvial and aeolian sand deposits of Pleistocene and Holocene ages (Roberts et al., 2006).

The region lies within a sub-tropical climate which experiences mainly austral summer rainfall of between 900 and 1200 mm/yr (Clulow et al., 2012), however, extreme dry periods have been recorded with a distinctive cyclical wet/dry pattern with an approximate 10 year periodicity (Tyson and Preston-Whyte, 2000; Taylor et al., 2006; Bate and Taylor, 2008). When regional precipitation is high, the riverine inflow is strong and there is an outflow to the Indian Ocean, resulting in decreased salinity levels. However, during extended periods of drought reduced fluvial inflow results in lake level falling below sea level.

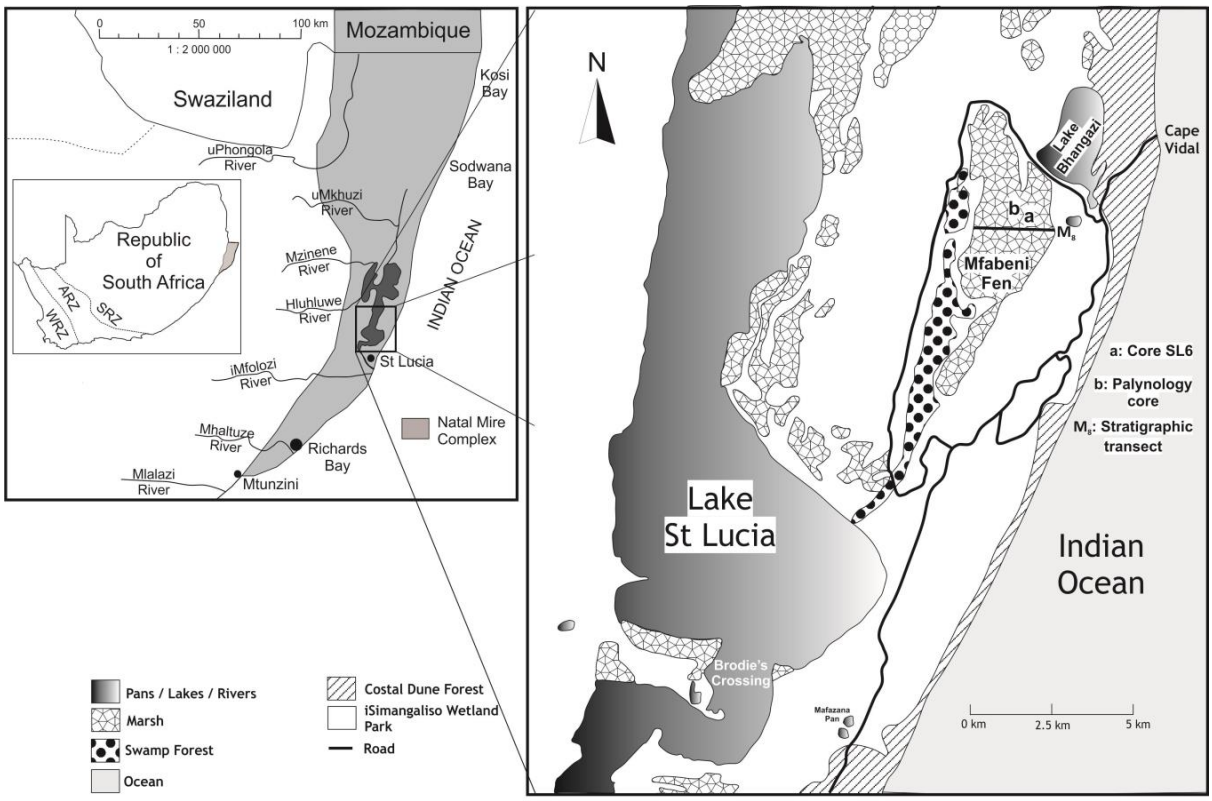

Figure 2: Location of core SL6 (a) in the Mfabeni peatland, iSimangaliso Wetland Park, northern Kwazulu-Natal, South Africa. Location of palynology core (b; Finch, 2005; Finch and Hill, 2008) and most proximal and deepest stratigraphic transect (M8; Grundling et al. 2013) included for orientation. WRZ = winter rainfall zone; ARZ = all-year rainfall zone; SRZ = summer rainfall zone.

If the estuary's mouth is open to the ocean, inflowing seawater replaces fresh water lost through evapotranspiration and salt concentrations can reach upwards of 120 ppt (3 times that of sea water) in the northern parts of the lake (Bate and Taylor, 2008). During extreme droughts, the only source of freshwater is groundwater seepage, with up to two-thirds originating from the Maputaland aquifer on the eastern shores (Taylor et al., 2006). The ecological significance of this freshwater input into the lake, is that the inflow persists even during extreme periods of drought (Vrdoljak and Hart, 2007) resulting in freshwater habitat refuges along the groundwater input points. The highest rainfall falls on the sand dune coastal barrier (>1200 mm/yr; Taylor et al., 2006), of which ca. 20% ends up as recharge into the Maputaland aquifer (Kelbe and Rawlins, 1993). As a result, the regional rainfall patterns have a strong influence on groundwater recharge and flow to the eastern shores of Lake St Lucia.

The Mfabeni peatland forms part of the greater Natal Mire Complex (NMC; Fig. 2), and lies within an interdunal depression on the eastern shores of Lake St Lucia. It has an extent of 10 x 3 km

(Clulow et al., 2012; Grundling et al., 2013), with a maximum depth of ca. 11 m (Grundling, 2001; Grundling et al., 2013) and lies ca. 11 m a.s.l. (Finch and Hill, 2008). The site was chosen for its varying freshwater inputs, high but variable rainfall pattern and pristine environmental conditions. In addition, the peatland was specifically targeted due its relative ancient age and continuous peat sedimentation record (Finch and Hill, 2008; Grundling et al., 2013). Even though the peatland is classified as minerotrophic (as opposed to ombrotrophic), it is only influenced by ground water and direct precipitation, resulting in mainly authochthonous sediment input (Finch and Hill, 2008). Peat started accumulating via valley infilling ca. 50 kcal yr BP as a result of the aggregational blockage of the Nkazana palaeochanel that used to link the peatland basin with Lake St Lucia and, sustained groundwater input (Grundling et al., 2013). The continuous ca. 50 kyr period of peat sedimentation, covering the late Pleistocene and Holocene, positions the Mfabeni peatland as one of the oldest continuous coastal peatland records in Southern Africa. The peat deposit owes its longevity to the protection against sea level fluctuations, and enhanced groundwater transmissibility (Grundling et al., 2013) of the adjacent coastal dune corridor (ca. 55 kcal yrs BP; Porat and Botha, 2008).

1.1.2. Geological setting, morphology and stratigraphy

According to Roberts et al. (2006), the iSimangaliso wetland park forms part of the Maputaland Group of coastal Cenozoic deposits, which is made up of, from oldest to youngest: Port Durnford, Kosi Bay, Isipingo, KwaMbonambi and Sibayi Formations. The basement consists of Cretaceous siltstones, which were deposited during the break-up of Gondwana, followed by eastward dipping consolidated Mesozoic and Neogene sedimentary rocks (Figure 3). On the eastern shore, mainly unconsolidated to semi-consolidated sediments of middle to late-Pleistocene age overlie the Mesozoic and Neogene rocks. They are made up of thin estuarine clays of the Port Durnford formation in the west and thicker dune sands of the Kosi Bay and Isipingo formation to the east. The youngest unit is the Holocene dune sands of the Sibayi Formation, which overlies the older strata in most of the area. The predominantly unconsolidated to semi-consolidated nature of the sand dune sediments in these formations contributes to their relatively high hydraulic conductivity and their suitability for water channelling (Vaeret and Sokolic, 2009). The terrain morphology of

the eastern shores of St Lucia Estuary has been described by Taylor et al. (2006). The terrain was subject to continuous river and coastal carving during the last two glacial/interglacial periods of the Pleistocene. The nucleus of the eastern shores terrain started as a barrier island in the St Lucia Bay marine environment. During the Weichselain regression, river incision created valleys that were subsequently filled in first with marine and then fluvial deposits during the Flandrian marine transgression and subsequent sea water exclusion after the coastal dune barrier was accreted. The contemporary eastern shore is proportioned into three terrains, comprising the (a) vegetated coastal dune barrier, (b) central undulating dune system, and (c) low-lying areas between the undulating dune systems that include the Mfabeni peatland.

Grundling et al. (2013) cored successive boreholes of between 100 and 200m intervals along eight transects from north to south in the Mfabeni basin (Figure 4). They described the morphology of the Mfabeni peatland as complex, with a main central depression that extends to a depth of 10.8m and smaller depressions on either side of the main basin with peat depths of no more than 2.5m. The peat surface slopes in a southerly direction in addition to a very gentle downwards slope from west to east. Grundling et al. (2013) recognised five distinctive peat layers that were occasionally interspersed with sandy layers, mostly in the eastern part of the basin, listed from the bottom up:-

1. The basal layer consists of brown coloured fibrous wood and sedge material in the deepest part of the basin along transect M8 (Figure 2 and 4);
2. dark finer-grained amorphous layer (gyttja) with sand lenses and more fibrous peat towards the top of the layer;
3. dark coloured fibrous package with wood and sedge remains;
4. amorphous dark sedge that become less decomposed with fibrous woody remains towards the top;
5. top layer is made up of poorly decomposed sedge and woody peat.

According to Grundling (2004), due to the linear gradient of the Mfabeni core ^{14}C ages versus peat thickness (regression value for the Pleistocene = 0.94 and Holocene = 1.00) the peatland

sediments are not compacted, supported by intact fresh water mollusc shells at a depth of 3m and more in the peat profile.

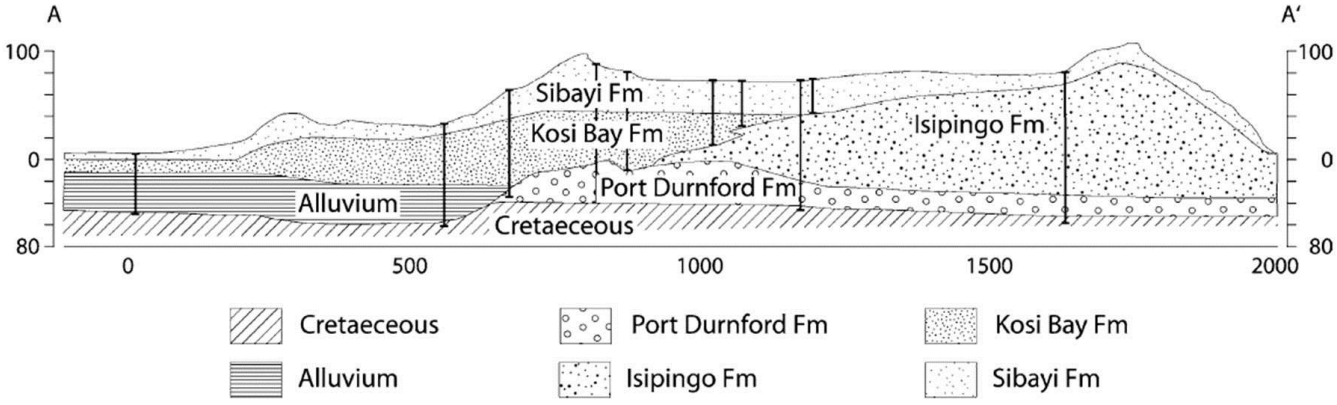

Figure 3: Geological cross section of the eastern shores boundary of Lake St Lucia. Vertical lines show position of exploration boreholes (from Taylor et al., 2006). Vertical scale in meters.

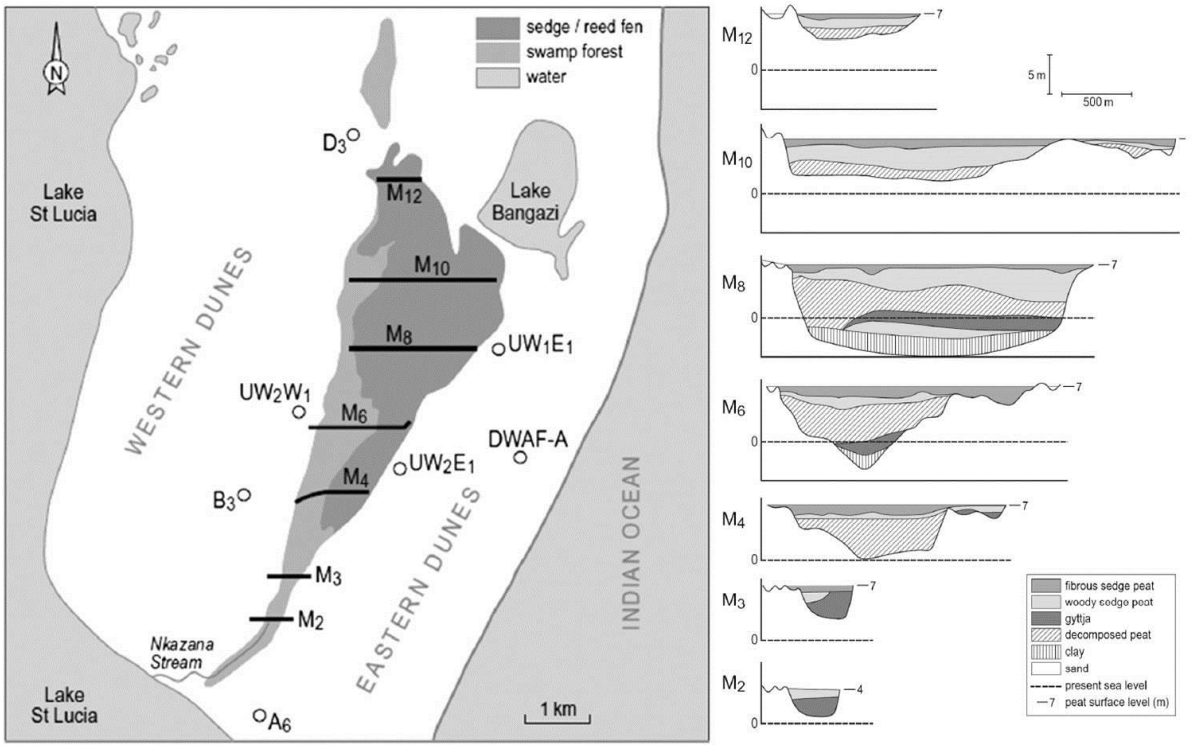

Figure 4: Sample sites and stratigraphy of Mfabeni peatland along eight transects from west to east. From Grundling et al. (2013).

1.1.3. Regional groundwater flow

Taylor et al. (2006) ran a groundwater flow simulation on the eastern shores of Lake St Lucia. They concluded that the relatively stable groundwater flow from the high coastal dune barrier has two flow components, one eastward towards the Indian Ocean and the other in a westerly direction that is intercepted by the low lying plain where the Mfabeni is situated. The Embomveni dune ridge is located in the central eastern shores, and lies between the Mfabeni peatland and Lake St Lucia. It acts as a mound that radiates groundwater into the Mfabeni peatland to the east and into the lake towards the north and west. The Embomveni part of the aquifer has fluctuating water levels of up to 5 m between extreme dry and wet conditions, and controls the variable discharge into the peatland and estuary. The Mfabeni basin is therefore fed by groundwater from both dune ridges, with the most varied flow emanating from the Embomveni dune ridge. According to Ramsay and Cooper (2002), the South African coastline sea level dropped up to -120m during the height of the LGM and raised ca. +3.5m above modern sea levels during the mid-Holocene. Since the Mfabeni is a coastal fen, there is a possibility that the fluctuating sea levels proposed since the Late Pleistocene could have influenced the water table levels in the basin as a result of lateral movement of groundwater. This in turn would have affected peat accumulation in the Mfabeni basin, which could have overprinted climatic signals in the archive. This does not seem to be the case, as comparisons with the physical parameters of peat accumulation (TOC and C accumulation) in the basin do not appear to have any strong correlation with sea level fluctuations. Therefore, it was assumed that sea level changes did not have a major influence on peat formation in the Mfabeni peatland.

1.1.4. Site vegetation

The park is spatially heterogeneous and ranges from saline to fresh water habitats, encompassing swamps, hygrophilous grasslands, salt marshes, mangroves, swamp and riparian forests (Vrdoljak and Hart, 2007). The extent and character of each habitat is determined largely by topography, hydrology, vegetation and historical land use. Mucina et al. (2006) broadly classified the eastern shore vegetation as Maputuland wooded grassland, coastal belt and sub-tropical freshwater wetland and northern coastal dune and swamp forests, whereas the fen itself is dominated by

herbaceous reed sedges and grasses (Finch, 2005). Venter (2003) undertook a plant community survey in the Mfabeni swamp and adjacent swamp forest. They classified 11 peatland and 3 swamp forest communities based on species and habitat (Table 1).

Table 1: Mfabeni peatland and swamp forest plant communities (Venter, 2003)

Name	Description	Location	Water table
Peatland communities			
Restio zuluensis - Andropogon appendiculatus	Closed low sedge and grass peatland	Grassland west of swamp forest	Fluctuating
Scleria poiformis	Closed tall sedge peatland	North to north-eastern parts of swamp	Shallow water
Rhynchospora holoschoenoides	Open to closed short sedge peatland	Eastern edge of swamp	Fluctuating shallow
Typha capensis - Ludwigia octovalvis	Closed high peatland	within swamp in deep water	Deep water
Eleocharis dulcis	Closed tall sedge peatland	North-eastern and northern parts of swamp	Deep water
Rhynchospora corymbosa	Closed low sedge peatland	Widespread	shallow variable
Fimbristylis bivalvis	Open to closed short sedge peatland	Widespread	Variable medium deep
Sphagnum trucatum - Xyris natalensis	Closed short moss peatland	Southern and central-northern parts of swamp	Shallow
Cladium mariscus	Closed high sedge peatland	Widespread	Shallow
Cyperus prolifer	Closed short sedge peatland	North-western to northern parts of swamp	Variable
Cyperus fastigiatus	Closed tall sedge peatland	Northern parts of swamp	Medium to deep
Swamp forest communities			
Syzygium cordatum - Stenochleana tenuifolia	Swamp forest	Central portion of swamp forest	Shallow variable
Ficus trichopoda - nephrolepis biserrata	Swamp forest	Northern and southern parts of swamp forest	Shallow variable
Barringtonia racemosa - Bridelia micrantha	Swamp forest	Southern portion of swamp forest along drainage lines	Medium

Apart from Venter (2003) study, there has been no other in-depth studies done on the contemporary plant communities in the peatland, which has resulted in a lack of information on the balance of C3 and C4 plants present and the effects of growing season temperatures and moisture availability on the $\delta^{13}C_{wax}$ signal of contemporary plants in the region.

1.2 Geochemical proxies

A geochemical proxy is a chemical compound that can be used to infer a relationship between a specific physical process and a corresponding change in the said chemical component. The most valuable proxies are those for which a single or dominant controlling factor can be identified, and the preserved signals are responsive to changes in on-going primary processes. Inherently, all proxies suffer from shortcomings that can be caused by limitations such as quantifying the geochemical relationship in modern systems and, preservation versus diagenetic effects after deposition which can complicate extrapolations (Sageman and Lyons, 2003). Therefore, it is essential that researchers use a multi-proxy approach to reduce uncertainties involved in delineating past climate and environmental changes within the different geochemical disciplines.

1.2.1 Bulk source indicators:

C/N ratio: Elemental analysis of OM is widely used to distinguish between algal and terrestrial plant sources in sediments (Meyers, 1994, 2003; Gälman et al., 2008). Due to absence of cellulose

and abundance of protein in algal-derived OM (Meyers and Ishiwatari, 1993; Meyers, 1997), the atomic C/N ratio provides an indication of the relative contribution of algal and terrestrial plant-derived OM into sediments. Algal sources typically have atomic C/N ratios of between 4 and 10, whereas vascular land plants have C/N ratios of 20 or greater. C/N ratios between 10 and 20 indicate a mixture of both algal and terrestrial plant OM (Meyers, 1997). In peatlands, the C/N proxy is employed in conjunction with C and N stable isotope signatures to elucidate OM preservation, redox depositional conditions and biogeochemical processes related to C and N cycling of sedimentary OM (Skrzypek et al., 2008; Jones et al., 2010; Andersson et al., 2012).

Stable Carbon (C) isotopes: The C isotopic composition of sedimentary OM reflects the dynamics of carbon assimilation during photosynthesis and isotopic composition of the carbon source. The $\delta^{13}C$ signal can be used to distinguish between different photosynthetic pathways employed by the plants in the peatland (Figure 4). C3 plants biochemically discriminate against ^{13}C during the Calvin cycle and produce an average $\delta^{13}C$ signal of ca. -27 ‰, while C4 plants use the Hatch-Slack pathway and produce an isotopic enriched average value of -14‰ (O'Leary, 1988; Meyers, 1994, 1997). Due to freshwater algae exclusively utilizing dissolved CO_2, which is usually in isotopic equilibrium with atmospheric CO_2, lake-derived OM is typically not distinguishable from other C sources emanating from the surrounding watershed (Meyers, 1994). On the other hand, marine algae utilises dissolved bicarbonate, which has a $\delta^{13}C$ value of approximately 0‰, and as a consequence commonly displays $\delta^{13}C$ values of -20 to -22‰. The distinct $\delta^{13}C$ signatures of OM produced by C3 versus C4 plants and marine algae have been used to trace OM sources in both terrestrial and marine sediments (Meyers and Ishiwatari, 1993; Meyers, 1997; Xue et al., 2014). In peatlands, the $\delta^{13}C$ signal can serve as an archive for changes in the relative contribution of C4 and C3 plants, which can be related to changes in environmental and climatic conditions (Skrzypek et al., 2008, 2010).

Stable nitrogen (N) isotopes: The N stable isotopic ratio is based on the premise that isotopic compositions of inorganic nitrogen sources to aquatic and land plants differ significantly (Meyer, 1997). In peatlands, higher plants form the dominant source of OM input; resulting in up to 95% of N originating from the degraded plant OM (Andersson et al., 2012).

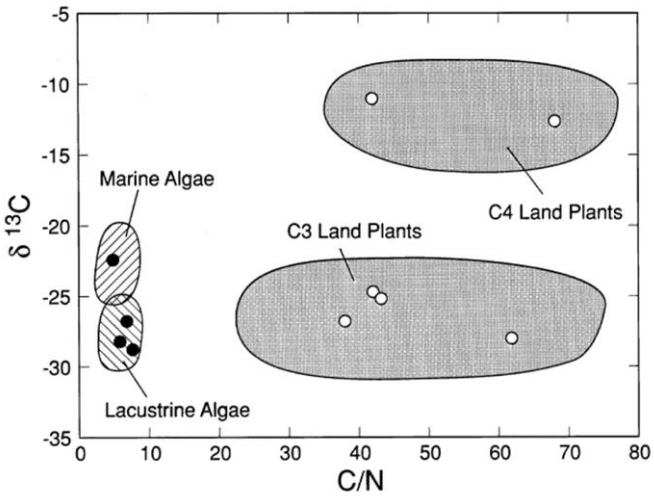

Figure 5: Elemental and isotopic identifiers for bulk organic matter (from Meyers, 1994, 1997)

Plants that receive their N predominantly from soil N fixers conventionally display $\delta^{15}N$ values within a small range (ca. -2 to +2‰) analogous to atmospheric $\delta^{15}N$ (± 0‰; Meyers and Ishiwatari, 1993). In contrast, plants deriving the majority of their N through microbially catalysed OM decomposition display characteristically more negative $\delta^{15}N$ values (ca. -2 to -8‰; Fogel and Cifuentes, 1993; Skrzypek et al., 2008). Bodelier and Laanbroek (2004) suggested that during increased rates of methanogenesis, and by that token increased temperatures and waterlogging in tropical peatlands, the high N demanding methanogenic bacteria produce a more isotopically light N source for plants, which ultimately causes the soil N isotopic signal to become depleted in ^{15}N.

1.2.2. Molecular source indicators:

Biomarkers are organic compounds that have specific biological origins and their preserved forms in sediments reflect enzymatic control on their molecular structures. This trait of retaining their biological signature has resulted in these compounds being referred to as “biological markers”, or as they are more commonly referred biomarkers (Meyers, 1997).

***n*-Alkane (*n*-alk):** are saturated straight-chained hydrocarbons that are relatively resistant to microbial alteration and decomposition during digenesis compared to other hydrocarbons (Meyer 1997). Hence *n*-alkanes are particularly valuable for identifying OM sources for palaeoenvironmental reconstructions.

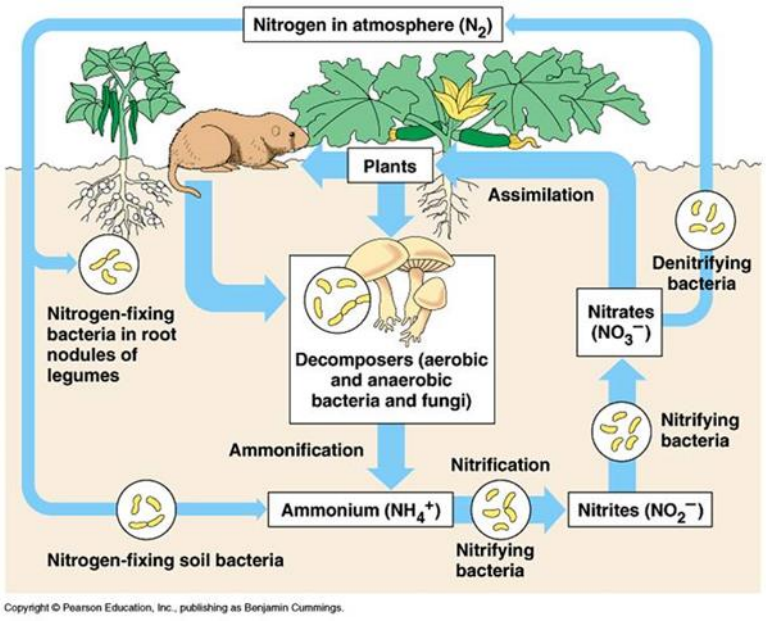

Figure 6: biogeochemical cycling of N in the ecosystem. (©2005 Pearson Education, Inc., publishing as Benjamin Cummings. http://bio2.shtechclub.org/cd/bc_campbell_biology_7/0,7052,3949437-,00.html)

The principle contributing distinction between algae, aquatic and vascular land plants is the differences in the principal chain lengths of their molecular groups. The predominance of C_{27}, C_{29} and C_{31} *n*-alkanes indicates that vascular emergent and land plant epicuticular waxes has been a major contributor to the sedimentary OM (Eglinton and Hamilton, 1967; Cranwell et al., 1987; Rieley et al., 1991). In contrast, aquatic / submerged plants are dominated by C_{23} and C_{25} *n*-alkanes (Cranwell, 1984; Ficken et al., 2000), whereas algal contributions are indicated by the abundance of C_{17} *n*-alkanes (Cranwell et al., 1987; Eglinton and Hamilton, 1967; Rieley et al., 1991).

***n*-Alkanoic Acid (*n*-FA)**: are more sensitive to degradation and modification than other types of biogenic lipids (Meyers and Ishiwatari, 1993), and so are more useful indicators of OM recycling as opposed to source indicators (Meyers, 2003). Degradation rates of short chained *n*-FAs have been estimated to be 6-7 times higher than for the long-chain *n*-FAs in coastal marine sediments (Haddad et al., 1992). Long chain *n*-FA (C_{24}, C_{26} and C_{28}) compounds are derived from the waxy cell wall of land plants, and are the non-reactive survivors of transport of land-derived debris into lake sediments (Meyers 2003). In contrast, shorter chain *n*-FAs (C_{12}, C_{14} and C_{16}) are more

prevalent in algal and bacterial lipids (Cranwell et al., 1987, Rieley et al., 1991). Plant cell membranes tend to be dominated by more abundant unsaturated *n*-alkanoic acids than their saturated counterparts (Zhou et al., 2005). Both Jeffries (1972) and Kawamura and Ishiwatari (1981) reported preferential microbial degradation of the unsaturated C_{16} and C_{18} *n*-alkanoic acids in tidal marsh and lake sediments. Therefore, the different rates at which saturated and unsaturated fatty acids degrade are suggested to be sensitive to environmental conditions (Meyers and Kawka, 1984), especially temperature (Kawamura and Ishiwatari, 1981; Zhou et al., 2005). Additionally, Zhou et al. (2010) attributed the discrepancies between *n*-alkane, *n*-alkanol, and *n*-alkanoic acid homologue distributions in the Hani peat sequence to partial replacement of the primary compounds by secondary microbial biomarkers. They attributed the dominance of C_{16} acid and corresponding absence of C_{24} acid in the upper part of their core to post-depositional, secondary synthesis of microbially produced acids as a consequence of increased microbial activity during the post-glacial and Holocene warming.

***n*-Alkanol (*n*-alc)**: is a relatively labile biomarker which is often partly diagenetically altered (Meyers, 1997; 2003), and commonly used to elucidate both OM sources and diagenetic alteration. They have similar chain length distributions to *n*-FA compounds corresponding to their origins, with chain lengths of C_{22} – C_{30} monomers predominantly produced in the epicuticular layers of terrestrial plants (Eglinton and Hamilton, 1967; Rieley et al., 1991), whereas aquatic microbes typically contribute towards the abundance of short chained *n*-alkanols in lake sediments (C_{16} – C_{22}; Cranwell et al., 1987; Volkman et al., 1999).

As a result of the Mfabeni atomic C/N ratio (Chapter 2, Figure 5) rarely dropping below 20 and the biomarker homologue distributions (Chapter 3, Figure S2) showing predominant long chain *n*-alkanes OM input throughout core SL6, it was concluded that algal OM input was at a minimum, and therefore, algal influences on the organic geochemical proxies in the core were not considered.

Biomarker ratios:

Carbon preference index (CPI): Plants (and other organisms) produce predominantly odd-numbered *n*-alkanes and even-numbered carbon chains of *n*-FAs and n-alcs in their cell wall lipids (Meyers, 1993). Because these compounds degrade during diagenesis, the odd over even or even over odd characteristic of OM diminishes. Bray and Evans (1961) devised the CPI ratio as a numerical representation of how much of the original biomarker is preserved in sediments as a way of quantifying OM maturity (Table 1). Variations in factors such as sedimentation rates and degree of lake water oxygenation impact the preservation of these biomarkers. However, Zhou et al. (2010) reported high CPI values for *n*-alkanoic acids in the Hani peatland which he attributed to the replacement of the primary acids with secondary microbial acids after deposition.

Average chain length (ACL): the main function of plant leaf epicuticular layers is to protect terrestrial and emergent plant species against desiccation. It has been suggested that plants adapt the chain lengths of lipid components in their waxy layer in response to changes in temperature (Gagosian and Peltzer, 1986) and moisture availability (Andersson et al., 2011; Bush and McInerney, 2013; Schefuß et al., 2003; Zhou et al., 2010, 2005). The ACL value is derived from the concentration-weighted mean of the respective long chain compounds (Table 1), and due to land plants biosynthesizing long chain compounds in warmer (and drier) climates, can be used to infer changes in palaeoclimate.

Aquatic plant *n*-alkane proxy (P_{aq}): was developed by Ficken et al. (2000) to reconstruct the palaeohydrology of lakes on Mt Kenya in East Africa (Table 1). They used the distinctive differences in *n*-alkane chain lengths prevalent in submerged macrophytes (C_{23} and C_{25}) versus higher plant matter (C_{29}, C_{27} and C_{31}) to reconstruct the relative proportions of the in-situ plant assemblages in response to changes in lake levels. Several studies have been done using this ratio to reconstruct moisture availability in wetlands and peats (Nichols et al., 2006; Nichols et al., 2009; Zhou et al., 2005; Zheng et al., 2007).

Table 2: Summary of biomarker proxies

Proxy	Acronym	Equation	Background	Indications	References
Carbon preference index (all)	CPI	$CPI_1 = [\Sigma(C_{21} - C_{29})\ odd + \Sigma(C_{23} - C_{31})\ odd]/\ 2\Sigma(C_{22} - C_{30})\ even$ $CPI_2 = [\Sigma(C_{20} - C_{30})\ even + \Sigma(C_{22} - C_{32})\ even]/2\Sigma(C_{21} - C_{31})\ odd$	Plants produce leaf wax with odd-over-even (*n*-alkane) or even-over-odd (*n*-alkanonic acid & *n*-alkanol) predominance. During diagenesis, this odd over even or even over odd characteristic diminishes.	↑ Better preserved or less labile OM source e.g. terrestrial vs submerged OM input; ↓ More degraded or more labile OM source	Rieley et al., 1991; Zhou et al.,2010, 2005; Andersson et al., 2012
Average chain length (all)	ACL	$ACL_1 = (\Sigma[Ci] \times i) / \Sigma[Ci]$, for i = 23 – 33 where Ci = conc. of n–alkane containing i carbon atoms; $ACL_2 = (\Sigma[Ci] \times i) / \Sigma[Ci]$, for I = 22 – 32 where Ci = conc. of n-alkanoic acid or n-alkanol containing i carbon atoms	Plants produce long chain leaf wax layers in response to drier and warmer conditions. Changes in ACL trends can be used to elucidate climatic conditions during photosynthesis.	↑ Longer average chain lengths in leaf wax layers e.g. hotter and drier conditions; ↓ shorter average chain lengths e.g. during cooler and wetter conditions	Gagosian and Peltzer, 1986; Schefuß et al., 2003; Zhou et al., 2005; Carr et al., 2014
Aquatic plant (*n*-alkanes only)	P_{aq}	$P_{aq} = \frac{C_{23} + C_{25}}{C_{23} + C_{25} + C_{29} + C_{31}}$	Aquatic plant leaf waxes are dominated by mid-chain alkanes (n-C_{23} & C_{25}). P_{aq} is used to elucidate relative amounts of aquatic vs. higher plant input.	↑ more aquatic plant OM input e.g. during higher water levels; ↓ More terrestrial plant OM input e.g. during low water levels	Cranwell, 1984; Ficken et al., 2000; Zhou et al., 2010, 2005; Andersson et al., 2011
Terrestrial plant (*n*-alkanes only)	P_{wax}	$P_{wax} = \frac{C_{27} + C_{29} + C_{31}}{C_{23} + C_{25} + C_{27} + C_{29} + C_{31}}$	Emergent and terrestrial plant leaf waxes have long-chain alkanes (n-C_{27}, C_{29} and C_{31}). P_{wax} indicates variation in terrestrial plant input in relation to bulk plant input.	↑ higher proportions of terrestrial plant OM input during low water levels; ↓ less terrestrial plant OM input during high water levels	Eglinton and Hamilton, 1967; Rieley et al., 1991; Zheng et al. 2007; Andersson et al., 2011
saturated vs. unsaturated (*n*-alkanoic acids only)	$Sat/unsat_{FA}$ $18:1/18:0_{FA}$ $16:1/180_{FA}$	Various ratios	Unsaturated short chain n-alkanoic acids are more susceptible to microbial reworking and the sat/unsat alkanoic acid ratios indicate microbial decomposition.	↑ higher proportions of saturated vs unsaturated n-alkanoic acids e.g. higher microbial reworking i.e. higher temperatures; ↓ less microbial reworking i.e. lower temperatures	Meyers & Kawka, 1984; Zhou et al., 2005

Terrestrial plant *n*-alkane proxy (P_{wax}): Zheng et al. (2007) used the same premise of characteristic carbon chain length distributions for submerged macrophyte versus emergent and terrestrial plant to develop the P_{wax} proxy (Table 1). They used the P_{wax} proxy to gauge relative proportions of emergent and terrestrial plant inputs in relation to all higher plants to reconstruct the palaeoprecipitation record of Zoige-Hongyuan peat deposit.

Saturated vs unsaturated *n*-alkanoic acid proxies ($sat/unsat_{FA}$, *n*-$C18:1/18:0_{FA}$ and *n*-$C16:1/16:0_{FA}$): Monounsaturated *n*-alkanoic acids are more susceptible to climate driven microbial reworking than their saturated counterparts (Matsuda and Koyama, 1977 a, b), hence unsaturated fatty acids are preferentially degraded during warm and wet climatic conditions (Zhou et al., 2005). The $sat/unsat_{FA}$ concentration ratios can therefore be used to reconstruct fluctuations in microbial activity and inferences can be made about environmental conditions that drove these fluctuations.

Leaf wax ^{13}C isotopes ($\delta^{13}C_{wax}$): is a powerful analytical tool that allows researchers to further explore OM source inputs and diagenetic changes. This proxy owes it analytical superiority to the fact that source specificity can be confidently inferred due to organisms fractionating C isotopes differently during C fixation and the $\delta^{13}C$ values are negligibly affected by diagenetic processes (Meyer, 1997). The different biochemical pathways employed during photosynthesis by C3 and C4 plants causes a variation in degrees of fractionation of the source CO_2 isotope, resulting in characteristic $\delta^{13}C$ bulk values ranging from -22‰ to -30‰ for C3 and -10‰ to -14‰ for C4 plants

(Bender 1971; Vogel et al., 1978). However, the bulk $\delta^{13}C$ signal encompasses many different inputs of C into the sediments, from inorganic and organic sources, which can complicate palaeoreconstructions. On the other hand, long chain *n*-alkane compounds (> C_{25}) are produced exclusively in the leaf waxes of emergent and terrestrial land plants (Eglinton and Hamilton, 1967; Rieley et al., 1991), and are generally accepted to be the most recalcitrant of all the hydrocarbons found in sediments (Meyers, 1997; Meyers and Ishiwatari, 1993). $\delta^{13}C_{wax}$ values of these long chained *n*-alkane compounds is primarily controlled by the C fixation pathways employed during photosynthesis, and to a lesser degree, changes in temperature, moisture and inorganic C source (Chikaraishi and Naraoka, 2003; Hayes et al., 1990; O'Leary, 1981; Schefuß et al., 2005). Hence, observed changes in peat $\delta^{13}C_{wax}$ trends can best be explained by the changes in relative abundance between C3 and C4 plant input, and thereupon a direct link can be made to the representational proportion of C3 and C4 higher terrestrial plants that were present at the time of peat formation. The causes for shifts in the proportions of C3 and C4 plants over time are still subject to intense scientific debate. Originally it was thought that the Hatch-Slack pathway employed by C4 plants during photosynthesis was more efficient and therefore favoured under low atmospheric CO_2 (Ehleringer et al., 1991; Cerling et al., 1997). However, more recent studies have indicated that changes in the balance of C3/C4 plants can also be affected by local environmental factors such as temperature and aridity (Castañeda et al., 2007; Huang et al., 2001; Khon et al., 2014; Schefuß et al., 2003; Scott, 2002; Xue et al., 2014; Yamamoto et al., 2010). Vogel et al. (1978) reported that although C3 plants are found throughout Southern Africa, the C4 distributions of grasses occur in distinct geographical areas, largely determined by growing season temperatures. They found that C4 grasses are predominantly found in the SRZ of Southern Africa, whereas C3 grasses are more dominant in the WRZ and higher altitudes of the eastern escarpment. Stock et al. (2004), on the other hand, suggested that C4 sedges evolved under wetland conditions in warm and wet tropical areas. When comparing the leaf wax and bulk $\delta^{13}C$ trends in core SL6 to global atmospheric CO_2 concentrations records (Ahn and Brook, 2008; Indermuhle et al., 1999) the Mfabeni archive does not correlate with the global pCO_2 records.

Therefore, the assumption was made that the changes in atmospheric pCO_2 did not have a major effect on the balance of C3 and C4 plants at the site.

1.3. Research objectives

The overall aim of this PhD project is to employ multi-proxy geochemical techniques to reconstruct the late Pleistocene and Holocene environment, and explore the palaeoclimatic controls governing peat accumulation in the Mfabeni peatland, northern KwaZulu Natal Province, South Africa. The principle objectives are as follows:-

- delineate primary production, bulk OM source inputs, OM preservation and diagenetic processes by using bulk geochemical proxy signatures such as: mass accumulation rate (MAR), total organic carbon (TOC), carbon accumulation rate (CAR) and bulk $\delta^{13}C$, $\delta^{15}N$ and C/N.
- employ a combination of established biomarker ratios to reconstruct fluctuations in different plant OM sources, palaeohydrology and microbial reworking.
- compare compound specific $\delta^{13}C_{wax}$, bulk $\delta^{13}C$ and total organic carbon (TOC) trends with proximal stratigraphic and palynology studies undertaken in the peatland, and reconstruct proportional inputs of C3 and C4 plants type assemblages.
- establish if peatland hydrology or climate was the dominant factor determining the fluctuations in peatland plant types.

We then use different combinations of these diagnostic palaeoenvironmental indicators to compare the Mfabeni archive with other regional climate records and investigate the climate signal preserved in the peatland. The new data generated by these multi-geochemical proxies will provide critical information about the impact of these changes in driving climate and palaeoenvironment conditions (e.g. rainfall intensity, vegetation adaption and palaeohydrology) in Southern Africa. The data will be particularly useful for modelling scenarios where high-resolution interpretations of such changes are generally absent from this region.

1.4. Thesis Structure

This thesis is written in the format of stand-alone scientific papers and consists of five chapters, the first chapter is an introduction, chapters two to four deal with different geochemical techniques and proxies which were used to delineate the changes in sedimentation regimes, OM input, degrees of preservation, microbial activity, diagenetic changes, peatland hydrology and plant assemblages both in and around the peatland. These multi-palaeoenvironmental indicators were combined and compared to other regional climate archives to reconstruction the climate in this sub-tropical coastal zone of north eastern South Africa from ca. 47 kcal yr BP to present. Chapter five is a synopsis of the research work undertaken in this thesis.

Chapter two explores the palaeoenvironmental controls on peat formation in the Mfabeni peatland by employing bulk geochemical records to delineate the physical parameters, namely: primary production, bulk OM source inputs, preservation and diagenetic processes that lead to peat accumulating continuously since the late Pleistocene. We then explored the climatic conditions under which peat accumulated, and observed correlations with other published regional climate archives. These results were published in Palaeogeography, Palaeoclimatology, Palaeoecology (Baker et al., 2014).

In chapter three we employed *n*-alkane, *n*-alkanoic acid and *n*-alkanol biomarker proxies to delineate between dominant submerged plant versus emergent and terrestrial land plant inputs to infer fluctuations in peatland hydrology and microbial activity to infer relative temperature changes. Although our *n*-alkane proxy results show that the dominant OM input into the peatland to be emergent and terrestrial plants, definite shallow lake periods, where submerged macrophytes predominated, was recorded, signalling dramatic variations in precipitation intensities since the late Pleistocene. The temperature sensitive *n*-alkanoic acid and *n*-alkanol proxies were used to disentangle local temperature and precipitation fluctuation. This chapter has been submitted to Palaeogeography, Palaeoclimatology, and Palaeoecology for review in April 2015. It was re-submitted with revisions in August 2015.

Chapter four details the molecular leaf wax $\delta^{13}C$ isotopes data, and previously published bulk C isotope and TOC data, and compared to palynology and stratigraphic studies done in the Mfabeni to reconstruct the plant type assemblage fluctuations since the inception of the peatland. Our results showed definitive shifts in the proportional contributions of C3 and C4 plants which correlated strongly with the comparative palynology and stratigraphic records. A manuscript documenting the full results from this investigation has been prepared for submission to the Journal of Quaternary Science.

Chapter five presents a brief synopsis of the thesis, providing a summary of the findings outlined in the preceding chapters. Additionally, possible avenues for future research and outstanding gaps in knowledge regarding palaeoenvironmental research in the region were identified.

A complete list of relevant references is listed at the end of each chapter, in the format specific to the target journal in which the manuscripts were published or submitted to. Appendix information relevant to each chapter is included at the end the pertinent chapters.

1.5. Abbreviations

Full terminology is listed in text wherever they first appear with the relevant abbreviation listed in brackets. Abbreviations that are frequently used in this thesis include:

A1 and A2 - Antarctic warming events
ACL - average chain length
ACR - Antarctic cold reversal
Alc – *n*-alkanols
Alk – *n*-alkanes
ARZ - all year rainfall zone
C - Carbon
CAR - carbon accumulation rate
C_{max} - carbon chain maximum
CPI - carbon preference index
DOC – dissolved organic carbon
FA – *n*-alkanoic acids / fatty acids

GC - gas chromatography

GHG – greenhouse gasses

H1-5 - Heinrich events

Hol - Holocene

ITCZ - Inter Tropical Convergence Zone

kcal yr BP - thousand years calibrated before present

KZN - KwaZulu Natal

LGM - Last Glacial Maximum

LARCA - long-term apparent C accumulation

LSR - linear sedimentation rate

MAR - mass accumulation rate

MS - mass-spectrometer

N - Nitrogen

NMC – Natal mire complex

NPP - net primary production

OM - organic matter

P_{aq} - *n*-alkane aquatic plant ratio

P_{wax} - *n*-alkane terrestrial leaf wax ratio

$Sat/unsat_{FA}$ - total saturated / unsaturated n-alkanoic acid ratio

SOM - soil organic matter

SRZ - summer rainfall zone

SST - sea surface temperature

TLE – total lipid extraction

TLE-A – acidic total lipid extraction fraction

TLE-N – neutral total lipid extraction fraction

TOC - total organic carbon

TRACA - true rate of carbon accumulation

WRZ - winter rainfall zone

YD - Younger Dryas

$\delta^{13}C_{bulk}$ - bulk carbon isotope

$\delta^{13}C_{wax}$ - leaf wax carbon isotope

References

Ahn, J., Brook, E.J., 2008. Atmospheric CO2 and climate on millennial time scales during the last glacial period. Science 322, 83–5.

Andersson, R.A., Meyers, P., Hornibrook, E., Kuhry, P., Mörth, C., 2012. Elemental and isotopic carbon and nitrogen records of organic matter accumulation in a Holocene permafrost peat sequence in the east European Russian arctic. Journal of Quaternary Science. 27 (6), 545-552.

Andersson, R. a., Kuhry, P., Meyers, P., Zebühr, Y., Crill, P., Mörth, M., 2011. Impacts of paleohydrological changes on n-alkane biomarker compositions of a Holocene peat sequence in the eastern European Russian Arctic. Organic Geochemistry. 42, 1065–1075.

Baker, A., Routh, J., Blaauw, M., Roychoudhury, a. N., 2014. Geochemical records of palaeoenvironmental controls on peat forming processes in the Mfabeni peatland, Kwazulu Natal, South Africa since the Late Pleistocene. Palaeogeography, Palaeoclimatology, Palaeoecology. 395, 95–106.

Bate, G.C., Taylor, R.H., 2008. Sediment salt-load in the St Lucia Estuary during the severe drought of 2002-2006. Environmental Geology. 55 (5), 1089-1098.

Bender, M.M., 1971. Variations in the 13C/12C ratios of plants in relation to the pathway of photosynthetic carbon dioxide fixation. Phytochemistry. 10, 1239–1244.

Blackford, J., 2000. Palaeoclimatic Records from Peat Bogs. Trends in Ecology & Evolution. 15, 193–198.

Bodelier, P.L.E., Laanbroek, H.J., 2004. Nitrogen as a regulatory factor of methane oxidation in soils and sediments. FEMS Microbial Ecology. 47 (3), 265-277.

Bray, E.., Evans, E.., 1961. Distribution of *n*-paraffins as a clue to recognition of source beds. Geochimica et Cosmochimica Acta. 22, 2–15.

Bush, R.T., McInerney, F. A., 2013. Leaf wax *n*-alkane distributions in and across modern plants: Implications for paleoecology and chemotaxonomy. Geochimica et Cosmochimica Acta. 117, 161–179.

Carr, A.S., Boom, A., Grimes, H.L., Chase, B.M., Meadows, M.E., Harris, A., 2014. Leaf wax n-alkane distributions in arid zone South African flora: Environmental controls, chemotaxonomy and palaeoecological implications. Organic Geochemistry. 67, 72–84.

Castañeda, I.S., Werne, J.P., Johnson, T.C., 2007. Wet and arid phases in the southeat African tropics since the Last Glacial Maximum. Geology 35, 823–826.

Cerling, T.E., Harris, J.M., Macfadden, B.J., Leakey, M.G., Quade, J., Eisenmann, V., Ehleringer, J.R., 1997. Global vegetation change through the Miocene / Pliocene boundary. Nature 389, 153–158.

Chase, B.M., Meadows, M.E., 2007. Late Quaternary dynamics of southern Africa's winter rainfall zone. Earth-Science Reviews. 84, 103–138.

Chase, B.M., Thomas, D.S.G., 2007. Multiphase late Quaternary aeolian sediment accumulation in western South Africa: Timing and relationship to palaeoclimatic changes inferred from the marine record. Quaternary International. 166, 29–41.

Chase, B.M., Meadows, M.E., Carr, A.S., Reimer, P.J., 2010. Evidence for progressive Holocene aridification in southern Africa recorded in Namibian hyrax middens: Implications for African Monsoon dynamics and the “African Humid Period”. Quaternary Research. 74, 36–45.

Chase, B.M., Quick, L.J., Meadows, M.E., Scott, L., Thomas, D.S.G., Reimer, P.J., 2011. Late glacial interhemispheric climate dynamics revealed in South African hyrax middens. Geology 39, 19–22.

Chase, B.M., Scott, L., Meadows, M.E., Gil-Romera, G., Boom, A., Carr, A.S., Reimer, P.J., Truc, L., Valsecchi, V., Quick, L.J., 2012. Rock hyrax middens: A palaeoenvironmental archive for southern African drylands. Quaternary Science Reviews. 56, 107–125.

Charman, D.J., Brown, A.D., Hendon, D., Kimmel, A., Karofeld E. 2004. Testing the relationship between Holocene peatland palaeoclimate reconstructions and instrumental data, Quaternary Science Reviews. 23, 137-143.

Chikaraishi, Y., Naraoka, H., 2003. Compound-specific δD–δ13C analyses of *n*-alkanes extracted from terrestrial and aquatic plants. Phytochemistry. 63, 361–371.

Chimner, R.A., Ewel, K.C., 2005. A tropical freshwater wetland: II. Production, decomposition, and peat formation. Wetlands Ecology and Management. 13 (6), 671-684.

Clulow, A.D., Everson, C.S., Mengistu, M.G., Jarmain, C., Jewitt, G.P.W., Price, J.S., Grundling, P., 2012. Measurement and modelling of evaporation from a coastal wetland in Maputaland, South Africa. Hydrology and Earth System Sciences. 16 (9), 3233-3247.

Cranwell, P.A., 1984. Lipid geochemistry of sediments from Upton Broad, a small productive lake. Organic Geochemistry. 7, 25–37.

Cranwell, P.A., Eglinton, G., Robinson, N., 1987. Lipids of aquatic organisms as potential contributors to lacustrine sediments-II. Organic Geochemistry. 11, 513–527.

Eglinton, G., Hamilton, R.J., 1967. Leaf Epicuticular Waxes. Science. 156, 1322–1335.

Ehleringer, J.R., Sage, R.F., Flanagan, L.B., Pearcy, R.W., 1991. Climate change and the evolution of C(4) photosynthesis. Trends in Ecology & Evolution. 6, 95–9.

Ficken, K.J., Li, B., Swain, D.L., Eglinton, G., 2000. An n-alkane proxy for the sedimentary input of submerged / floating freshwater aquatic macrophytes. Organic Geochemistry. 31, 745–749.

Finch, J.M., 2005. Late Quaternary palaeoenvironments of the Mfabeni peatland, northern Kwazulu Natal. MSc Thesis, University of KwaZulu-Natal, Pietermaritzburg.

Finch, J.M., Hill, T.R., 2008. A late Quaternary pollen sequence from Mfabeni Peatland, South Africa: Reconstructing forest history in Maputaland. Quaternary Research. 70 (3), 442-450.

Fogel, M.L., Cifuentes, L.A., 1993. Isotope fractionation during primary production. Organic geochemistry: Principles and applications, 73-98.

Gagosian, R.B., Peltzer, E.T., 1986. The importance of atmospheric input of terrestrial material to deep sea sediments. Organic Geochemistry. 10, 661–669.

Gälman, V., Rydberg, J., De-Luna, S.S., Bindler, R., Renberg, I., 2008. Carbon and nitrogen loss rates during aging of lake sediment: Changes over 27 years studied in varved lake sediment. Limnology and Oceanography. 53 (3), 1076-1082.

Grundling, P.L., 2001. The Quaternary peat deposits of Maputaland, Northern Kwazulu-Natal, South Africa: categorisation, chronology and utilisation. MSc Thesis, University of Johannesburg.

Grundling, P.L., 2004. The role of sea-level rise in the formation of peatlands in Maputaland. [WWW Document]. OceanDocs. URL http://www.oceandocs.org/handle/1834/703 (accessed 10.24.12).

Grundling, P., Grootjans, A.P., Price, J.S., Ellery, W.N., 2013. Development and persistence of an African mire: How the oldest South African fen has survived in a marginal climate. Catena. 110, 176-183.

Haddad, R.I., Martens, C.S., Farrington, J.W., 1992. Quantifying early diagenesis of fatty acids in a rapidly accumulating coastal marine sediment. Organic Geochemistry. 19, 205–216.

Hayes, J.M., Freeman, K.H., Popp, B.N., Hoham, C.H., 1990. Compound-specific isotopic analyses: a novel tool for reconstruction of ancient biogeochemical processes. Organic Geochemistry. 16, 1115–1128.

Holmgren, K., Lee-Thorp, J. a., Cooper, G.R.J., Lundblad, K., Partridge, T.C., Scott, L., Sithaldeen, R., Talma, a. S., Tyson, P.D., 2003. Persistent millennial-scale climatic variability over the past 25,000 years in Southern Africa. Quaternary Science Reviews. 22, 2311–2326.

Holzkämper, S., Holmgren, K., Lee-Thorp, J., Talma, S., Mangini, A., Partridge, T., 2009. Late Pleistocene stalagmite growth in Wolkberg Cave, South Africa. Earth and Planetary Science Letters. 282, 212–221.

Huang, Y., Street-Perrott, F.A., Metcalfe, S.E., Brenner, M., Moreland, M., Freeman, K.H., 2001. Climate Change as the Dominant Control on Glacial-Interglacial Variations in C 3 and C 4 Plant Abundance. Science. 293, 1647–1651.

Immirzi, C.P., Maltby, E., Clymo, R.S., 1992. The global status of peatlands and their role in carbon cycling: A report for the Friends of the Earth. Wetlands Ecosystems Research Group, Department of Geography, University of Exeter, London.

Indermuhle, A., Stocker, T.F., Joos, F., Fischer, H., Smith, H.J., Wahlen, M., Deck, B., Mastroianni, D., Tschumi, J., Blunier, T., Meyer, R., Stauffer, B., 1999. Holocene carbon-cycle dynamics based on CO2 trapped in ice at Taylor Dome, Antarctica. Nature 398, 121–126.

Jeffries, H.P., 1972. Fatty-acid ecology of a tidal marsh. Limnology and Oceanography. 17, 433–440.

Jones, M.C., Peteet, D.M., Sambrotto, R., 2010. Late-glacial and Holocene δ15N and δ13C variation from a Kenai Peninsula, Alaska peatland. Palaeogeography, Palaeoclimatology, Palaeoecology. 293 (1-2), 132-143.

Kawamura, K., Ishiwatari, R., 1981. Polyunsaturated fatty acids in lacustrine sediment as a possible indicator of paleoclimate. Geochimica et Cosmochimica Acta. 45, 149–155.

Kelbe, B., Rawlins, B., 1993. Geohydrology of the eastern shores of St Lucia, in: Taylor, R.H. (Ed.), Proceedings of the Workshop on Water Requirements for Lake St Lucia. Department of Environmental Affairs, Pretoria, South Africa, pp. 32–38.

Khon, V.C., Wang, Y. V, Krebs-Kanzow, U., Kaplan, J.O., Schneider, R.R., Schneider, B., 2014. Climate and CO2 effects on the vegetation of southern tropical Africa over the last 37,000 years. Earth and Planetary Science Letters. 403, 407–417.

Kristen, I., Wilkes, H., Vieth, a., Zink, K.-G., Plessen, B., Thorpe, J., Partridge, T.C., Oberhänsli, H., 2010. Biomarker and stable carbon isotope analyses of sedimentary organic matter from Lake Tswaing: evidence for deglacial wetness and early Holocene drought from South Africa. Journal of Paleolimnology. 44, 143–160.

Lee-Thorp, J.A., Holmgren, K., Lauritzen, S.E., Linge, H., Moberg, A., Partridge, T.C., Stevenson, C., Tyson, P.D., 2001. Rapid climate shifts in the southern African interior throughout the mid to late Holocene. Geophysical Research Letters. 28, 4507–4510.

Matsuda, H., Koyama, T., 1977a. Early diagenesis of fatty acids in lacustrine sediments—I. Identification and distribution of fatty acids in recent sediment from a freshwater lake. Geochimica et Cosmochimica Acta. 41, 777–783.

Matsuda, H., Koyama, T., 1977b. Early diagenesis of fatty acids in lacustrine sediments—II. A statistical approach to changes in fatty acid composition from recent sediments and some source materials. Geochimica et Cosmochimica Acta. 41, 1825–1834.

Meadows, M., 2001. The role of Quaternary environmental change in the evolution of landscapes: case studies from southern Africa. Catena. 42, 39–57.

Meadows, M.E., Baxter, A.J., 1999. Late Quaternary palaeoenvironments of the southwestern Cape, South Africa: A regional synthesis. Quaternary International. 57-58, 193–206.

Meadows, M., Baxter, A., Parkington, J., 1996. Late Holocene environments at Verlorenvlei, Western Cape Province, South Africa. Quaternary International. 33, 81–95.

Meyers, P. A., 1994. Preservation of elemental and isotopic source identification of sedimentary organic matter. Chemical Geology. 114, 289–302.

Meyers, P. A., 1997. Organic geochemical proxies of paleoceanographic, paleolimnologic, and paleoclimatic processes. Organic Geochemistry. 27, 213–250.

Meyers, P. A., 2003. Applications of organic geochemistry to paleolimnological reconstructions: A summary of examples from the Laurentian Great Lakes. Organic Geochemistry. 34, 261–289.

Meyers, P. A., Ishiwatari, R., 1993. Lacustrine organic geochemistry—an overview of indicators of organic matter sources and diagenesis in lake sediments. Organic Geochemistry. 20, 867–900.

Meyers, P.A., Kawka, O.E., 1984. Geolipid, pollen and diatom stratigraphy in postglacial lacustrine sediments. Organic Geochemistry. 6, 727–732.

Moore, T., Basiliko, N. 2006. Decomposition, In Boreal Peatland Ecosystems, Wieder, R.K., Vitt, D.H. (eds.), Ecological Studies Vol. 188, Springer-Verlag, Berlin, pp. 126-143.

Moore, T.R., Dalva, M. 1993. The influence of temperature and water table position on carbon dioxide and methane emissions from laboratory columns of peatland soils, Journal of Soil Science. 44, 651-661.

Mucina, L., Adams, J.B., Knevel, I.C., Rutherford, M.C., Powrie, L.W., Bolton, J.J., van der Merwe, J.H., Anderson, R.J., Bornman, T.G., le Roux, A., Janssen, J.A.M., 2006. Coastal Vegetation of South Africa, in: Mucina, L., Rutherford, M.C. (Eds.), The vegetation of South

Africa, Lesotho and Swaziland. South African National Biodiversity Institute, Pretoria, pp. 658-696.

Nash, D.J., Meadows, M.E., 2012. Africa, in: Metcalfe, S.E., Nash, D.J. (Eds.), Quaternary Environmental Change in the Tropics. John Wiley and Sons, Ltd., UK, pp. 79–150.

Neumann, F.H., Stager, J.C., Scott, L., Venter, H.J.T., Weyhenmeyer, C., 2008. Holocene vegetation and climate records from Lake Sibaya, KwaZulu-Natal (South Africa). Review of Palaeobotany and Palynology. 152, 113–128.

Neumann, F.H., Scott, L., Bousman, C.B., van As, L., 2010. A Holocene sequence of vegetation change at Lake Eteza, coastal KwaZulu-Natal, South Africa. Review of Palaeobotany and Palynology. 162, 39–53.

Nichols, J.E., Booth, R.K., Jackson, S.T., Pendall, E.G., Huang, Y., 2006. Paleohydrologic reconstruction based on *n*-alkane distributions in ombrotrophic peat. Organic Geochemistry. 37, 1505–1513.

Nichols, J.E., Walcott, M., Bradley, R., Pilcher, J., Huang, Y., 2009. Quantitative assessment of precipitation seasonality and summer surface wetness using ombrotrophic sediments from an Arctic Norwegian peatland. Quaternary Research. 72, 443–451.

Norström, E., Scott, L., Partridge, T.C., Risberg, J., Holmgren, K., 2009. Reconstruction of environmental and climate changes at Braamhoek wetland, eastern escarpment South Africa, during the last 16,000 years with emphasis on the Pleistocene-Holocene transition. Palaeogeography, Palaeoclimatology, Palaeoecology. 271, 240–258.

O'Leary, M.H., 1988. Carbon isotopes in photosynthesis. Bioscience. 38: 328-451.

Orme A R (1990) Wetland morphology, hydrodynamics and sedimentation. In:

Williams M (ed) Wetlands: a threatened landscape. Basil, Blackwell, pp 42–94.

Page, S.E., Rieley, J.O., Banks, C.J., 2011. Global and regional importance of the tropical peatland carbon pool. Global Change Biology. 17 (2), 798-818

Partridge, T.C., 2002. Were Heinrich events forced from the southern hemisphere? South African Journal of Science. 98, 43–46.

Porat, N., Botha, G., 2008. The luminescence chronology of dune development on the Maputaland coastal plain, southeast Africa. Quaternary Science Reviews. 27 (9-10,) 1024-1046.

Preston-Whyte, R.A., Tyson, P.D., 1998. The atmosphere and weather of southern Africa. Oxford University Press, South Africa.

Quick, L.J., Meadows, M.E., Bateman, M.D., Kirsten, K.L., Mäusbacher, R., Haberzettl, T., Chase, B.M., 2015a. Vegetation and climate dynamics during the last glacial period in the fynbos-afrotemperate forest ecotone, southern Cape, South Africa. Quaternary International. doi:10.1016/j.quaint.2015.08.027

Quick, L.J., Carr, A.S., Meadows, M.E., Boom, A., Bateman, M.D., Roberts, D.L., Reimer, P.J., Chase, B.M., 2015b. A late Pleistocene-Holocene multi-proxy record of palaeoenvironmental change from Still Bay, southern Cape Coast, South Africa. Journal of Quaternary Science. 30, 870–885.

Ramsay, P.J., Cooper, J. a G., 2002. Late Quaternary Sea-Level Change in South Africa. Quaternary Research. 57, 82–90. doi:10.1006/qres.2001.2290Rawlins, B.K., Kelbe, B.E., 1991. Case study on the hydrological response of a shallow coastal aquifer to afforestation, in: Vienna Symposium. pp. 357 – 366.

Rieley, G., Collier, R.J., Jones, D.M., Eglinton, G., Eakin, P.A., Fallick, A.E., 1991. Sources of sedimentary lipids deduced from stable carbon-isotope analyses of individual compounds. Nature. 352, 425–427.

Rieley J.O., Ahmad-Shah A.A., Brady M.A., 1996. The extent and nature of tropical peat swamps - Tropical Lowland Peatlands of Southeast Asia. In: Maltby E., Immirzi C.P., Safford R.J. (Eds.), Tropical Lowland Peatlands of Southeast Asia -proceedings of a workshop on integrated planning and management of tropical lowland peatlands: workshop on integrated planning and management of tropical lowland peatlands. IUCN, Gland, Switzerland.

Roberts, D.L., Botha, G.A., Maud, R.R. and Pether, J. 2006, "Coastal Cenozoic Deposits" in Geology of South Africa, eds. M.R. Johnson and Anhaeusser, C.R. and Thomas, R.J., 1st edn, Geological Society of South Africa / Council of Geosciences, Johannesburg / Pretoria, pp. 605-628.

Scott, L., 2002. Grassland development under glacial and interglacial conditions in southern Africa: Review of pollen, phytolith and isotope evidence. Palaeogeography, Palaeoclimatology, Palaeoecolgy. 177, 47–57.

Scott, L., Holmgren, K., Partridge, T.C., 2008. Reconciliation of vegetation and climatic interpretations of pollen profiles and other regional records from the last 60 thousand years in the Savanna Biome of Southern Africa. Palaeogeography. Palaeoclimatology. Palaeoecology. 257, 198–206.

Sageman, B. B., Lyons, T. W., 2003. Geochemistry of fine-grained sediments and sedimentary rocks, in Treatise on Geochemistry, vol. 7, edited by F. Mackenzie, pp. 115– 158, Elsevier, New York.

Schefuß, E., Schouten, S., Schneider, R.R., 2005. Climatic controls on central African hydrology during the past 20,000 years. Nature. 437, 1003–1006.

Schefuß, E., Ratmeyer, V., Stuut, J.B.W., Jansen, J.H.F., Sinninghe Damsté, J.S., 2003. Carbon isotope analyses of n-alkanes in dust from the lower atmosphere over the central eastern Atlantic. Geochimica et Cosmochimica Acta. 67, 1757–1767.

Skrzypek, G., Paul, D., Wojtun, B., 2008. Stable isotope composition of plants and peat from Arctic mire and geothermal area in Iceland. Polish Polar Research. 29 (4), 365-376.

Skrzypek, G., Jezierski, P., Szynkiewicz, A., 2010. Preservation of primary stable isotope signatures of peat-forming plants during early decomposition - observation along an altitudinal transect. Chemical Geology. 273, 238–249.

Strack, M., 2008. Peatlands and climate change. International Peat Society, Jyvaskyla, Finland

Stock, W.D., Chuba, D.K., Verboom, G. a., 2004. Distribution of South African C3 and C4 species of Cyperaceae in relation to climate and phylogeny. Austral Ecology. 29, 313–319.

Stokes, S., Thomas, D.S.G., Washington, R., 1997. Multiple episodes of aridity in southern Africa since the last interglacial period. Nature. 388, 154–158.

Talma, A.S., Vogel, J.C., 1992. Late Quaternary paleotemperatures derived from a speleothem from Cango Caves, Cape Province, South Africa. Quaternary Research. 37, 203–213.

Taylor, R., Kelbe, B., Haldorsen, S., Botha, G. a., Wejden, B., Været, L., Simonsen, M.B., 2006. Groundwater-dependent ecology of the shoreline of the subtropical Lake St Lucia estuary. Environmental Geology. 49, 586–600.

Tyson, P.D., Preston-Whyte, R.A., 2000. The Weather and Climate of Southern Africa, 2nd ed. Oxford University Press Incorporated, Cape Town, South Africa.

Vaeret, L., Sokolic, F., 2009. Methods for studying the distribution of groundwater-dependent wetlands: a case study from Eastern Shores, St Lucia, South Africa, in: Responses to global change and management actions in coastal groundwater resources, Norwegian University of Life Sciences.

Valsecchi, V., Chase, B.M., Slingsby, J. a., Carr, A.S., Quick, L.J., Meadows, M.E., Cheddadi, R., Reimer, P.J., 2013. A high resolution 15,600-year pollen and microcharcoal record from the Cederberg Mountains, South Africa. Palaeogeography, Palaeoclimatology, Palaeoecology. 387, 6–16.

Venter, C.E., 2003. Vegetation ecology of Mfabeni peat swamp, St Lucia, MSc, KwaZulu-Natal. University of Pretoria.

Vogel, J.C., Fuls, A., R.P., E., 1978. The geographical distribution of Kranz grasses in South Africa. South African Journal of Science. 58, 373 – 377.

Volkman, J.K., Barrett, S.M., Blackburn, S.I., 1999. Eustigmatophyte microalgae are potential sources of C29 sterols, C22–C28 *n*-alcohols and C28–C32 *n*-alkyl diols in freshwater environments. Organic Geochemistry. 30, 307–318.

Vrdoljak, S.M., Hart, R.C., 2007. Groundwater seeps as potentially important refugia for freshwater fishes on the Eastern Shores of Lake St Lucia, KwaZulu-Natal, South Africa. African Journal of Aquatic Science. 32 (2), 125-132.

Walther, S.C., Neumann, F.H., 2011. Sedimentology, isotopes and palynology of late Holocene cores from Lake Sibaya and the Kosi Bay system (KwaZulu-Natal, South Africa). South African Geographical Journal. 93, 133–153.

Xue, J., Zhong, W., Cao, J., 2014. Changes in C3 and C4 plant abundances reflect climate changes from 41,000 to 10,000yr ago in northern Leizhou Peninsula, South China. Palaeogeography, Palaeoclimatology, Palaeoecology, 396, 173–182.

Yamamoto, S., Kawamura, K., Seki, O., Meyers, P. a., Zheng, Y., Zhou, W., 2010. Environmental influences over the last 16ka on compound-specific δ13C variations of leaf wax n-alkanes in the Hani peat deposit from northeast China. Chemical Geology. 277, 261–268.

Zheng, Y., Zhou, W., Meyers, P. A., Xie, S., 2007. Lipid biomarkers in the Zoigê-Hongyuan peat deposit: Indicators of Holocene climate changes in West China. Organic Geochemistry. 38, 1927–1940.

Zhou, W., Xie, S., Meyers, P. A., Zheng, Y., 2005. Reconstruction of late glacial and Holocene climate evolution in southern China from geolipids and pollen in the Dingnan peat sequence. Organic Geochemistry. 36, 1272–1284.

Zhou, W., Zheng, Y., Meyers, P. A., Jull, a. J.T., Xie, S., 2010. Postglacial climate-change record in biomarker lipid compositions of the Hani peat sequence, Northeastern China. Earth and Planetary Science Letters. 294, 37–46.

CHAPTER 2:

Geochemical records of palaeoenvironmental controls on peat forming processes in the Mfabeni peatland, KwaZulu Natal, South Africa since the Late Pleistocene

A presentation of the research paper

This paper was published by the research journal *Palaeogeography, Palaeoclimatology, Palaeoecology* in January 2014. I am the first author with Dr Joyanto Routh, Dr Maarten Blaauw and Prof Alakendra Roychoudhury being co-authors.

Dr Routh and I were responsible for extracting the 810 cm long core from the Mfabeni peatland. I was responsible for describing, processing and preparing the 1 – 2 cm sample intervals and commissioned the geochemical analysis, which included elemental and stable isotope analysis by the isotope lab at the Department of Archaeology, University of Cape Town and ^{14}C dating at the Poznań Radiocarbon Laboratory, Poland. The uncalibrated ages were then converted to calibrated dates on the Bacon software and the age-depth model was produced by Dr Blaauw. I was responsible for the data processing, generation of all the figures and data tables, concept design and write up of the article. The manuscript was revised and improved based on oral and written feedback from Dr Routh. Prof Roychoudhury and Dr Blaauw assisted in the final editing of the manuscript.

Geochemical records of palaeoenvironmental controls on peat forming processes in the Mfabeni peatland, KwaZulu Natal, South Africa since the Late Pleistocene

A. Baker[a], J. Routh[b*], M. Blaauw[c], A.N. Roychoudhury[a]

[a]Department of Earth Sciences, Stellenbosch University, Private Bag X1, Matieland, 7600, South Africa

[b]Department of Water and Environmental Studies, Linköping University, 581 83 Linköping, Sweden

[c]School of Geography, Archaeology and Palaeoecology, Queen's University Belfast, Belfast BT7 1NN, U.K.

Abstract

The Mfabeni peatland is the only known sub-tropical coastal fen that transcends the Last Glacial Maximum (LGM). This ca. 10 m thick peat sequence provides a continuous sedimentation record spanning from the late Pleistocene to present (basal age ca. 47 kcal yr BP). We investigated the palaeoenvironmental controls on peat formation and organic matter source input at the Mfabeni fen by: 1) exploring geochemical records (mass accumulation rate, total organic carbon, carbon accumulation rate, $\delta^{13}C$, $\delta^{15}N$ and C/N ratio) to delineate primary production, organic matter source input, preservation and diagenetic processes, and 2) employ these geochemical signatures to reconstruct the palaeoenvironmental conditions and prevailing climate that drove carbon accumulation in the peatland. We established that the Mfabeni peat sediments have undergone minimal diagenetic alteration. The peat sequence was divided into 5 linear sedimentation rate (LSR) stages indicating distinct changes in climate and hydrological conditions: *LSR stage 1* (ca. 47 to ca. 32.2 kcal yr BP): predominantly cool and wet climate with C4 plant assemblages, interrupted by two short warming events. *LSR stage 2* (ca. 32.2 to ca. 27.6 kcal yr BP): dry and

windy climate followed by a brief warm and wet period with increased C4 sedge swamp vegetation. *LSR stage 3* (ca. 27.6 to ca. 20.3 kcal yr BP): initial cool and wet period with prevailing C4 sedge plant assemblage until ca. 23 kcal yr BP; then an abrupt change to dry and cool glacial conditions and steady increases in C3 grasses. *LSR stage 4* (ca. 20.3 to ca. 10.4 kcal yr BP): continuation of cool and dry conditions and strong C3 grassland signature until ca. 15 kcal yr BP, after which precipitation increases. *LSR stage 5* (ca. 10.4 kcal yr BP to present): characterized by extreme fluctuations between pervasive wet and warm to cool interglacial conditions with intermittent abrupt millennial-scale cooling/drying events and oscillations between C3 and C4 plant assemblages. In this study we reconstructed a high-resolution record of local hydrology, bulk plant assemblage and inferred climate since the Late Pleistocene, which suggest an anti-phase link between Southern African and the Northern Hemisphere, most notably during Heinrich (5 to 2) and Younger Dryas events.

1. Introduction

Peatlands play a pivotal role in the global carbon (C) cycle, serving as a direct link between the short-term (atmosphere, biosphere and hydrosphere) and long-term (geosphere) carbon reservoirs. Under sequestering conditions, peatlands serve as sinks for atmospheric CO_2, important sources of CH_4 and exporters of fluvial dissolved and particulate organic carbon to down-stream ecosystems (Worrall et al., 2003). The balance between ecosystem productivity and respiration, controlled primarily by precipitation, temperature, water table fluctuation and local topography, determines if a peatland acts as a C sink or source.

Contemporary global peatland C stocks have been estimated to be in excess of 450 Petagrams (1 Pg = 10^{15}g), equivalent to 75% of CO_2 stored in the atmosphere at any given time (Strack, 2008). The vast majority (~90%) of peatlands are found in the Northern Hemisphere temperate and boreal regions, with tropical and sub-tropical peatlands constituting the balance (Immirzi et al., 1992; Page et al., 2011). However, because of their relatively higher carbon accumulation rate (CAR; Chimner and Ewel, 2005; Strack, 2008), tropical peatlands are estimated to represent up to a quarter of the potential global peatland C stock (Strack, 2008; Page et al., 2011), and they are at a

greater risk of degradation and overexploitation due to their proximity to populated areas and climate change (Rieley et al., 1996). Currently, there is limited scientific understanding of the processes that regulate C cycling and accumulation in tropical peatlands (Chimner and Ewel, 2005), and how changing climate and increasing anthropogenic pressures will affect low latitude peatland systems and their ability to sequester C.

Southern Africa is situated at the interface of tropical and temperate climate systems. The region is influenced by the largest asymmetrical cross-continental tropical convection (Stokes et al., 1997) as a consequence of seasonal fluctuations in the Inter Tropical Convergence Zone (ITCZ), and large temperature gradients between the warm Agulhas and cold Benguela oceanic currents (Preston-Whyte and Tyson, 1998; Tyson and Preston-Whyte, 2000). Due to the topography and semi-arid climate of Southern Africa, archives are not commonly preserved, and few continuous palaeoenvironment records exist (Chase and Meadows, 2007), despite strong evidence of climate variability from Antarctic ice cores and low latitude African hydrological investigations (Bard et al., 1997; Blunier et al., 1998; Gasse, 2000; Stocker, 2000; Stenni et al., 2001). A few detailed limnology studies have been undertaken in regional lakes (Meadows et al., 1996; Meadows and Baxter, 1999; Partridge, 2002; Kristen et al., 2010), but due to the fact that most of southern Africa is water scarce, freshwater lakes are uncommon. Speleothem archives from South African caves have yielded high-resolution climate records (Talma and Vogel, 1992; Lee-Thorp et al., 2001 Holmgren et al., 2003; Holzkämper et al., 2009), but these records either do not span the Last Glacial Maximum (LGM) or are incomplete with at least one or more hiatuses of between 2.5 and 10 kyr. Several palynology studies have been undertaken in regional coastal peatlands and hyrax midden deposits (Finch and Hill, 2008; Neumann et al., 2008, 2010; Walther et al., 2011; Valsecchi et al., 2013) however, with the exception of the Mfabeni peatland study (Finch and Hill, 2008) the palynology records are limited to the deglacial and Holocene periods. To our knowledge, the only geochemical palaeoclimatic study undertaken on the sub-tropical Braamhoek peatland in the austral summer rainfall region of South Africa is by Norström et al. (2009). This inland wetland is located on the Eastern escarpment at 1700 m a.s.l. and lies over 290 km from the nearest coastline with a palaeorecord extending only as far back as ca. 16 kcal yr BP.

The lack of high-resolution terrestrial palaeoclimate records on the African sub-continent continues to hinder the understanding of past climate forcing factors and their environmental impacts (Chase and Meadows, 2007; Gasse et al., 2008). Additional high resolution multi-proxy and multi-archive studies are therefore needed to elucidate past climate fluctuations and modelling of the ensuing environmental responses to these changes in the future. In this context, organic matter (OM) rich peat deposits are ideally suited for palaeoenvironmental studies as they are well preserved archives that are subject to mainly autochthonous depositional regimes that are largely regulated by climate (Strack, 2008). The aim of this research is to investigate climatic and environmental conditions that have prevailed in the southern African region since the Late Pleistocene. Our objective is to reconstruct the palaeoenvironmental controls on past C accumulation and OM source input at the sub-tropical coastal Mfabeni fen by: 1) delineating primary production, OM source input, OM preservation and diagenetic processes which affected the formation of these peat deposits, and 2) using multiple geochemical proxy signatures such as, mass accumulation rate (MAR), total organic carbon (TOC), carbon accumulation rate (CAR), $\delta^{13}C$, $\delta^{15}N$ and C/N, to reconstruct the palaeoenvironmental conditions and prevailing climate in the peatland over the last ca. 47 kcal yr BP.

2. Methods

2.1. Site description

St Lucia is one of the largest estuarine systems on the African continent (Vrdoljak and Hart, 2007). It falls within the UNESCO World Heritage iSimangaliso Wetland Park, situated on the northern shores of Kwazulu-Natal province, South Africa (Fig. 1). Lake St Lucia, the dominant north-south aligned water body, has an extent of 350 km^2 and an average depth of only 90 cm. At its northern end, the lake is fed by four regional rivers with a combined catchment of approximately 6085 km^2, namely the uMkhuze, Nyalazi, Mzinene and Hluhluwe rivers. To the south, a narrow 22 km long

waterway sporadically links the lake to the Indian Ocean, and to the east the lake is fed with fresh water by the large Maputuland unconfined aquifer (Kelbe et al., 1995; Taylor et al., 2006a).

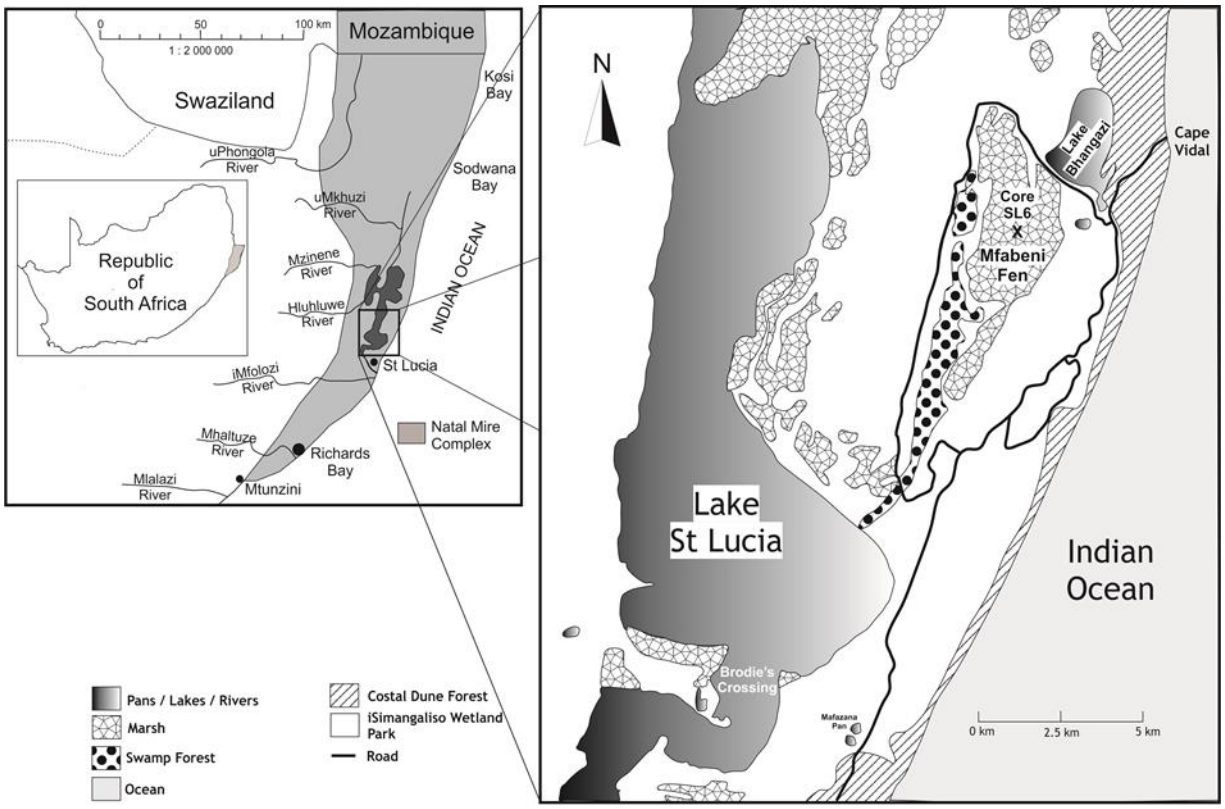

Figure 1: Mfabeni Peatland, iSimangaliso Wetland Park, St Lucia, northern KwaZulu Natal, South Africa with major habitat groups and dominant water bodies represented.

The Mfabeni fen lies within an interdunal valley (Botha and Porat, 2007) on the eastern shores of Lake St Lucia, running parallel to the coastline and measuring ca. 10 x 3 km (Clulow et al., 2012; Grundling et al., 2013), and thickness of up to ca. 11 m (Grundling, 2001; Grundling et al., 2013). The hydrological regime of the fen is controlled by local precipitation and circum-neutral Ca^{2+} and HCO_3^- dominated groundwater emanating from the Maputaland aquifer (Venter, 2003; Taylor et al., 2006b; Grundling et al., 2013). The region lies within a humid, sub-tropical climate which experiences primarily austral summer rainfall of between 900 and 1200 mm/yr (Grundling, 2001; Taylor et al., 2006a). However, modern rainfall data indicate distinctive wet and dry cyclical events which can effectively halve the annual precipitation for extended periods (Bate and Taylor, 2008). The surface waters on the eastern part of the minerotrophic Mfabeni peatland drain northwards

into the southern part of Lake Bhangasi, while the western sections drain southwards into Lake St Lucia (Grundling, 2001; Clulow et al., 2012).

The Mfabeni fen forms part of the greater Natal Mire Complex (NMC; Fig. 1) that extends from southern Mozambique to the south of Richards Bay, Kwazulu-Natal (Smuts, 1992). The NMC falls within the Maputaland group of coastal Cenozoic deposits, constrained in the west by the Lebomobo monocline, uPongola and uMkhuze River valleys (Botha and Porat, 2007). The Mfabeni peatland accumulated by valley infilling on a lacustrine or intertidal non-permeable clay layer (Grundling et al., 2013) within the reworked late Pleistocene KwaMbonanbi Formation coastal dune depression (Smuts, 1992), as a consequence of blockage of the Nkazana palaeo-channel and sustained groundwater input from the Maputaland aquifer (Grundling et al., 2013).

The iSimangaleso wetland park encompasses several heterogeneous habitats, mainly as a response to topography, hydrology and historical land use (Vrdoljak and Hart, 2007). Mucina et al. (2006) broadly categorised the wetland habitats as Maputaland wooded grassland, coastal belt and sub-tropical freshwater wetlands surrounded by northern coastal forests.

The Mfabeni fen vegetation is largely represented by herbaceous reed sedge vegetation (Finch, 2005), and is dominated by *Rhynchospora holoschoenoide, Fimbristylis bivalve, Panicum glandulopaniculatum* and *Ischaemum fasciculatum* (Lubke et al., 1992; Vaeret and Sokolic, 2008).

2.2. Sampling techniques

A 810 cm long sediment core, SL6, was extracted from the middle of the peatland (28.15021°S; 32.52508°E) using a 5 cm diameter x 50 cm length Russian peat corer in June 2011. The core was logged in the field and described and sectioned into 1–2 cm increments in the laboratory. All samples were weighed before freeze-drying, then again afterwards to calculate bulk density and porosity of each segment.

2.3. Radiocarbon dating / age model

Evenly spaced samples were sent for ^{14}C dating at the Poznań Radiocarbon Laboratory, Poland. The sediments were chemically pre-treated as described by Brock et al. (2010) with the exception

of using 0.25M instead of 1M HCl; samples SL1 31-32 and SL4 89-90 were not treated with NaOH due to their low carbon content. The samples were combusted with CuO and Ag wool at 900^0C for 10 hrs and the CO_2 was reduced to pure graphite in a vacuum line as described by Czernik and Goslar (2001). Coal or IAEA C1 Carrara Marble and international modern Oxalic Acid II standards were subjected to the same pre-treatment and combustion procedure. The ^{14}C content of the samples were measured on a Compact Carbon AMS (National Electrostatics Corporation, USA) as described by Goslar et al. (2004). The conventional ^{14}C age was calculated using a correction factor for isotopic fractionation as per Stuiver and Polach (1977).

Since the ages of some of the ^{14}C dates lie beyond the limit of the southern hemisphere calibration curve (McCormac et al., 2004), dates were calibrated using the Northern hemisphere terrestrial calibration curve IntCal09 (Reimer et al., 2006) while applying a southern hemisphere offset of 40 ±20 ^{14}C years (McCormac et al., 1998). Post-bomb ages were calibrated using the southern hemisphere post-bomb curve of Hua and Barbetti (2004). All ages were adjusted within the Bayesian framework, using age-depth modelling software Bacon (Blaauw and Christen, 2011). This method divides a core into sections and models the accumulation rate for each of these sections. Accumulation rates were constrained by prior information (here a gamma distribution with mean 50 yr/cm and shape 1.5), and the variability of accumulation rate from one depth to the next was constrained by a 'memory' parameter (here using the default beta distribution with mean 0.7 and strength 4). Stable runs were obtained using multiple Markov Chain Monte Carlo (MCMC) iterations.

2.4. Elemental and stable isotope analyses

Selection of acid treated and raw samples were analysed for C and N stable isotopes composition and elemental ratios at the Department of Archaeology, University of Cape Town. Peat samples were combusted in a Thermo Scientific Flash 2000 organic elemental analyser, coupled to a Thermo Scientific Delta V Plus isotope ratio mass spectrometer via a Thermo Scientific Conflo IV gas control unit (detection limit 5µg). The sand samples (low C and N wt%) were combusted in a Thermo Finnigan Flash EA 1112 series elemental analyzer, coupled to a Thermo electron Delta

Plus XP isotope ratio mass spectrometer via a Thermo Finnigan Conflo III gas control unit (detection limit 15 µg). In-house standards used were: chocolate/egg mixture, Australian National University sucrose, Merck proteinaceous gel and dried lentils, calibrated against International Atomic Energy Agency standards (N1, N2, NBS 18, 19, SMOW and SLAP). The precision for both analytical systems was 0.05 and 0.08‰ for N and C, respectively. Nitrogen (N) isotopic composition is expressed relative to atmospheric N, whereas C is expressed relative to Pee-Dee Belemnite.

2.5. C3/C4 plant mass balance

To broadly gauge the relative proportions of C input from C4 and C3 plants during peat accumulation in Mfabeni, a mass balance equation was used as per Gillson et al. (2004) and Boutton et al. (1998):

$$\delta^{13}C_{SOM} = (\delta^{13}C\ C4_{plants})\ (x) + (\delta^{13}C\ C3_{plants})\ (1-x) \qquad \textbf{(Equation 1)}$$

Where:
- $\delta^{13}C_{SOM}$ bulk stable carbon isotope composition of C_{org} in sample
- $\delta^{13}C\ C4_{plants}$ and $\delta^{13}C\ C3_{plants}$ are the average stable C isotope values from regional C4 (-13.2‰) and C3 (-27.5‰) vegetation (Muzuka, 1999).
- x is the proportion of C from C4 plant sources and (1-x) the proportion of C from C3 plants.

3. Results

3.1. Core description

Core SL6 consists of 7 different sediment types (Fig. 2), dominated by peat with occasional sandy lenses of varying thicknesses: black fine-grained amorphous peat (810-610 cm), dark brown fine-grained peat with grey sand mottled zones (610 – 535 cm), black fine-grained peat with grey sand mottled zones (535 – 440 cm), black fine-grained amorphous peat with increasing sandy texture with depth (440 - 340 cm), black fined-grained amorphous peat with minimal rootlets (340 - 110

cm), black fine-grained amorphous peat, with extensive rootlets (110 - 61 cm), and dark brown "fibrous" peat transitioning to fine grained black amorphous peat sediments with depth (61 - 0 cm).

The peat sediments show an average bulk density of 0.29, 0.34, 0.28, 0.28, 0.24 g.cm^{-3} for linear sedimentation rate (LSR, see section 3.2 for explanation) stages 1 to 5, respectively (Table 1). The average core porosity for the dominant peat sediment was calculated to be 0.7.

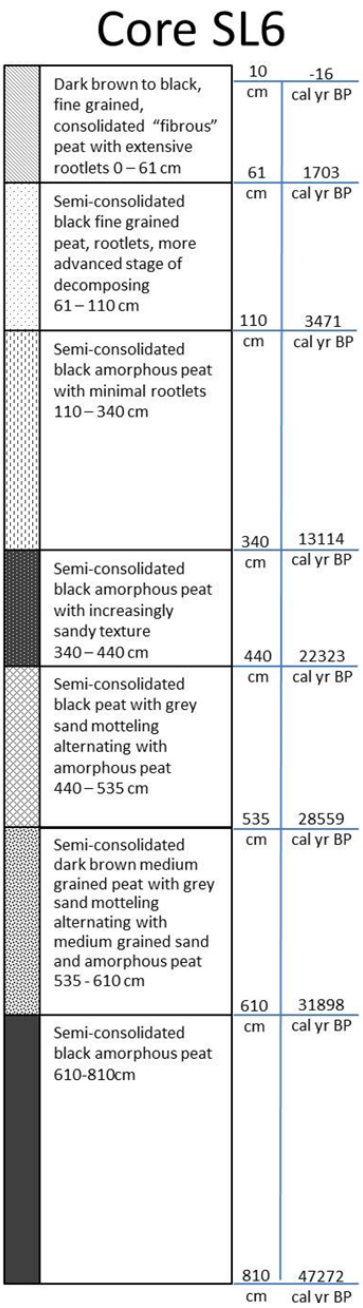

Figure 2: Core SL6 stratigraphic profile with modelled ages

3.2. Age model

The SL6 basal age recorded at 805 cm is ca. 47.0 kcal yr BP (Table 2; Fig. 3). Peat sediments dominate (Fig. 2) from the base of the core up to the age of ca. 31.9 kcal yr BP (609 cm). Above this a succession of sand lenses cross cut the core, with relatively low C% up to ca. 28.8 kcal yr BP (540 cm). A fining up transition occurs from "sandy" peat to peaty sediments until a modelled age of ca. 14.3 kcal yr BP (350 cm), after which amorphous peat sediments with increasing rootlet content dominate (340 - 61 cm), ending in the top "fibrous" surface peat layer.

The linear sedimentation rates (LSR) calculated for core SL6 suggests several changes in sedimentation regimes (Fig. 4; Table 1). When a trendline is fitted to grouped data points, the lower third of the core, spanning ca. 47.0 to ca. 32.4 kcal yr BP, displays an average LSR of0.13 mm.yr^{-1} (LSR Stage 1). The average LSR increases to 0.22 mm.yr^{-1} between ca. 32.1 and ca. 27.9 kcal yr BP (LSR Stage 2), declining to 0.14 mm.yr^{-1} (ca. 27.6 to ca. 20.3 kcal yr BP; LSR Stage 3) before dropping to its lowest average rate of 0.10 mm.yr^{-1} between ca. 19.8 and ca. 10.4 kcal yr BP (LSR Stage 4). Thereafter, a marked increase in average LSR to 0.29 mm.yr^{-1} occurs during the Holocene (LSR Stage 5).

3.3. Past sedimentation and C measurements

3.3.1. Mass accumulation rate (MAR)

MAR in core SL6 fluctuates between a minimum of 20.8 (ca. 14.3 kcal yr BP) and a maximum of 103 $g.m^{-2}.yr^{-1}$ (ca. 3.5 kcal yr BP) with a total core MAR average of 57.5 $g.m^{-2}.yr^{-1}$ (Fig. 4 and Table 1). LSR stages 1, 3 and 4 display overall lower than core average MAR values of 37.6, 41.4 and 28.1 $g.m^{-2}.yr^{-1}$, respectively, punctuated by abrupt shifts to above core average MAR values for LSR stages 2 and 5 (76.4 and 70.9 $g.m^{-2}.yr^{-1}$, respectively). LSR stage 5 shows the least consistency with overall elevated MAR values, and short intermittent excursions to below average MAR values at ca. 7.1, ca. 5.3, ca. 4.7 and ca. 1.4 kcal yr BP.

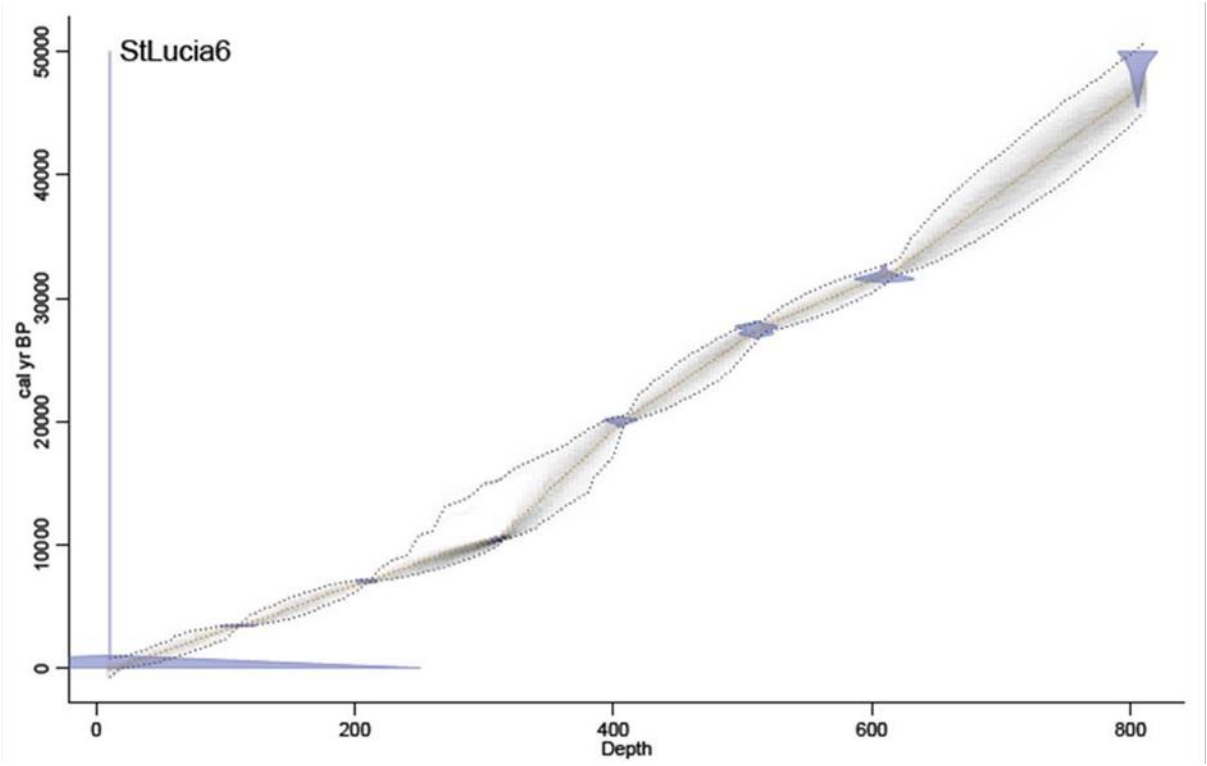

Figure 3: Core SL6 age-depth model with uncertainty ranges. AMS ^{14}C dates were calibrated with IntCal09 curve (Reimer et al., 2006) with a southern Hemisphere offset of ca. 40 ±20 ^{14}C years (McCormac et al., 1998). Postbomb dates calibrated with southern Hemisphere postbomb curve by Hua and Barbetti (2004). All dates were adjusted within the Bayesian framework, using Bacon age depth modelling software (Blaauw and Christen 2011).

Table 1: Sediment properties with averaged accumulation data for the five LSR stages in core SL6

Core #	n	Sediment type	Porosity	Bulk Density g.cm^{-3}	LSR[a] mm.yr^{-1}	MAR[b] g.m^{-2}.yr^{-1}	TOC gC.m^{-2}	C Accumulation g C.m^{-2}.yr^{-1}
Averages								
LSR 1	38	Peat	0.73	0.29	0.13	37.6	1068	13.6
LSR 2	20	Peaty sand	0.64	0.34	0.22	76.4	553	12.4
LSR 3	22	Peat	0.73	0.28	0.15	41.4	896	13.0
LSR 4	20	peat	0.72	0.28	0.10	28.1	711	7.4
LSR 5	98	peat	0.69	0.24	0.29	70.9	1108	32.3

[a] LSR = Linear Sedimentation Rate

[b] MAR = Mass Accumulation Rate

Table 2: Chronology of Mfabeni peatland core SL6 with uncalibrated AMS ^{14}C dates, corresponding percentage total organic carbon (TOC) and bulk stable carbon isotope values

Sample code	Depth (cm)	Material	uncalibrated date	% C	$\delta^{13}C_{TOC}$
SL6 10-11	10	Peat	109 ± 0.35 pMC	45.1	-21.8
SL6 109-110	109	Peat	3240 ± 30 BP	51.9	-16.8
SL6 209-210	209	Peat	6170 ± 30 BP	19.2	-24.5
SL6 309-310	309	Peat	9270 ± 70 BP	37.1	-21.5
SL6 405-406	405	Peat	16940 ± 80 BP	14.7	-19.1
SL6 510-511	510	Peat	22800 ± 130 BP	29.6	-18.6
SL6 609-610	609	Peat	27600 ± 190 BP	22.5	-19.0
SL6 709-710	709	Peat	>48000 BP	28.1	-17.6
SL6 805-806	805	Peat	49000 ± 2200 BP	12.2	-20.1

3.3.2. Total organic carbon (TOC)

The sediment TOC of core SL6, for the most part, trends similarly but opposite to MAR records, fluctuating between a minimum of 9.65 g C.m-2 (ca. 30.4 kcal yr BP) and a maximum of 1600 g C.m-2 (ca. 44.6 kcal yr BP) with a total core average of 981 g C.m-2 (Fig. 4; Table 1). During LSR stage 1, TOC fluctuates dynamically between the core maximum and 327 g C.m-2 at ca. 35.6 kcal yr BP. LSR stage 2 displays the lowest TOC stage average (553 g C.m-2) with the exception of an abrupt increase of 584 g C.m-2 towards the latter part of the stage (28.5 kcal yr BP). LSR stage 3 fluctuates around the core average until a sharp decrease occurs at ca. 22.3 kcal yr BP followed by a relatively low TOC values till ca. 14.3 (350 cm) kcal yr BP. Thereafter TOC increases in the lead

up to and during the Holocene which exhibits the highest stage TOC average (1108 g C.m-2 ; LSR stage 5), , despite sporadic sharp declines associated with increases in MAR at ca. 5.3 kcal yr BP and ca. 7.7 kcal yr BP.

3.3.3. Carbon accumulation rate (CAR)

From the bottom of core SL6 up until ca. 10.2 kcal yr BP, the CAR fluctuates below the total core average of 22.05 g C.m-2.yr-1 (stages 1 – 4 core average = 11.9 g C.m-2.yr-1), with the exception of between ca. 28.6 and ca. 27.9 kcal yr BP where the CAR maximises at just below 28 g C.m-2.yr-1 (Fig. 4; Table 1). The lowest CAR values occur between ca. 30.4 and ca. 30.0 kcal yr BP (LSR stage 2), coinciding with an increase in sand dominated sediments. The top quarter of core SL6 (LSR stage 5) displays an elevated average CAR of 32.3 C.m-2.yr-1 , notwithstanding three sharp declines at ca. 7.1, between ca. 5.5 and ca. 5.3 and ca. 1.4 and ca. 1.3 kcal yr BP.

3.4. Elemental and stable isotopes measurements

3.4.1. C/N ratio

The atomic C/N ratio for core SL6 displays a range of between 16.9 (ca. 1.4 kcal yr BP) and 71.1 (ca. 24.2 kcal yr BP) with a core average of 40.5 (Fig. 5). The C/N ratio at the base starts out below 30.0, but steadily increases to 57.3 at ca. 38.7 kcal yr BP before sharply declining to 37.6 at ca. 37.5 kcal yr BP. The C/N signal then stabilises to between 36 and 52 until ca. 24.5 kcal yr BP, where a significant positive shift occurs to a maximum of 71.1, followed by a return to a below core average of 29.9 at ca. 17.1 kcal yr BP. Thereafter, the C/N signal gradually increases until ca. 1.9 kcal yr BP, where it sharply declines from 57.7 to the core minimum value of 16.9 at ca. 1.4 kcal yr BP.

3.4.2. Stable N isotopes

$\delta^{15}N$ values for core SL6 range between 1.9 (ca. 41.5 kcal yr BP) and -2.9‰ (ca. 0.44 kcal yr BP) and show an overall depletion in ^{15}N up core (Fig. 5). The $\delta^{15}N$ signal shifts to enriched ^{15}N values from the base of the core till the core maximum at ca. 41.5 kcal yr BP. Thereafter, the $\delta^{15}N$ signal steadily trends to depleted ^{15}N values, with the exception of a period of enrichment in ^{15}N between

ca. 30.0 and ca. 24.5 kcal yr BP, and a sharp positive incursion to enriched ^{15}N from -1.5 to 0.9‰ at ca. 1.4 kcal yr BP.

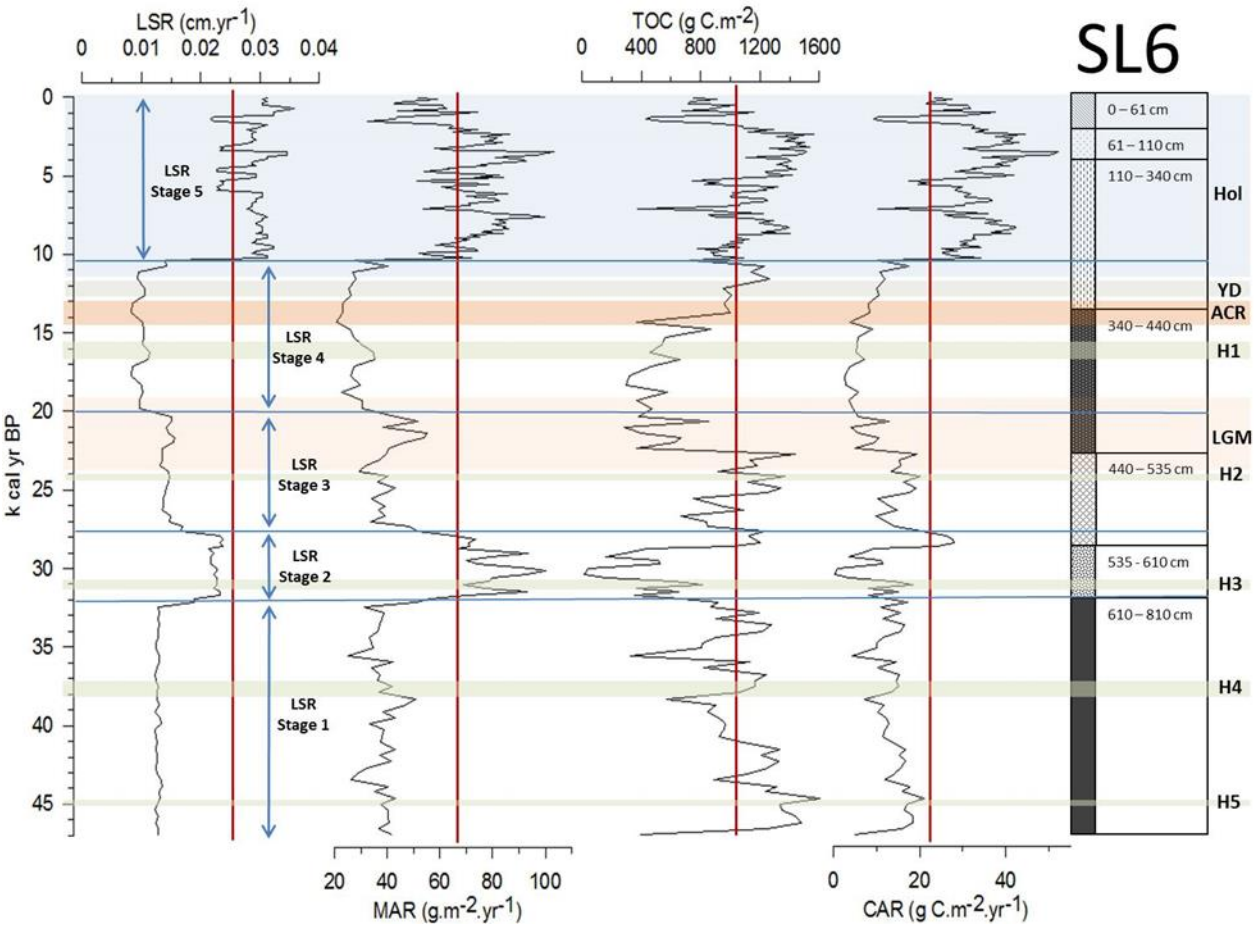

Figure 4: Downcore profile of Core SL6 presenting linear sedimentation rate (LSR), mass accumulation rate (MAR), total organic carbon (TOC) and carbon accumulation rate (CAR) with age and depth. Red line represents total core average. Hol = Holocene, YD = Younger Dryas; H1-5 = Heinrich events, LGM = Last Glacial Maximum. Heinrich dates after Hemming (2004).

3.4.3. Stable C isotopes

$\delta^{13}C$ signal fluctuates between a maximum of -15.5‰ (ca. 24.2 kcal yr BP) and minimum of -25.3 (ca. 9.4 kcal yr BP), with no discernible overall trend (Fig. 5). With the exception of the base interval, the $\delta^{13}C$ signal becomes enriched in ^{13}C up core from -22.9 to -17.4‰ between ca. 46.6 and ca. 38.3 kcal yr BP before sharply decreasing to -22.3‰. Thereafter, the $\delta^{13}C$ signal increases steadily to the core maximum value at ca. 24.2 kcal yr BP, and then declines again to the core minimum at ca. 9.4 kcal yr BP. For the remaining part of the upper core, the $\delta^{13}C$ signal becomes enriched in ^{13}C through a succession of fluctuating cycles displaying pronounced

enrichment shifts in ^{13}C of 4.5‰ (ca. 8.8 to ca. 8.4 kcal yr BP), 8.2‰ (ca. 6.5 to ca. 4.7 kcal yr BP) and 4.5‰ (ca. 1.2 to ca. 0.15 kcal yr BP).

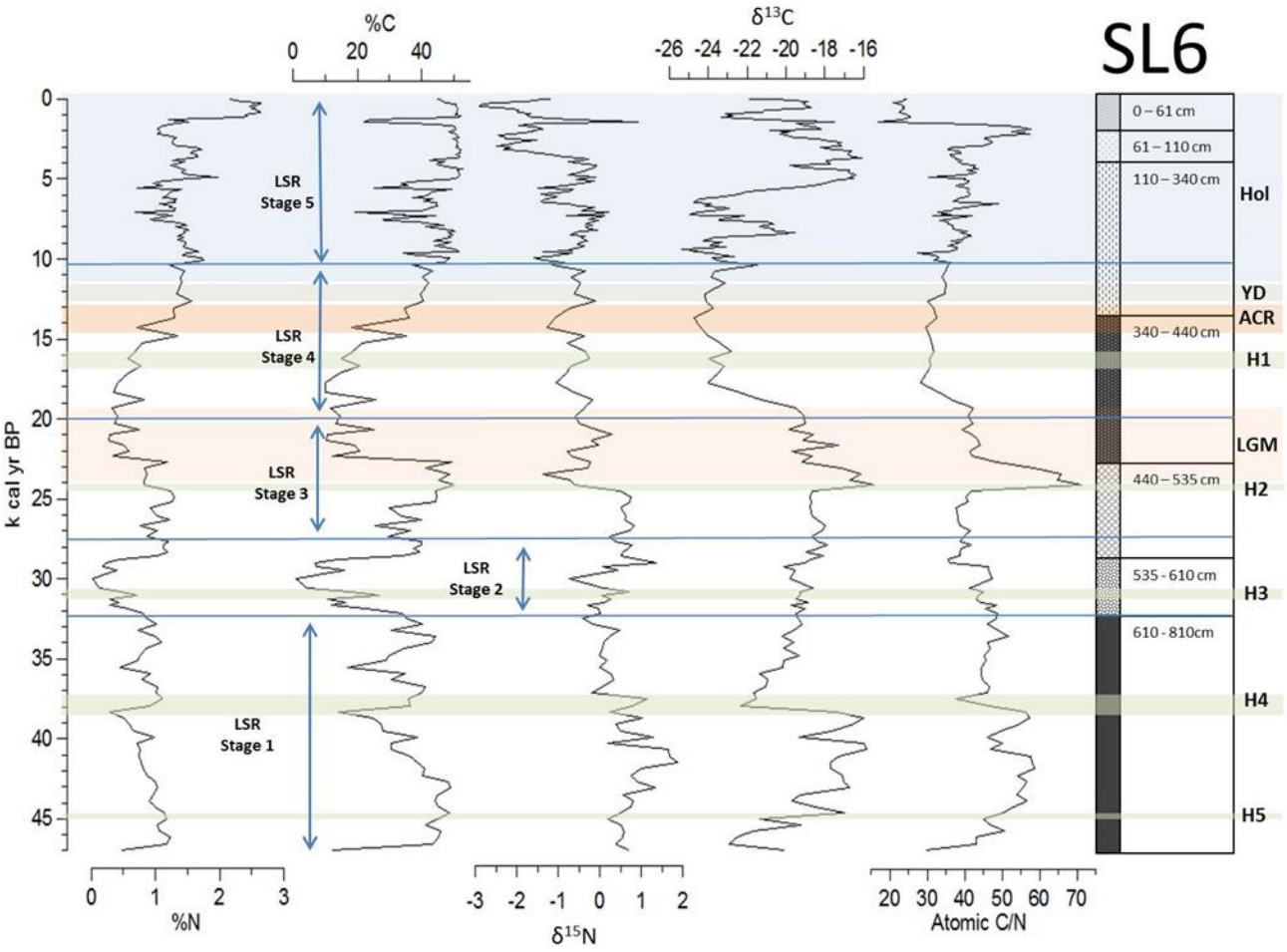

Figure 5: SL6 down core profile representing stable C and N isotope signals, elemental weight percentages for C and N and atomic C/N ratio. Hol = Holocene, H1-5 = Heinrich events, LGM = Last Glacial Maximum. Heinrich dates after Hemming (2004).

4. Discussion

4.1. Sedimentation and carbon accumulation

Core SL6 returned a basal ^{14}C age of ca. 47.0 kcal yr BP (805 cm), spanning the late Pleistocene and Holocene, positioning it as one of the oldest continuous coastal peatland records globally. According to Strack (2008), low lying coastal peat deposits in the (sub) tropics tend to accumulate faster than their temperate / boreal counterparts, however, most of the extensive coastal peatlands

surveyed in SE Asia (Anderson and Muller, 1975; Staub and Esterle, 1994) only originated in the middle to late Holocene after the last sea level transgression. The Mfabeni peatland, therefore, is unique and owes its longevity to the protection against sea level fluctuations, and enhanced groundwater transmissibility (Grundling et al., 2013) of the adjacent coastal dune corridor (ca. 55 kcal yrs BP; Porat and Botha; 2008).

The varying LSR, MAR and CAR throughout core SL6 (Fig. 4) are indicative of changes in sedimentation regimes which are ultimately controlled by local climate. The total core LSR of between 0.10 and 0.29 $mm.yr^{-1}$ calculated for SL6 compares favourably with the average C accumulation rate reported by Grundling (2001, 2013) in the Mfabeni peatland. Peat accumulates when Net Primary Production (NPP) outstrips decomposition (Chimner and Ewel, 2005). In sub-arctic and boreal peatlands, the low to sub-zero temperatures retard microbial decomposition causing peat to accumulate (Francez and Vasander, 1995), notwithstanding the short growing seasons. However in the tropics, peatlands are subject to consistent hot and often humid conditions that are associated with rapid rates of decomposition. Although elevated temperatures facilitate microbial decomposition and rapid turnover of OM in tropical regions, it also increases NPP due to longer growing seasons and relatively higher precipitation, with plant roots mooted as the primary source of peat accumulation in tropical regions (Chen and Twilley, 1999; Chimner et al., 2002). The overriding dominant control on (sub) tropical peat formation is waterlogging, which enables prevailing anaerobic depositional conditions that ultimately retard the rate of decomposition and permits OM rich peat sediments to accumulate (Rieley et al., 1996). Waterlogging in peatlands results from an in-balance between moisture input and evapotranspiration, facilitated by local geology/ topography, impermeable mineral base layers, basin geomorphology and groundwater input (Cameron et al., 1989).

The SL6 CAR profile (Fig. 4) can be divided into two distinct segments, the top quarter of the core, spanning the Holocene, averages 32 g $C.m^{-2}.yr^{-1}$, with the rest of the core averaging only 12 g $C.m^{-2}.yr^{-1}$. Estimates for Holocene CAR for the northern hemisphere peatlands have been published (Gorham, 1991; Turunen et al., 2002; Charman et al., 2013), with some authors using a statistical model developed by Clymo et al. (1992), to convert long-term apparent C accumulation (LARCA)

rates to contemporary true rate of carbon accumulation (TRACA), with limited success (Gorham, 1991; Clymo et al., 1998). The LARCA average rate calculated for a northern Swedish fen was reported to be 25 g $C.m^{-2}.yr^{-1}$ (Oldfield et al., 1997) and 24 g $C.m^{-2}.yr^{-1}$ for a proximal fen 70 km away (Nilsson et al., 2008). Gorham (1991), on the other hand, published a global LARCA estimate of 29 g $C.m^{-2}.yr^{-1}$, which is more representative of the CAR (32 g $C.m^{-2}.yr^{-1}$) in the Mfabeni peatland during the Holocene.

4.2. Elemental and isotopic proxies

Atomic C/N ratios are often used as a proxy to delineate OM sources in lakes and marine environments (Meyers, 1994, 2003; Gälman et al, 2008). In peatlands, the C/N proxy has been employed in conjunction with C and N stable isotope signatures to elucidate OM preservation, redox depositional conditions and biogeochemical processes related to C and N cycling of sedimentary OM (Skrzypek et al., 2008; Jones et al., 2010; Andersson et al., 2012).

Palaeoresearchers commonly employ the $\delta^{15}N$ proxy as an indicator for bulk OM source input into lake / marine sediments and changes in palaeoproductivity (Meyers and Ishiwatari, 1993; Meyers, 1997, 2003; Routh et al., 2004; Choudhary et al., 2009). In peatlands, higher plants form the overwhelmingly dominant source of OM input; resulting in up to 95% of N originating from the degraded plant OM (Andersson et al., 2012). The premise for the N isotope bulk OM source proxy is based on the isotopically different sources of inorganic N available to plants. Plants that receive their N predominantly from soil N fixers conventionally display $\delta^{15}N$ values within a small range (approximately -2 to +2‰) analogous to atmospheric $\delta^{15}N$ (± 0‰). In contrast, plants sourcing the majority of their N through microbially catalysed OM decomposition display characteristically more negative $\delta^{15}N$ ranges (ca. -2 to -8‰; Fogel and Cifuentes, 1993; Skrzypek et al., 2008). Bodelier and Laanbroek (2004) suggested that during increased rates of methanogenesis, and by that token increased temperatures and waterlogging in tropical peatlands, the high N demanding methanogenic bacteria tend to consume large quantities of ^{14}N to produce a more isotopically light N source for plants, which ultimately causes the peat N isotopic signal to become depleted in ^{15}N.

Stable carbon isotope signatures, in conjunction with atomic C/N ratios, have also proven to be robust indicators of OM sources, diagenetic alteration and primary production (Meyers and Ishiwatari, 1993; Meyers, 2003). C4 and C3 plants fractionate against ^{13}C differently, which results in significantly more positive bulk $\delta^{13}C$ values for C4 plant biomass in comparison with that of C3 plants. Therefore, the $\delta^{13}C$ signal in peat sediments can serve as an archive for changes in the relative contribution of C4 and C3 plants, which can be related to changes in environmental and climatic conditions (Skrzypek et al., 2008, 2010). The bulk $\delta^{13}C$ isotopic values in core SL6 demonstrates a strong correlation with concordant isotopic values of the leaf wax *n*-alkanes ($r=0.88$, $P=0.01$, $n=27$; in Baker et al., in preparation), suggesting the major OM source in the Mfabeni sediments are of terrestrial plant origin. A detailed study of how individual plant species identified in Mfabeni could potentially react to changes in moisture and temperature is beyond the scope of this research. We assume, therefore, that these environmental factors have a negligible effect on the $\delta^{13}C$ value of bulk OM in comparison with shifts in C3/C4 vegetation.

Finch and Hill (2008) undertook an extensive palynological study in the Mfabeni peatland and documented the changes in the pollen record. They observed a local vegetation taxa dominated by varying proportions of *Poaceae* and *Cyperaceae* since the late Pleistocene (ca. 44 kcal yr BP to present). Even though the *Paoceae* and *Cyperaceae* plant families are comprised of both C3 and C4 species, Stock et al., (2004) and Vogel and Fuls (1978) observed a definite geographical distribution between the two photosynthetic pathways in southern Africa. The C4 grasses and sedges occur more abundantly in the north eastern austral summer rainfall areas, while the C3 species are more dominant in the winter rainfall areas and high altitude regions of the south Western Cape and eastern Escarpment. Kotze and O'Connor (2000) did a study of contemporary vegetation within and around wetlands along an altitudinal gradient in the Kwazulu-Natal region. They documented the percentage variations of the two dominant species, namely C3/C4 grasses and sedges, in wetlands with varying hydrological conditions. The Mongolwane wetland, at 550 m elevation, recorded relative proportions of 49.2, 39.6, 9.5 and 1.7% for C4 sedges, C3 grasses, C3 sedges and C4 grasses, respectively, in permanently inundated sections, and 57.6, 21.0, 13.2 and 8.2% for C4 sedges, C4 grasses, C3 grasses and C3 sedges, respectively, in seasonally

inundated areas. This represents a shift from ~50:50 split between C3 and C4 plant species in permanent wetlands to ~20:80 ratio in favour of C4 plant species in seasonal wetlands. Kotze and O'Connor (2000) also recorded an increase to near absolute C4 grasses dominance as a result of moisture reduction in low-lying wetlands.

Throughout core SL6, the C/N ratio does not fall below 20 (Fig. 5), except at 54 cm (17; ca. 1.4 kcal yr BP), supporting the suggestion that the predominant OM input into the Mfabeni peatland being vascular land plants. The elemental C and N wt% values exhibit a strong correlation throughout the core (total core: r = 0.77; P=0.01; n = 196; refer to Table 3 for individual LSR stages and Fig. 5), which represents a MAR, as opposed to diagenetic relationship for C and N concentrations with depth (Andersson et al., 2012). Kuhry and Vitt (1996) used the elemental C/N relationship to explore diagenetic effects in acrotelm and catotelm peat layers. They proposed that in the aerobic acrotelm layer, N is preferentially lost during OM breakdown, resulting in increased bulk C/N ratio with depth, whereas in the anaerobic catotelm layer, a decrease in C/N should be observed as a result of methanogenesis and N becoming immobile under anoxic conditions. The SL6 C/N ratio shows no overall trends down core, supporting the inference based on the wt% C and N relationship, that diagenetic alteration did not play a major role during overall peat formation in Mfabeni peatland.

The $\delta^{15}N$ signal in core SL6 displays a general increasing trend with depth, with values ranging between -2.9 and 1.9‰ suggesting the predominant source of bioavailable N during photosynthesis is N-fixing bacteria and not microbial reworking of OM. In contrast, the $\delta^{13}C$ profile fluctuates between -25.3 and -15.5‰, inferring an interchangeable source of C3 and C4 plant end members (Fig. 5 and 6). It has been shown that the lighter ^{12}C (Nichols et al., 2009; Jones et al., 2010) and ^{14}N isotopes (Amundson et al., 2005) are preferential removed during extensive microbial remineralisation, resulting in an enrichment in both the ^{13}C and ^{15}N isotopes in the remaining soil (and more ^{14}N available for plant uptake; Bodelier and Laanbroek, 2004).

Table 3: Statistical relationships between isotopic and elemental profiles for LSR stages in Core SL6. (Two tail test, P=probability level, df=degrees of freedom)

	δ^{15}N : C/N	δ^{13}C : C/N	δ^{15}N : δ^{13}C	%N : %C
LSR Stage 1				
r	0.34	0.61	0.39	0.90
(P=0.01; df=36)		**Sig**		**Sig**
LSR Stage 2				
r	-0.78	-0.66	0.52	0.99
(P=0.01; df=15)	**Sig**	**Sig**		**Sig**
LSR Stage 3				
r	-0.69	0.83	-0.36	0.84
(P=0.01; df =20)	**Sig**	**Sig**		**Sig**
LSR Stage 4				
r	0.25	0.84	-0.36	0.98
(P=0.01; df=18)		**Sig**		**Sig**
LSR Stage 5				
r	0.06	0.16	-0.18	0.46
(P=0.01; df=97)				**Sig**

Therefore a significant statistical correlation can be expected between the $\delta^{13}C$, $\delta^{15}N$ and C/N signals in extensively decomposed soils (Engel et al., 2010), or conversely, an insignificant correlation in highly preserved soils where minor isotopic C and N fractionation occurred during diagenesis (Jedrysek and Skrzypek, 2005; Jones et al., 2010; Skrzypek at al., 2010). By comparing the isotopic and elemental signals for each of the five LSR stages in core SL6, the statistical relationships can be used to infer the relative degree of SOM preservation / rates of decomposition for each LSR stages.

There is a general absence of any significant correlation between the $\delta^{15}N$ and $\delta^{13}C$ signals (Table 3) in all five of the LSR stages endorsing the Mfabeni sediments as highly preserved. When comparing the $\delta^{13}C$ and C/N signals, a significant correlation is exhibited in LSR stages 1 – 4, while the $\delta^{15}N$ and C/N comparison only shows a significant correlation during LSR stages 2 and 3. This unbalanced correlation between the isotopic and elemental combinations up core suggests the degree of OM preservation was influenced predominantly by environmental factors during deposition and diagenesis, as opposed to peat maturity (age), permitting us to gauge relative rates

of decomposition during each LSR stage, and surmise the environmental factors affecting not only sedimentation but decomposition rates (Engle et al., 2010).

4.3. Palaeo reconstruction

4.3.1 LSR Stage 1 (ca. 47.0 – ca. 32.4 kcal yr BP)

LSR Stage 1 (average LSR = 0.13 mm.yr^{-1}) occurred in conjunction with relatively low MAR; high average TOC, below average C accumulation (Fig. 4), and relatively low rates of decomposition (Table 3) suggesting a cool and wet period, with extended phases of waterlogging, but slow peat accumulation probably as a result of lower NPP. The δ^{15}N values are comparatively more positive, ranging between -0.4 and +1.9‰, indicating a predominant atmospheric N fixing source while the δ^{13}C signal fluctuates between -22.9 and -15.8‰, representing a C4 plant dominated OM input (Fig. 5). Finch and Hill (2008) found evidence of high frequencies of forest tree pollen, with a locally dominant signal of grasses, and to a lesser extent sedges, between ca. 44 and ca. 33 kcal yr BP, which they interpreted to represent a cool and wet period. A cooler climate could have resulted in lower rates of methanogenesis, and a reduction in bioavailable ^{14}N (Skrzype et al., 2008; Jones et al., 2010). For the δ^{13}C signal, however, the C isotope signature is only significantly influenced by the relative proportions of C3 and C4 plant OM input. Stock et al. (2004) concluded that C4 sedges endemic throughout South Africa appeared to have evolved more as a response to low atmospheric CO_2, as opposed to limited nutrient and hydrologic adaptations, which are more typical of the regional C4 grasses. The shifts in δ^{13}C during this stage trends similarly, but opposite to the CO_2 records reported in the Byrd ice cores (Stocker, 2000) reinforcing the proposed evolutionary relationship between C4 plants and lower atmospheric pCO_2.

Notably, the core TOC maximum occurs in this stage at ca. 44.6 kcal yr BP (1600 g C.m^{-2}), together with another abrupt increase in average TOC values between ca. 37.9 and ca. 35.9 kcal yr BP, concordant with the A2 and A1 warming event (and Heinrich 5 (H5) and Heinrich 4 (H4) cooling event in the Northern hemisphere) identified by δ^{18}O and δ^{2}H signals in the Byrd and Vostok ice cores from Antarctica (and GRIP ice core in Greenland; Blunier et al., 1998; Stocker, 2000). Bard et al. (1997) reported an overall 1.6 ^{0}C gradual decline in alkenone proxy sea surface

temperatures (SST) from a marine sediment core (MD79257) extracted at 20^{0}S in the Mozambique Channel during this same period. However, included in this general decline, two prominent spikes were observed at ca. 44.5 and ca. 35.5 kcal yr BP, which correspond to the A2 and A1 warming events, respectively (Blunier et al., 1998; Stocker, 2000). Although the stable isotope signature does not definitively reflect the A2 warming event (or H5, 44.5 kcal yr BP), a shift of -4.1‰ to more negative δ^{13}C values and a decrease in C4 plant contribution (Fig. 6) is observed starting at ca. 38 kcal yr BP (A2; H4). This δ^{13}C negative shift is followed closely by a negative shift in δ^{15}N values, which suggests an increase in microbial sources of ^{14}N isotopes as a response to the A1 warming event. It is postulated that the prominent change in physical and geochemical parameters during the A1 (and A2) warming event was a result of permanent waterlogging and increased contributions from C3 grasses relative to C4 sedges during a period of permanent inundation (Kotze and O'Connor, 2000), accompanied by increased rates of methanogenesis towards the latter part of LSR Stage 1.

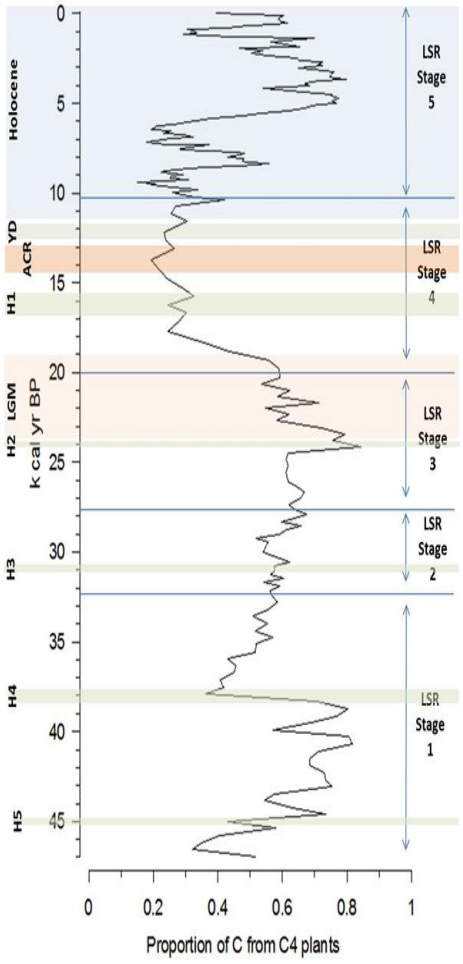

Figure 6: Proportion of carbon input from C4 plants (Equation 1, see methods section 2.5). Hol = Holocene, H1-5 = Heinrich events, LGM = Last Glacial Maximum. Heinrich dates after Hemming

4.3.2. LSR stage 2 (ca. 32.1 – ca. 27.9 kcal yr BP)

The next LSR stage (Fig. 4) displays an increased average LSR of 0.22 mm.yr-1, overall high MAR, low TOC and CAR, which was accompanied by a gradual overall positive trends in δ^{13}C and δ^{15}N values (Fig. 5) and an increase in decomposition rates compared to LSR stage 1 (Table 3). These parameters infer a period of minimal water logging at the site, and a shift to sand dominated sedimentation, most likely due to a shift to drier and windier conditions. Conversely, a sharp increase in TOC and C accumulation to above core average values, concordant with more negative δ^{15}N values occurred in the latter part of LSR stage 2 (ca. 28.6 to ca. 27.9 kcal yr BP), suggesting a short period of wet and warm conditions, in contrast to the general overall trend

towards glacial conditions. The $\delta^{13}C$ signal, however, continues along an overall positive trend, inferring a continued increase in C4 plant input which can be correlated to overall decreasing pCO_2 (compared to the Byrd Ice core; Stocker, 2000). This interpretation is supported by a general decline over the same timescale, punctuated by an abrupt increase of 1^0C at ca. 28 kcal yr BP in the MD79257 core derived alkenone SST (Bard et al., 1997), and a decline in forest pollen and switch towards sedge dominated swamp vegetation (Finch and Hill, 2008). Likewise, the Vostok ice core registered a noticeable return to more positive δ^2H values at ca. 28 kcal yr BP (Stocker, 2000). Talma and Vogel (1992) calculated late Quaternary ambient temperatures from speleothem $\delta^{18}O$ values in the Cango Caves (22^0E, 33^0S), which is situated in the perennial rainfall region of the southern Cape, South Africa. They observed a slow overall decline in temperature leading up to the LGM (ca. 19 to ca. 17 kyr BP), punctuated by a ~1.5 ^0C temperature reversal at ca. 28.5 kyr BP. It could also be argued that with the large abrupt increase in CAR observed at the conclusion of LSR stage 2, the Mfabeni peatland switched from being a temporary to a seasonally inundated fen resulting in an increase in C4 sedge dominance as reported by Kotze and O'Connor (2000). Partridge (2002) similarly recorded a peak in precipitation levels using a rainfall time series sediment proxy extracted from the Tswaing impact crater lake in north eastern South Africa around ca. 28 kcal yr BP, before the onset of full glacial conditions.

4.3.3. LSR stage 3 (ca. 27.6 – ca. 20.3 kcal yr BP)

During LSR stage 3 (Fig. 4), the LSR drops to an average of 0.14 $mm.yr^{-1}$ accompanied by below average MAR, average to high TOC and near average CAR until ca. 22.7 kcal yr BP, after which a sharp decline in TOC and to a lesser extent CAR is observed. A significant correlation between both $\delta^{15}N$ and $\delta^{13}C$ with C:N ratio suggests an overall elevated rate of decomposition during the LGM (Table 3). The $\delta^{15}N$ and $\delta^{13}C$ values remain relatively stable until ca. 24.2 kcal yr BP. The N and C stable isotope records subsequently diverge (H2, Fig. 5), the $\delta^{15}N$ values become more negative, whereas the $\delta^{13}C$ and C/N ratio values abruptly increase, coincidental with elevated TOC and average CAR. These changing parameters can be interpreted as an initial shift to cooler temperatures and a peak in waterlogging (precipitation) and increased dominance of widespread C4 wetland sedges (Kotze and O'Conner, 2000), before a shift to cooler and drier conditions after

ca. 23 kcal yr BP. The sharp increase in C/N ratio at ca. 24.2 k cal yr BP could possibly be due to an increase in peat accumulation, as a result of higher plant preservation during extensive waterlogging suggested by the elevated TOC and more subtle increases in the LSR and CAR. Thereafter, the $\delta^{13}C$ signal steadily decreases, coinciding with a sharp drop in TOC and CAR, which we conclude as an overall increase in relative abundance of C3 grasses, which have an advantage over C4 grasses / sedges at lower growing season temperatures (Sage et al., 1999; Kotze and O' Conner, 2000; Finch and Hill, 2008; Fig. 6). The SST of core MD79257 displayed stable temperatures around 26 ^{0}C until ca. 24 kcal yr BP (H2) after which the signal steadily declines towards the lowest core SST of 24.2 ^{0}C at ca. 20 kcal yr BP (Bard et al., 1997). The Byrd Antarctic ice core $\delta^{18}O$ signal oscillates between -41.5 and -39.0‰ until ca. 24 kcal yr BP, after which the signal declines to lowest levels for the next ca. 3.5 kyr (Blunier et al., 1998). Finch and Hill (2008) observed an abrupt change from swamp sedge to grassland vegetation after ca. 24 kcal BP which they interpreted as an abrupt shift to drier, cooler local conditions at the onset of the LGM (ca. 24 kcal yr BP) indicated by a sudden increases in Poaceae pollen frequencies and a steady decline in Cyperaceae pollen. Likewise, the Cold Air cave stalagmite located in Makapansgat Valley (24^{0}S, 29^{0}E) in the summer rainfall area of South Africa recorded drier conditions in conjunction with lower temperatures between 23 – 21 kyr (Holmgren et al., 2003).

4.3.4. LSR Stage 4 (ca. 19.8 – ca. 10.4 kcal yr BP)

The lowest core average LSR (0.10 mm.yr^{-1}) occurs in LSR stage 4 (Fig. 4), corresponding to a period of low MAR, low but steadily increasing TOC and CAR dominated by an abrupt shift to negative $\delta^{13}C$ values. This trend is accompanied by fluctuating $\delta^{15}N$ values near the core average (Fig. 5) and relative reduction in decomposition rates (Table 3). Between ca. 14.3 and ca. 10.8 kcal yr BP, a sharp overall increase in TOC values occurs, whereas other physical and geochemical parameters remain relatively constant. These observations can be interpreted as a continuation of dry and cool late glacial conditions up until ca. 15 kcal yr BP, after which an abrupt increase in precipitation and waterlogging occurs. The sharply negative $\delta^{13}C$ values could have been as a result of increases in C3 grass input which is supported by the sharp decline in the proportion of C from C4 plants mass balance at the onset of LSR stage 4 (Fig. 6), and then a

switch to C3 swamp forest vegetation after ca. 15 kcal yr BP due to the abrupt increase in precipitation. Finch and Hill (2008) documented a continued dominance of grasslands over wetland sedges during this stage, which leads us to speculate that the predominant photosynthetic pathway employed by Poaceae grasses was C3 as a consequence of the better adaptation to lower growing season temperatures and general dry conditions compared to C4 plants (Sage et al., 1999) up to ca. 15 kcal yr BP.

Norström et al. (2009) used palynology, and C and N stable isotope proxies to infer a cool and dry climate between 16 and 14.3 kyr, then a shift to more humid conditions culminating at 13.2 kyr before returning to drier conditions in the Braamhoek peatland (28^0S, 29^0E). Talma and Vogel (1992) recorded a reversal of the generally declining ambient air temperatures in the Cango cave speleothem after ca. 15.5 kyr BP, with the temperature steadily increasing up until stalagmite growth ceased at ca. 13.8 kyr BP. The Cold Air cave stalagmite δ^{18}O signature inferred drier and cooler conditions around ca. 19.5 - 17.5 and ca. 15 – 13.5 kyr, with warming interludes (Holmgren et al., 2003), while biomarker and stable isotope proxies from Lake Tswaing (25^0S, 28^0E) suggested the period between ca. 14 and ca. 10 kcal yr BP experienced increased temperatures and moisture (Kristen et al., 2010).

Chase et al. (2011) recorded relative dry conditions between ca. 19.5 and ca. 17.5 kcal yr BP, followed by an increase in moisture up to the early Holocene in hyrax midden deposits located in the winter rainfall zone of the SW Cape, with the exception of a conspicuous period of drier conditions concomitant with the Younger Dryas (YD). On the contrary, Schefusz et al. (2011) observed large inputs of terrestrial sedimentary and plant input into the Zambezi catchment area (18^0 33.9' S, 37^0 22.8' E) during the H1 and YD northern hemisphere cold events, indicating significant increases in adjacent continental austral summer rainfall precipitation, while the proximal Mozambique channel MD79257 core alkenone SST recorded a warming trend after ca. 15 kyr BP (H1; Bard et al., 1997).

Stocker (2000), compared the Greenland GRIP ice core with the Vostok and Byrd Antarctic ice cores, and documented asynchronous responses to climate change between the two latitudinal

hemispheres during the last deglaciation. The similarity between these trends in core SL6 and other regional climate records implies that the Mfabeni peat deposit faithfully recorded both regional and global late glacial climatic events and displays a comparable opposite phasing in trend and magnitude when compared to northern hemisphere Heinrich and YD climate events.

4.3.5. LSR stage 5 (ca. 10.2 kcal yr BP – present)

The transition to interglacial conditions at the Pleistocene / Holocene boundary displays a prominent shift to highly fluctuating climatic conditions. Gasse (2000) concluded that dramatic Holocene hydrological changes documented in low latitudes on the African continent appear to rival fluctuations observed during the preceding glacial period. The LSR stage 5 is represented by elevated and highly variable sedimentation, displaying the highest LSR stage average (0.29 $mm.yr^{-1}$), accompanied by high MAR, overall high TOC and CAR (Fig. 4), with an ever decreasing $\delta^{15}N$ and fluctuating $\delta^{13}C$ signature (Fig. 5). The lack of any significant correlations between either of the stable isotopes and elemental ratio, suggests low rates of decomposition during the Holocene (Table 3). These parameters can be interpreted as significant increases in humidity and temperatures typical of an interglacial period, punctuated by a collection of millennial-scale cooling events. Three abrupt excursions to low TOC and CAR values occur at ca. 7.1, ca. 5.3 and ca. 1.4 kcal yr BP, which coincide with decreases in Mozambique Channel alkenone and Zambezi delta TEX_{86}-derived SST (Bard et al., 1997; Schefuß et al., 2011), and signs of general aridity in the Kalahari Desert (Stokes et al., 1997). Norström et al. (2009) recorded similar large oscillations in the Braamhoek wetland proxies that are in general agreement with the Mfabeni peatland parameters, with the exception of between 7.5 and 2.5 ka which indicate a relatively dry and warm period, whereas core SL6 recorded overall elevated CAR values, excluding the two millennial-scale drying events at ca. 7 and ca. 5.3 kcal yr BP. Norström et al. (2009) however did stipulate that this time period can only be used to infer general palaeoenvironmental conditions due to the comparative low rate of peat accumulation and low chronological resolution in the Braamhoek record.

After ca. 10.5 kcal yr BP, the CAR abruptly increases while the $\delta^{13}C$ record displays the minimum core value (-25.3‰; ca. 9.4 kcal yr BP) and lowest C4 plant C contribution (Fig. 6) suggesting a

significant increase in local precipitation and C3 plant abundance in and around the Mfabeni peatland. The palynology record showed rapidly increasing *Podocarpus* forest (C3) pollen after ca. 11 kcal yr BP, which is interpreted to represent a period of cool and wet conditions (Finch and Hill, 2008). In contrast, Valsecchi et al. (2013) documented a shift from Protea-type pollen to arboreal pollen and attributed the change to warmer and wetter conditions in the winter rainfall fynbos area of the south Western Cape. The Cold Air cave stalagmite returned the lowest $\delta^{13}C$ values at ca. 9 kyr, indicating a significant increase in C3 plant influence on the precipitating aragonite (Holmgren et al., 2003). At ca. 9 kcal yr BP, the $\delta^{13}C$ values reverse their decreasing trend and rapidly become more positive, peaking at ca. 8.4 kcal yr BP, after which the signal returns to more negative values up until ca. 7.2 kcal yr BP (first of the millennium scale cooling events), emulated by similar trending TOC and CAR. Finch and Hill (2008) documented a rapid increase in swamp forest vegetation, with sustained levels of Podocarpus pollen, during the Holocene Altithermal (ca. 8 to ca. 6 kcal yr BP), which they interpreted to signify a warming trend with high precipitation levels, supported by a corresponding 0.6 ^{0}C increase in the Mozambique Channel core SST data at ca. 9 kcal yr BP (Bard et al., 1997). The enriched ^{13}C signal at ca. 8.4 kcal yr BP, could possibly be a result of a spike in C4 wetland sedge populations (Fig 6) contributing to the enrichment of ^{13}C during a brief period of intensive waterlogging in the peatland, reinforced by a peak in levels of concordant SL6 CAR (Fig. 4). The $\delta^{13}C$ signal returns steadily to more negative values up until ca. 7 kcal yr BP, suggesting a return to swamp forest (C3) dominance, and humid and warm climatic conditions, supported by increases in TOC up until ca. 7 kcal yr BP cooling event. Pudsey and Evans (2001) studied changes in glacial till deposits from floating ice sheets at the edge of the Antarctic Peninsula. They documented large deglaciation in the northern James Ross Island, and proposed the full disappearance of the George VI Ice shelf ca. 6.5 kyr BP, signifying a warming trend in Antarctic. The Mfabeni $\delta^{13}C$ signal increases by more than ca. 5‰, coinciding with a decrease in $\delta^{15}N$ values, between ca. 7 and ca. 6 kcal yr BP inferring a shift to C4 sedge dominated plant OM input (Kotze and O'Conner, 2000 and Fig. 6) and increased methanogenesis. These signatures indicate a short wet period before a shift to cool dry conditions at the second millennium-scale ca. 5.3 kcal yr BP cooling event, delineated by the abrupt decrease in TOC and

CAR. After ca. 6 kcal yr BP, Finch and Hill (2008) observed a steady decline in the abundance of Podocarpus forest pollen and an increase in Poaceae and Cyperaceae frequency, indicating a move to grassland / savannah dominance, and inferred a cooling and drying trend towards the middle Holocene.

Relatively more positive $\delta^{13}C$ values occur between ca. 5 to ca. 3 kcal yr BP, coinciding with elevated TOC and CAR and continuance of wetland C4 sedge dominance (Finch and Hill, 2008; Fig. 6), signalling a return to warm and moist conditions. Anthropogenic farming practices become apparent from the palynology record after ca. 5 kcal yr BP, specifically attributed by Finch and Hill (2008) to the decline in Podocarpus (C3) forests which could have artificially elevated the $\delta^{13}C$ climate signal. As a consequence, bulk parameters need to be interpreted with caution from ca. 5 kcal yr BP as human influence on the palaeoenvironment signal increased. An overall C4 peatland signature of the $\delta^{13}C$ trend and a shift to more negative $\delta^{15}N$ up until ca. 1.4 kcal yr BP suggests the continued dominance of C4 sedge input (and perhaps anthropogenic forest thinning) due to extensive waterlogging. Finch and Hill (2008) concluded an increase in savannah / grassland pollen to infer a drying trend from ca. 3 kcal yr BP to present. However, we interpret core SL6 data to suggest a warming and moist trend over this period (with the exception of the 1.4 kcal yr BP cooling event) as indicated by ever decreasing $\delta^{15}N$ and overall positive $\delta^{13}C$ signals during this same period, signalling waterlogged conditions. The last of the abrupt cooling/drying events (ca. 1.4 kcal yr BP) occurs in conjunction with a prominent decrease in both TOC and CAR, a positive 2.4‰ deviation in $\delta^{15}N$ and an initial increase, followed by a decrease in $\delta^{13}C$ values. The changes in the proxy parameters indicate that this abrupt cooling event reduced the rate of methanogensis, reducing the amount of bioavailable ^{14}N and an increase in C4 grass input (Fig. 6) in response to sudden and brief period of dry conditions. The swift return to the more elevated TOC and CAR and the lowest $\delta^{15}N$ core values, accompanied by oscillating $\delta^{13}C$ signal infers a return to cyclical climate conditions and once again highlights the extreme climatic fluctuations characteristic of the Holocene, both regionally and globally (Gasse, 2000; Mayewski et al., 2004).

The Mfabeni record's overall opposite environmental response to better known climatic events in the Northern hemisphere suggests an anti-phase coupling to the southern hemisphere (Figs. 4 and

5). Core SL6 shows a trend in both physical and geochemical parameters towards increased C accumulation during cold Heinrich events (particularly H5 to H2 and YD), suggesting elevated precipitation, and arguably temperatures, which is in direct contrast to findings from the northern hemisphere records. Varying degrees of anti-phased interhemisphere coupling has also been observed by other authors (Bard et al., 1997; Blunier et al., 1998; Schmittner et al., 2003; Chase et al., 2011; Schefuß et al., 2011) with several different mechanisms for climate forcing postulated; signalling a crucial requirement for additional regional palaeoenvironment studies to corroborate or challenge these hypotheses.

5. Conclusions

We employed several known geochemical indicators of peat forming processes and related them to changes in past primary production, OM preservation, OM sources and digenetic alteration after deposition. By relating the bulk parameters to physical and biogeochemical processes, we were able to reconstruct the palaeoenvironment that controlled peat formation at the Mfabeni peatland and hypothesise the probable climate on the north east coast of South Africa since the late Pleistocene. We established that the Mfabeni peat sediments have undergone minimal diagenetic alteration, confirming the archive's high degree of preservation and accurate recording of palaeoenvironmental conditions. We surmise the following sequence of palaeoenvironmental conditions and their climatic controls from ca. 47 kcal yr BP to present:-

LSR stage 1 (ca. 47 – ca. 32.2 kcal yr BP): we inferred a predominantly cool and wet climate with extensive waterlogged but low NPP, and C4 plant dominant OM source assemblage, punctuated by two short warming events, A2 (ca. 44.5 k cal yr BP) and A1 (ca. 37 kcal yr BP). The latter events were delineated by elevated TOC attributed to increased NPP and extensive waterlogging. *LSR stage 2* (ca. 32.2 to ca. 27.6 kcal yr BP): a distinct period of sand dominated deposition as a result of negligible waterlogging, suggesting dry and windy conditions, followed by a brief period of warm and wet conditions (ca. 28 kcal yr BP) indicated by an abrupt increases in CAR and C4 sedge swamp vegetation abundance. *LSR stage 3* (ca. 27.6 – ca. 20.3 kcal yr BP): began with cool and wet conditions with a peak in waterlogging at ca. 24 kcal yr BP represented by high TOC and

prevailing C4 sedge assemblage. After ca. 23 kcal yr BP (LGM), an abrupt change to dry and cool conditions indicated by a sharp drop in TOC and steady increase in C3 grasses relative to C4 sedges as waterlogging receded. *LSR stage 4* (ca. 20.3 – ca. 10.4 kcal yr BP): continuance of cool and dry conditions inferred by limited waterlogging and strong C3 grassland signature until ca. 15 kcal yr BP, after which, increases in waterlogging and precipitation during waning of the ACR and lead up to the Pleistocene/Holocene boundary. This trend further accentuates the apparent opposite climate phasing between the Northern and southern hemispheres. *LSR stage 5* (ca. 10.4 kcal yr BP – present): the Holocene epoch is characterized by fluctuations between pervasive wet and warm to cool / dry interglacial conditions, with intermittent abrupt millennial-scale cooling / dry events (ca. 7.1, ca. 5.3, ca. 1.4 kcal yr BP). The MAR, TOC and CAR values are distinctly elevated, with large abrupt magnitudes of variability accompanied by frequent changes between C3 and C4 plant assemblages in comparison to the late glacial period.

In this study, we delineated the Mfabeni peat sequence to produce a high resolution record of past local hydrology and bulk plant assemblages, and by using these signals, we inferred regional climate variability since the Late Pleistocene. There has long been a quest amongst palaeoclimatologists to understand the interhemispheric climate coupling relationship. The Mfabeni archive suggests an anti-phase link between southern Africa and the Northern hemisphere, most notably during H5 to H2 and YD events. Many more analogous palaeoclimate studies need to be undertaken to firm up our understanding of the triggers and change mechanisms responsible for LGM climate variability in southern Africa.

6. Acknowledgments

Alistair Clulow helped facilitate field access and site identification. A Russian peat corer was loaned to the project by Piet-Louis Grundling. iSimangaliso Authority and Ezemvelo KZN Wildlife granted access and sampling permission. The following people assisted with laboratory set up, equipment, protocols and analysis: Esmé Spicer, Cynthia Sanchez-Garrido, Renata Smit, Ian Newton, Lena Lundman, Tomaz Gozlar, Eric Ward and Megan Hill. Nikolai Pedentchouk and Michael Meadows gave valuable manuscript input. The project was supported through a bilateral

funding agreement by the Swedish Research Link-South Africa program. Student support was supplied by the Department of Science and Technology, National Research Foundation and InKaba yeAfrica (AEON). This is an Inkaba ye Africa publication no. 78 and AEON publication no. 118.

7. References

Amundson, R., Austin, A.T., Schuur, E.A.G., Yoo, K., Matzek, V., Kendall, C., Uebersax, A., Brenner, D. and Baisden, W.T., 2003. Global patterns of the isotopic composition of soil and plant nitrogen. Global Biogeochemical Cycles 17(1), 31-41.

Anderson, J.A.R., Muller, J., 1975. Palynological study of a Holocene peat and a Miocene coal deposit from NW Borneo. Review of Palaeobotany and Palynology 19 (4), 291-317.

Andersson, R.A., Meyers, P., Hornibrook, E., Kuhry, P., Mörth, C., 2012. Elemental and isotopic carbon and nitrogen records of organic matter accumulation in a Holocene permafrost peat sequence in the east European Russian arctic. Journal of Quaternary Science 27 (6), 545-552.

Bard, E., Rostek, F., Sonzogni, C., 1997. Interhemispheric synchrony of the last deglaciation inferred from alkenone palaeothermometry. Nature 385 (6618), 707-710.

Bate, G.C., Taylor, R.H., 2008. Sediment salt-load in the St Lucia Estuary during the severe drought of 2002-2006. Environmental Geology 55 (5), 1089-1098.

Blaauw, M., Christeny, J.A., 2011. Flexible paleoclimate age-depth models using an autoregressive gamma process. Bayesian Analysis 6 (3), 457-474.

Blunier, T., Chappellaz, J., Schwander, J., Dällenbach, A., Stauffer, B., Stocker, T.F., Raynaudt, D., Jouzel, J., Clausen, H.B., Hammer, C.U., Johnsen, S.J., 1998. Asynchrony of Antarctic and Greenland climate change during the last glacial period. Nature 394 (6695), 739-743.

Bodelier, P.L.E., Laanbroek, H.J., 2004. Nitrogen as a regulatory factor of methane oxidation in soils and sediments. FEMS Microbial Ecology 47 (3), 265-277.

Botha, G., Porat, N., 2007. Soil chronosequence development in dunes on the southeast African coastal plain, Maputaland, South Africa. Quaternary International 162-163, 111-132.

Boutton, T.W., Archer, S.R., Midwood, A.J., Zitzer, S.F., Bol, R., 1998. δ13C values of soil organic carbon and their use in documenting vegetation change in a subtropical savanna ecosystem. Geoderma 82(1–3), 5-41.

Brock, F., Higham, T., Ditchfield, P., Ramsey, C.B., 2010. Current pretreatment methods for ams radiocarbon dating at the oxford radiocarbon accelerator unit (orau). Radiocarbon 52 (1), 103-112.

Cameron, C.C., Esterle, J.S., Palmer, C.A., 1989. The geology, botany and chemistry of selected peat-forming environments from temperate and tropical latitudes. International Journal of Coal Geology 12 (1–4), 105-156.

Charman, D.J., Beilman, D.W., Blaauw, M., Booth, R.K., Brewer, S., Chambers, F.M., Christen, J.A., Gallego-Sala, A., Harrison, S.P., Hughes, P.D.M., Jackson, S.T., Korhola, A., Mauquoy, D., Mitchell, F.J.G., Prentice, I.C., Van Der Linden, M., De Vleeschouwer, F., Yu,

Z.C., Alm, J., Bauer, I.E., Corish, Y.M.C., Garneau, M., Hohl, V., Huang, Y., Karofeld, E., Le Roux, G., Loisel, J., Moschen, R., Nichols, J.E., Nieminen, T.M., MacDonald, G.M., Phadtare, N.R., Rausch, N., Sillasoo, U., Swindles, G.T., Tuittila, E.-., Ukonmaanaho, L., Väliranta, M., Van Bellen, S., Van Geel, B., Vitt, D.H., Zhao, Y., 2013. Climate-related changes in peatland carbon accumulation during the last millennium. Biogeosciences 10 (2), 929-944.

Chase, B.M., Quick, L.J., Meadows, M.E., Scott, L., Thomas, D.S. and Reimer, P.J., 2011. Late glacial interhemispheric climate dynamics revealed in South African hyrax middens. Geology 39 (1), 19-22.

Chase, B.M., Meadows, M.E., 2007. Late Quaternary dynamics of southern Africa's winter rainfall zone. Earth-Science Reviews 84 (3-4), 103-138.

Chen, R., Twilley, R.R., 1999. A simulation model of organic matter and nutrient accumulation in mangrove wetland soils. Biogeochemistry 44 (1), 93-118.

Chimner, R.A., Ewel, K.C., 2005. A tropical freshwater wetland: II. Production, decomposition, and peat formation. Wetlands Ecology and Management 13 (6), 671-684.

Chimner, R.A., Cooper, D.J., Parton, W.J., 2002. Modeling carbon accumulation in Rocky mountain fens. Wetlands 22 (1), 100-110.

Choudhary, P., Routh, J., Chakrapani, G.J., 2009. An environmental record of changes in sedimentary organic matter from Lake Sattal in Kumaun Himalayas, India. Science of the Total Environment 407 (8), 2783-2795.

Clulow, A.D., Everson, C.S., Mengistu, M.G., Jarmain, C., Jewitt, G.P.W., Price, J.S., Grundling, P., 2012. Measurement and modelling of evaporation from a coastal wetland in Maputaland, South Africa. Hydrology and Earth System Sciences 16 (9), 3233-3247.

Clymo, R.S., 1992. Models of peat growth. Suo 43 (4-5), 127-136.

Clymo, R.S., Turunen, J., Tolonen, K., 1998. Carbon accumulation in peatland. Oikos 81 (2), 368-388.

Czernik, J., Goslar, T., 2001. Preparation of graphite targets in the Gliwice radiocarbon laboratory for AMS^{14}C dating. Radiocarbon 43 (2), 283-291.

Engel, Z., Skrzypek, G., Paul, D., Drzewicki, W., Nývlt, D., 2010. Sediment lithology and stable isotope composition of organic matter in a core from a cirque in the Krkonoše Mountains, Czech Republic. Journal of Paleolimnology 43 (4), 609-624.

Finch, J.M., 2005. Late Quaternary palaeoenvironments of the Mfabeni peatland, northern Kwazulu Natal. MSc Thesis, University of KwaZulu-Natal, Pietermaritzburg.

Finch, J.M., Hill, T.R., 2008. A late Quaternary pollen sequence from Mfabeni Peatland, South Africa: Reconstructing forest history in Maputaland. Quaternary Research 70 (3), 442-450.

Francez, A.J., Vasander, H., 1995. Peat accumulation and peat decomposition after human disturbance in French and Finnish mires. Acta Oecologica 16 (5), 599-608.

Fogel, M.L., Cifuentes, L.A., 1993. Isotope fractionation during primary production. Organic geochemistry: Principles and applications, 73-98.

Gälman, V., Rydberg, J., De-Luna, S.S., Bindler, R., Renberg, I., 2008. Carbon and nitrogen loss rates during aging of lake sediment: Changes over 27 years studied in varved lake sediment. Limnology and Oceanography 53 (3), 1076-1082.

Gasse, F., 2000. Hydrological changes in the African tropics since the Last Glacial Maximum. Quaternary Science Reviews 19 (1-5), 189-211.

Gasse, F., Chalié, F., Vincens, A., Williams, M.A.J., Williamson, D., 2008. Climatic patterns in equatorial and southern Africa from 30,000 to 10,000 years ago reconstructed from terrestrial and near-shore proxy data. Quaternary Science Reviews 27 (25-26), 2316-2340.

Gillson, L., Waldron, S., Willis, K.J., 2004. Interpretation of soil $\delta^{13}C$ as an indicator of vegetation change in African savannas. Journal of Vegetation Science 15 (3), 339-350.

Gorham, E., 1991. Northern peatlands: role in the carbon cycle and probable responses to climatic warming. Ecological Applications 1 (2), 182-195.

Goslar, T., Czernik, J., Goslar, E., 2004. Low-energy ^{14}C AMS in Poznań Radiocarbon Laboratory, Poland. Nuclear Instruments and Methods in Physics Research Section B: Beam Interactions with Materials and Atoms (223–224), 5-11.

Grundling, P.L., 2001. The Quaternary peat deposits of Maputaland, Northern Kwazulu-Natal, South Africa: categorisation, chronology and utilisation. MSc Thesis, University of Johannesburg.

Grundling, P., Grootjans, A.P., Price, J.S., Ellery, W.N., 2013. Development and persistence of an African mire: How the oldest South African fen has survived in a marginal climate. Catena 110, 176-183.

Hemming, S.R., 2004. Heinrich events: Massive late Pleistocene detritus layers of the North Atlantic and their global climate imprint. Reviews of Geophysics 42 (1), 1-43.

Holmgren, K., Lee-Thorp, J.A., Cooper, G.R.J., Lundblad, K., Partridge, T.C., Scott, L., Sithaldeen, R., Siep Talma, A., Tyson, P.D., 2003. Persistent millennial-scale climatic variability over the past 25,000 years in southern Africa. Quaternary Science Reviews 22 (21-22), 2311-2326.

Holzkämper, S., Holmgren, K., Lee-Thorp, J., Talma, S., Mangini, A., Partridge, T., 2009. Late Pleistocene stalagmite growth in Wolkberg Cave, South Africa. Earth and Planetary Science Letters 282 (1-4), 212-221.

Hua, Q., Barbetti, M., 2004. Review of tropospheric bomb C-14 data for carbon cycle modelling and age calibration purposes. Radiocarbon, 46 (3), 1273-1298.

Immirzi, C.P., Maltby, E., Clymo, R.S., 1992. The global status of peatlands and their role in carbon cycling: A report for the Friends of the Earth. Wetlands Ecosystems Research Group, Department of Geography, University of Exeter, London.

Jedrysek, M., Skrzypek, G., 2005. Hydrogen, carbon and sulphur isotope ratios in peat: The role of diagenesis and water regimes in reconstruction of past climates. Environmental Chemistry Letters 2 (4), 179-183.

Jones, M.C., Peteet, D.M., Sambrotto, R., 2010. Late-glacial and Holocene $\delta^{15}N$ and $\delta^{13}C$ variation from a Kenai Peninsula, Alaska peatland. Palaeogeography, Palaeoclimatology, Palaeoecology 293 (1-2), 132-143.

Kelbe, B.E., Rawlins, B.K., Nomquphu, W., 1995. Geohydrological modelling of Lake St Lucia. Report, University of Zululand, KwaDlangezwa 3886 KwaZulu-Natal.

Kotze, D.C., O'Connor, T.G., 2000. Vegetation variation within and among palustrine wetlands along an altitudinal gradient in KwaZulu-Natal, South Africa. Plant Ecology 146 (1), 77-96.

Kristen, I., Wilkes, H., Vieth, A., Zink, K., Plessen, B., Thorpe, J., Partridge, T.C., Oberhänsli, H., 2010. Biomarker and stable carbon isotope analyses of sedimentary organic matter from

Lake Tswaing: Evidence for deglacial wetness and early Holocene drought from South Africa. Journal of Paleolimnology 44 (1), 143-160.

Kuhry, P., Vitt, D.H., 1996. Fossil carbon/nitrogen ratios as a measure of peat decomposition. Ecology 77 (1), 271-275.

Lee-Thorp, J., Holmgren, K., Lauritzen, S.E., Linge, H., Moberg, A., Partridge, T., Stevenson, C., Tyson, P., 2001. Rapid climate shifts in the southern African interior throughout the mid to late Holocene. Geophysical Research Letters 28 (23), 4507-4510.

Lubke, R.A., Moll, J.B., Avis, A.M., 1992. Rehabilititaion ecology in coastal and environmental services: eastern shores of Lake St Lucia. Kingsa/Tojan lease area special reports 1, biophysical environment, Council of Scientific and Industrial Research, Pretoria, South Africa.

Mayewski, P.A., Rohling, E.E., Stager, J.C., Karlén, W., Maasch, K.A., Meeker, L.D., Meyerson, E.A., Gasse, F., van Kreveld, S., Holmgren, K., Lee-Thorp, J., Rosqvist, G., Rack, F., Staubwasser, M., Schneider, R.R., Steig, E.J., 2004. Holocene climate variability. Quaternary Research 62 (3), 243-255.

McCormac, F.G., Hogg, A.G., Higham, T.F.G., Lynch-Stieglitz, J., Broecker, W.S., Baillie, M.G.L., Palmer, J., Xiong, L., Pilcher, J.R., Brown, D., Hoper, S.T., 1998. Temporal variation in the interhemispheric 14C offset. Geophysical Research Letters. 25, 1321–1324.

McCormac, F.G., Hogg, A.G., Blackwell, P.G., Buck, C.E., Higham, T.F.G., Reimer, P.J., 2004. SHCal04 southern Hemisphere calibration, 0-11.0 cal kyr BP. Radiocarbon 46 (3), 1087-1092.

Meadows, M.E., Baxter, A.J., Parkington, J., 1996. Late Holocene environments at Verlorenvlei, Western Cape Province, South Africa. Quaternary International 33 (1), 81-95.

Meadows, M.E., Baxter, A.J., 1999. Late Quaternary palaeoenvironments of the southwestern Cape, South Africa: A regional synthesis. Quaternary International 57-58, 193-206.

Meyers, P.A., 2003. Applications of organic geochemistry to paleolimnological reconstructions: A summary of examples from the Laurentian Great Lakes. Organic Geochemistry 34 (2), 261-289.

Meyers, P.A., 1997. Organic geochemical proxies of paleoceanographic, paleolimnologic, and paleoclimatic processes. Organic Geochemistry 27, (5-6), 213-250.

Meyers, P.A., 1994. Preservation of elemental and isotopic source identification of sedimentary organic matter. Chemical Geology 114 (3-4), 289-302.

Meyers, P.A., Ishiwatari, R., 1993. Lacustrine organic geochemistry-an overview of indicators of organic matter sources and diagenesis in lake sediments. Organic Geochemistry 20 (7), 867-900.

Mucina, L., Adams, J.B., Knevel, I.C., Rutherford, M.C., Powrie, L.W., Bolton, J.J., van der Merwe, J.H., Anderson, R.J., Bornman, T.G., le Roux, A., Janssen, J.A.M., 2006. Coastal Vegetation of South Africa, in: Mucina, L., Rutherford, M.C. (Eds.), The vegetation of South Africa, Lesotho and Swaziland. South African National Biodiversity Institute, Pretoria, pp. 658-696.

Muzuka, A.N.N., 1999. Isotopic compositions of tropical East African flora and their potential as source indicators of organic matter in coastal marine sediments. Journal of African Earth Sciences 28 (3), 757-766.

Neumann, F.H., Scott, L., Bousman, C.B., van As, L., 2010. A Holocene sequence of vegetation change at Lake Eteza, coastal KwaZulu-Natal, South Africa. Review of Palaeobotany and Palynology 162 (1), 39-53.

Neumann, F.H., Stager, J.C., Scott, L., Venter, H.J.T., Weyhenmeyer, C., 2008. Holocene vegetation and climate records from Lake Sibaya, KwaZulu-Natal (South Africa). Review of Palaeobotany and Palynology 152 (3-4), 113-128.

Nichols, J.E., Walcott, M., Bradley, R., Pilcher, J., Huang, Y., 2009. Quantitative assessment of precipitation seasonality and summer surface wetness using ombrotrophic sediments from an Arctic Norwegian peatland. Quaternary Research 72 (3), 443-451.

Nilsson, M., Sagerfors, J., Buffam, I., Laudon, H., Eriksson, T., Grelle, A., Klemedtsson, L., Weslien, P., Lindroth, A., 2008. Contemporary carbon accumulation in a boreal oligotrophic minerogenic mire, a significant sink after accounting for all C-fluxes. Global Change Biology 14 (10), 2317-2332.

Norström, E., Scott, L., Partridge, T.C., Risberg, J., Holmgren, K., 2009. Reconstruction of environmental and climate changes at Braamhoek wetland, eastern escarpment South Africa, during the last 16,000 years with emphasis on the Pleistocene-Holocene transition. Palaeogeography, Palaeoclimatology, Palaeoecology 271 (3-4), 240-258.

Oldfield, F., Thompson, R., Crooks, P.R.J., Gedye, S.J., Hall, V.A., Harkness, D.D., Housley, R.A., McCormac, F.G., Newton, A.J., Pilcher, J.R., Renberg, I., Richardson, N., 1997. Radiocarbon dating of a recent high latitude peat profile: Stor Amyran, northern Sweden. Holocene 7 (3), 283-290.

Page, S.E., Rieley, J.O., Banks, C.J., 2011. Global and regional importance of the tropical peatland carbon pool. Global Change Biology 17 (2), 798-818.

Partridge, T.C., 2002. Were Heinrich events forced from the southern hemisphere? South African Journal of Science 98 (1-2), 43-46.

Porat, N., Botha, G., 2008. The luminescence chronology of dune development on the Maputaland coastal plain, southeast Africa. Quaternary Science Reviews 27 (9-10,) 1024-1046.

Preston-Whyte, R.A, Tyson, P.D., 1998. The atmosphere and weather of southern Africa. Oxford University Press, South Africa.

Pudsey, C.J., Evans, J., 2001. First survey of Antarctic sub-ice shelf sediments reveals mid-Holocene ice shelf retreat. Geology 29 (9), 787-790.

Reimer, P.J., Baillie, M.G.L., Bard, E., Beck, J.W., Blackwell, P.G., Buck, C.E., Burr, G.S., Edwards, R.L., Friedrich, M., Guilderson, T.P., 2006. Comment on: Radiocarbon calibration curve spanning 0 to 50,000 years BP based on paired 230Th/234U/238U and ^{14}C dates on pristine corals by RG Fairbanks et al., 2005. Quaternary Science Reviews 24, 1781-1796 and Extending the radiocarbon calibration beyond 26,000 years before present using fossil corals by Chiu, T.C., 2005. Quaternary Science Reviews 24, 1797-1808. Quaternary Science Reviews 25, 855-862.

Rieley J.O., Ahmad-Shah A.A., Brady M.A., 1996. The extent and nature of tropical peat swamps - Tropical Lowland Peatlands of Southeast Asia. In: Maltby E., Immirzi C.P., Safford R.J. (Eds.), Tropical Lowland Peatlands of Southeast Asia -proceedings of a workshop on integrated planning and management of tropical lowland peatlands: workshop on integrated planning and management of tropical lowland peatlands. IUCN, Gland, Switzerland.

Routh, J., Meyers, P.A., Gustafsson, O., Baskaran, M., Hallberg, R., Scholdström, A., 2004. Sedimentary geochemical record of human-induced environmental changes in the Lake Brunnsviken watershed, Sweden. Limnology and Oceanography 49 (5), 1560-1569.

Sage, R.F., Wedin, D.A., Li, M., 1999. The Biogeography of C4 Photosynthesis: Patterns and Controlling Factors in: Sage, R.F., Monson, R.K. (Eds.), C4 Plant Biology. Academic Press, San Diego, pp. 313-373.

Schefuß, E., Kuhlmann, H., Mollenhauer, G., Prange, M. and Patzold, J., 2011. Forcing of wet phases in southeast Africa over the past 17,000 years. Nature Geoscience 480 (7378), 509-512

Schmittner, A., Saenko, O.A., Weaver, A.J., 2003. Coupling of the hemispheres in observations and simulations of glacial climate change. Quaternary Science Reviews 22 (5-7), 659-671.

Skrzypek, G., Jezierski, P., Szynkiewicz, A., 2010. Preservation of primary stable isotope signatures of peat-forming plants during early decomposition - observation along an altitudinal transect. Chemical Geology 273 (3-4), 238-249.

Skrzypek, G., Paul, D., Wojtun, B., 2008. Stable isotope composition of plants and peat from Arctic mire and geothermal area in Iceland. Polish Polar Research 29 (4), 365-376.

Smuts, W.J., 1992. Peatlands of the Natal mire complex: geomorphology and characterization. South African Journal of Science 88 (9-10), 474-483.

Staub, J.R., Esterle, J.S., 1994. Peat-accumulating depositional systems of Sarawak, East Malaysia. Sedimentary Geology 89 (1-2), 91-106.

Stenni, B., Masson-Delmotte, V., Johnsen, S., Jouzel, J., Longinelli, A., Monnin, E., Röthlisberger, R., Selmo, E., 2001. An oceanic cord reversal during the last deglaciation. Science 293 (5537), 2074-2077.

Stock, W.D., Chuba, D.K., Verboom, G.A., 2004. Distribution of South African C3 and C4 species of Cyperaceae in relation to climate and phylogeny. Austral Ecology 29 (3), 313-319.

Stocker, T.F., 2000. Past and future reorganizations in the climate system. Quaternary Science Reviews 19 (1-5), 301-319.

Stokes, S., Thomas, D.S.G., Washington, R., 1997. Multiple episodes of aridity in southern Africa since the last interglacial period. Nature 388 (6638), 154-158.

Strack, M., 2008. Peatlands and climate change. International Peat Society, Jyvaskyla, Finland.

Stuiver, M., Polach, H.A., 1977. Discussion: Reporting on ^{14}C data. Radiocarbon 19 (3), 355-363.

Talma, A., Vogel, J.C., 1992. Late Quaternary paleotemperatures derived from a speleothem from Cango caves, Cape Province, South Africa. Quaternary Research 37 (2), 203-213.

Taylor, R., Kelbe, B., Haldorsen, S., Botha, G.A., Wejden, B., Varet, L., Simonsen, M.B., 2006a. Groundwater-dependent ecology of the shoreline of the subtropical Lake St Lucia estuary. Environmental Geology 49 (4), 586-560.

Taylor, R., Adams, J.B., Haldorsen, S., 2006b. Primary habitats of the St Lucia estuarine system, South Africa, and their responses to mouth management. African Journal of Aquatic Science 31 (1), 31-41.

Turunen, J., Tomppo, E., Tolonen, K., Reinikainen, A., 2002. Estimating carbon accumulation rates of undrained mires in Finland - Application to boreal and subarctic regions. Holocene 12 (1), 69-80.

Tyson, P.D., Preston-Whyte, R.A., 2000. The weather and climate of southern Africa, Oxford University Press Incorporated, Cape Town, South Africa.

Vaeret, L., Sokolic, F., 2008. Methods for studying the distribution of groundwater-dependent wetlands: a case study from Eastern Shores, St Lucia, South Africa, in: Responses to global change and management actions in coastal groundwater resources, Norwegian University of Life Sciences.

Valsecchi, V., Chase, B.M., Slingsby, J.A., Carr, A.S., Quick, L.J., Meadows, M.E., Cheddadi, R. and Reimer, P.J., 2013. A high resolution 15,600-year pollen and microcharcoal record from the Cederberg Mountains, South Africa. Palaeogeography, Palaeoclimatology, Palaeoecology 387, 6-16.

Venter, C.E., 2003. The vegetation ecology of Mfabeni peat swamp, St Lucia, KwaZulu-Natal. MSc Thesis, University of Pretoria.

Vogel, J.C., Fuls, A., 1978. The Geographical Distribution of Kranz Grasses in South Africa. South African Journal of Science 74, 209-215.

Vrdoljak, S.M., Hart, R.C., 2007. Groundwater seeps as potentially important refugia for freshwater fishes on the Eastern Shores of Lake St Lucia, KwaZulu-Natal, South Africa. African Journal of Aquatic Science 32 (2), 125-132.

Walther, S.C., Neumann, F.H., 2011. Sedimentology, isotopes and palynology of late Holocene cores from Lake Sibaya and the Kosi Bay system (KwaZulu-Natal, South Africa). South African Geographical Journal 93 (2), 133-153.

Worrall, F., Reed, M., Warburton, J., Burt, T., 2003. Carbon budget for a British upland peat catchment. Science of the Total Environment 312 (1-3), 133-146.

Chapter 3:

Biomarker records of palaeoenvironmental variations in subtropical Southern Africa since the late Pleistocene: evidences from a coastal peatland

A presentation of the submitted research paper

This manuscript has been submitted to the research Journal *Palaeogeography, Palaeoclimatology, Palaeoecology* and has been under review since April 2015.

The Biomarker samples were extracted, separated, analysed and compounds identified by myself under the guidance of Dr Routh. I was responsible for the data processing, generation of all the figures and data tables, concept design and write up of the article. The manuscript was revised and improved based on oral and written feedback from Dr Routh. Prof Roychoudhury assisted in the final editing of the manuscript.

Biomarker records of palaeoenvironmental variations in subtropical Southern Africa since the late Pleistocene: evidences from a coastal peatland

Andrea BAKER[1], Joyanto ROUTH[2], Alakendra N. ROYCHOUDHURY[1]*

[1]Department of Earth Sciences, Stellenbosch University, Stellenbosch, South Africa

[2]Department of Thematic Studies – Environmental Change, Linköping University, 58183, Linköping, Sweden

Abstract

Southern Africa's unique global position has given rise to a dynamic climate influenced by large sea surface temperature gradients and seasonal fluctuations in the Inter Tropical Convergence Zone. Due to the region's semi-arid climate, terrestrial palaeorecords are rare and our understanding of the long-term sensitivity of these ecosystems to climatic drivers is ambiguous. An 810 cm continuous peat core was extracted from the Mfabeni peatland with a ^{14}C basal age of ca. 47 thousand years calibrated before present (kcal yr BP), positioning it as one of the oldest known coastal peatlands. This peat core provides an opportunity to investigate palaeoenvironment changes in sub-tropical Southern Africa since the late Pleistocene. Biomarker (*n*-alkane, *n*-alkanoic acid and *n*-alkanol) analysis, in conjunction with previously published bulk geochemical data, was employed to reconstruct organic matter (OM) sources, rates of OM remineralisation and peatland hydrology. Our results showed that the principal OM source into the peatland was emergent and terrestrial plants with exception of during shallow lake conditions when submerged

macrophytes dominated (ca. 44.5 – 42.6, 29.7, 26.1 – 23.1, 16.7 – 7.1 and 2.2 kcal yr BP). *n*-Alkane proxies suggest that local plant assemblages were predominantly influenced by peatland hydrology. By incorporating temperature sensitive *n*-alkanoic acid and *n*-alkanol proxies, it was possible to disentangle the local temperature and precipitation changes. Based on the results, we report variations in precipitation intensities, but subdued temperature fluctuations during the late Pleistocene. The Holocene period was characterised by overall elevated temperatures and precipitation compared to the preceding glacial period, interspersed with a millennial scale cooling event. A close link between the Mfabeni archive and adjacent Indian Ocean marine core records was observed, suggesting regional ocean surface temperatures to be the dominant climate driver in the region since the late Pleistocene.

Keywords: Southern Africa; Biomarkers; Late Pleistocene; Holocene; Palaeoenvironment; Sub-tropical peatland.

1. Introduction

Southern Africa is situated at a dynamic junction between tropical, sub-tropical and temperate climate systems. The region is dominated by large seasonal fluctuations in the Inter Tropical Convergence Zone (ITCZ; Stokes et al., 1997), and high sea surface temperature (SST) gradients between the warm Agulhas and cold Benguela oceanic currents fringing the region (Preston-Whyte and Tyson, 1998; Tyson and Preston-Whyte, 2000). Uncertainty, however, still surrounds the mechanism of interaction between these different climate drivers and whether terrestrial ecosystems in the region responded abruptly or gradually to the ensuing climatic shifts, most notably during the transition from the last glacial maximum (LGM) to the Holocene. The biggest hindrance to understanding Southern Africa palaeoclimate (and the environmental responses to climate fluctuations) is the general lack of continuous terrestrial archives (Nash and Meadows, 2012; Scott et al., 2008), mainly due to the region's topography and a semi-arid climate not being conducive for the preservation of climate archives (Chase and Meadows, 2007).

Regional terrestrial archives in Southern Africa that have been explored vary from speleothems (Holmgren et al., 2003; Holzkämper et al., 2009; Lee-Thorp et al., 2001; Talma and Vogel, 1992), coastal or inland lake sediments (Kristen et al., 2010; Meadows et al., 1996; Neumann et al., 2008, 2010; Partridge, 2002; Walther and Neumann, 2011) and regional peatlands (Baker et al., 2014; Finch and Hill, 2008; Norström et al., 2009) to *hyrax* midden deposits (Chase et al., 2010, 2011, 2012; Valsecchi et al., 2013) and multi-archive studies (Chase and Meadows, 2007; Chase and Thomas, 2007; Meadows, 2001; Meadows and Baxter, 1999; Scott et al., 2008). Nonetheless, these archives record site specific palaeoenvironmental conditions over varying time intervals, and only a few extending as far back as the LGM. Many records are temporally discontinuous, suffer from dating uncertainties and tend to be geographically clustered resulting in lack of ubiquitous distribution of archives across the region. In addition, conclusions derived from different proxies often yield different results and magnitudes in response to the perceived climate variability in the region. Therefore, additional high resolution multi-proxy and multi-archive regional studies are required to elucidate terrestrial environmental responses to past climatic shifts in Southern Africa.

Peat deposits are ideally suited for palaeoclimate research. Their high degree of preservation and predominantly climate regulated autochthonous depositional regimes (Strack et al., 2008); make them conducive for reconstructing environmental responses to climate fluctuations. Although some studies have been done on peatlands in the tropics (Anderson and Muller, 1975; Dommain et al., 2011, 2014; Kurnianto et al., 2014; Norström et al., 2009; Page et al., 2011; Staub and Esterle, 1994), the majority of peatland research undertaken has mainly focused on northern Hemisphere boreal/temperate peatlands, and as a result, limited scientific understanding exists of the processes that regulate carbon (C) cycling in sub-tropical and tropical peatlands (Chimner and Ewel, 2005), and how peatland C flux responds to climate change. The Mfabeni peatland core returned a basal ^{14}C age of ca. 47 thousand years calibrated before present (kcal yr BP; 805 cm), positioning it as one of the oldest continuous coastal peatland records globally (Baker et al., 2014; Finch and Hill, 2008; Grundling et al., 2013). The peatland owes its longevity to the protection against sea level fluctuation, and enhanced groundwater transmissivity (Grundling et al., 2013) of a ca. 100 m high coastal dune corridor (ca. 55 kcal yrs BP; Porat and Botha; 2008) that separates

the Mfabeni basin from the Indian Ocean. This unique archive offers us an opportunity to explore, in high-resolution, environmental responses to palaeoclimatic fluctuations in Southern Africa since the late Pleistocene.

Of special interest for palaeoclimate researchers are the records of molecular proxies preserved in geological archives. Biomarker proxies have been widely used by researchers to delineate organic matter (OM) sources, moisture, preservation and ambient temperatures in boreal / temperate peatlands and lakes (Andersson et al., 2012, 2011; Bai et al., 2009; Ficken et al., 1998; Ishiwatari et al., 2005; Nichols et al., 2006; Ogura et al., 1990; Rieley et al., 1991; Routh et al., 2014; Wang et al., 2012; Xie et al., 2004; Zheng et al., 2011a, 2007; Zhou et al., 2010); sub-tropical lakes, estuaries and wetlands (Al-Mutlaq et al., 2008; Ficken and Farrimond, 1995; Huang et al., 1999; Jaffé et al., 2001; Mead et al., 2005; Ranjan et al., 2015; Zhou et al., 2005); marine sediments (Hu et al., 2002; Pancost and Boot, 2004), aerosols (Bendle et al., 2007, 2006; Schefuß et al., 2003) and semi-arid soils (Carr et al., 2014). However, while these biomarker palaeoproxies are established tools for elucidating palaeoenvironments (Meyers 2003), they each individually suffer from unique limitations, and therefore should be interpreted with caution and always employed within a multi-proxy approach to mitigate their inadequacies.

The aim of our study is to explore the late Pleistocene and Holocene environment and to reconstruct the climatic controls governing the Mfabeni peatland in southern Africa (Figure 1). We employ a combination of established biomarker ratios as part of a multi-proxy study to reconstruct fluctuations in OM sources, palaeohydrology and microbial reworking. These reconstructions are then used to infer climatic conditions that could have driven these environmental changes. We substantiate our findings by comparing the Mfabeni archive with other regional climate records.

2. Methods

2.1. Site description

The UNESCO World Heritage iSimangaliso Wetland Park is situated on the northern shores of Kwazulu-Natal province, South Africa (Figure 1). Within the park, the shallow 350 km^2 St Lucia

Lake forms part of the largest estuarine wetland system on the African continent (Vrdoljak and Hart, 2007). On the eastern shores of Lake St Lucia, the Mfabeni fen lies within an interdunal valley (Botha and Porat, 2007) measuring ca. 10 x 3 km (Clulow et al., 2012; Grundling et al., 2013), and up to 11 m deep (Grundling et al., 2013; Grundling, 2001).

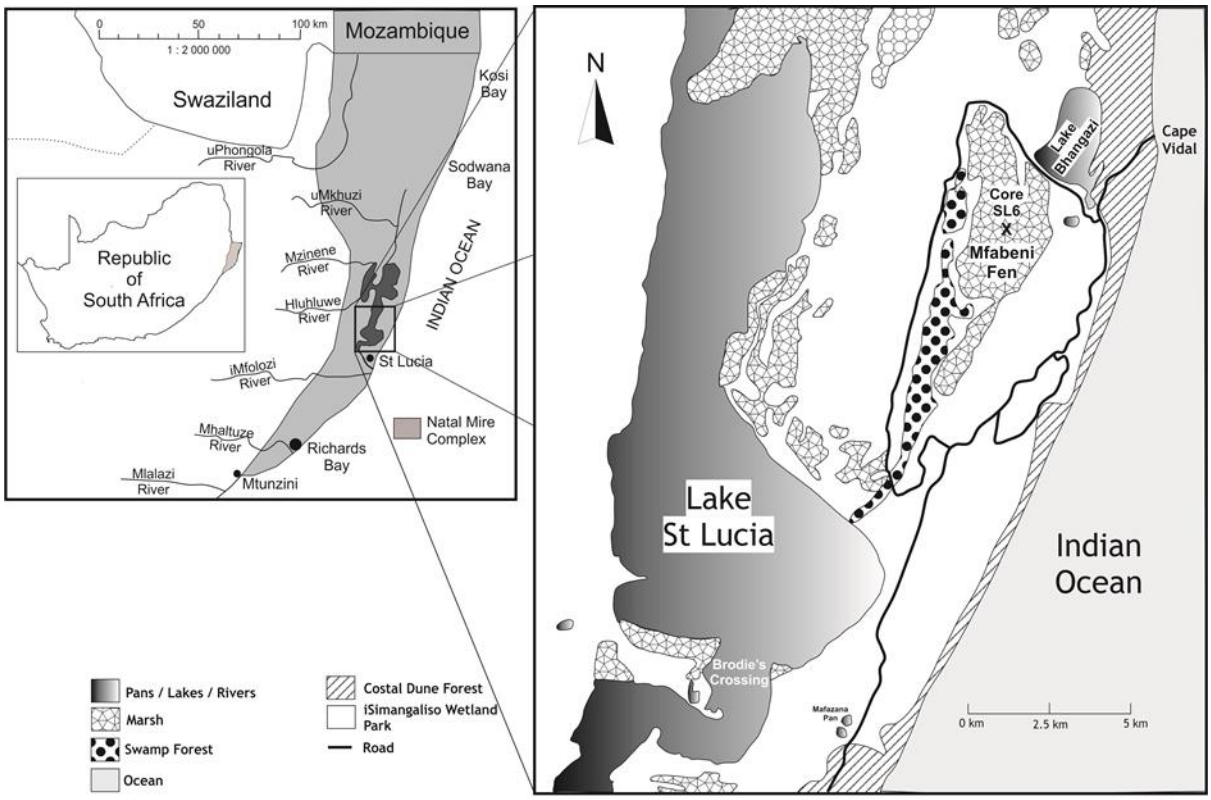

Figure 1: Core SL6, Mfabeni peatland, iSimangaliso Wetland Park, Kwazulu-Natal, South Africa

The fen's hydrology is influenced primarily by the Maputaland aquifer, that is structurally controlled by the north-south aligned coastal dune corridor, (Grundling et al., 2013; Taylor et al., 2006a; Venter, 2003) and local precipitation. The region has a sub-tropical climate and experiences mainly austral summer rainfall of between 900 and 1200 mm/yr (Grundling, 2001; Taylor et al., 2006b). However, distinct cyclical dry-wet periods have been identified in the contemporary rainfall records from this region (Bate and Taylor, 2008). The Mfabeni fen forms part of the greater Natal Mire Complex (NMC; Figure 1) that extends from southern Mozambique to the south of Richards Bay, Kwazulu-Natal, and was formed by valley infilling within the KwaMbonanbi formation coastal dune depression (Smuts, 1992). The iSimangaliso wetland park vegetation is made up of Maputaland wooded grassland, coastal belt and sub-tropical freshwater wetland and northern

coastal forests (Mucina et al., 2006), whereas the fen itself is dominated by herbaceous reed sedges and grasses (Finch, 2005).

2.2. Sampling techniques

Core SL6 was extracted from the middle of the Mfabeni fen (28.15021^{0}S; 32.52508^{0}E) to a depth of 810 cm in consecutive coring events, using a Russian peat corer consisting of a 5 cm diameter and 50 cm long core chamber. The continuous core samples were logged in the field, and later described and sectioned into 1-2 cm intervals in the laboratory, after which the sediments were freeze-dried for various analysis.

2.3. Radiocarbon dating / age model

^{14}C radiocarbon dating and age-depth modelling was done as per methods listed in Baker et al. (2014) and references therein. Nine selected raw peat samples were measured on a Compact Carbon AMS and conventional ^{14}C ages were calculated using a correction factor for isotopic fractionation (supplementary data Table A1). These ages were then calibrated using the northern hemisphere terrestrial calibration curve IntCal09 with a 40 ±20 ^{14}C year southern hemisphere offset (McCormac et al., 1998; supplementary data figure S1). Ages were then adjusted using the age-depth Bacon modelling software (Blaauw and Christeny, 2011).

2.4. Lipid extraction

A modified lipid extraction was undertaken as per the protocol set out by Wakeham et al. (2002) on 36 selected peat samples spanning the length of core SL6 and analysed for *n*-alkane, *n*-alkanoic acid and *n*-alkanol concentrations. The geochemical analyses were measured on the same intervals (including the nine ^{14}C radiocarbon dated samples). Approximately 2g of freeze-dried sediment, including recovery standard (deuterated hexatriacontane), was extracted with a mixture of CH_2Cl_2 and CH_3OH (9:1 v/v) on a Dionex automated solvent extractor for two successive cycles (1000 psi at 75^{0}C and 140^{0}C, respectively). An aliquot of the extracted total lipid extract (TLE) was saponified with 0.5N KOH (in methanol) at 100 ^{0}C for 2 hours. After cooling, 5% NaCl was added to the TLE, agitated and then washed with successive aliquots of hexane to separate the neutral (TLE-N) and acidic (TLE-A) fractions. The TLE-N fraction was then introduced into a long glass

column packed with deactivated 60 mesh silica gel. The *n*-alkane (F1) fraction was first eluted by passing 10 mL of hexane and then 5 mL of 25% toluene: 75% hexane solution, while the *n*-alkanol (F2) fraction was eluted by sequentially introducing 5 mL aliquots of increasing percentages of ethyl acetate in hexane (5% ethyl acetate: 95% hexane; 10% ethyl acetate: 90% hexane; 15% ethyl acetate: 85% hexane and 20% ethyl acetate: 80% hexane). The condensed F2 extract was then derivitized with BSTFA and pyridine at 70 ^{0}C for 2 hours. The TLE-A fraction was acidified with 6N HCL, extracted with hexane and derivitized with 10% BF3 (in methanol) for 2 hours at 100 ^{0}C. All extracts were spiked with internal deuterated-tetracosane and androstane standards. The samples were then injected in splitless mode into an Agilent 6890N gas chromatography (GC) interfaced to a 5973 MSD mass-spectrometer (MS) with a DB-5 (5%phenyl, 95% dimethyl polysiloxane) fused silica capillary column (30 m length x 0.25 mm i.d. x 0.25 µm film thickness). The GC oven was started at 35 °C held isothermally for 1 min, and increased to 130 °C at 20 °C min-1, the temperature was further increased to 320 °C at 6 °C min-1 and held isothermally for 15 min. The MS was operated at 70 eV under full-scan mode (m/z 50-500), with a run-time of 57.42 min. The compounds were identified based on their retention time and fragmentation patterns using the NIST MS Library (Version 2.0) / Lipid library (2011) and S-4066 standard (*n*-alkanes C_{14} – C_{32}even + Pristane/Phytane from CHIRON). Recovery of deuterated hexatriacontane added prior to initial extraction ranged from 75-85%. Internal standards detection limits ranged from 0.1 to 1 ng/mg and sample reproducibility was ± 10%. Biomarker GCMS counts were normalised with respect to % total organic carbon (TOC).

2.5. Proxies

A geochemical proxy is a chemical compound that can be used to infer a relationship between a specific physical process and a corresponding change in the said chemical component as a result of on-going processes or one that happened in the past (Hillaire-Marcel and de Vernal, 2007). The most valuable proxies are those for which a single or dominant controlling factor can be identified, and for which, preserved signals are responsive to changes in the primary process. The biomarker literature has numerous examples of its applications in tracing changes in terrestrial, lacustrine and oceanographic settings (Meyers, 2003, 1997; Peters et al., 2004). Some of these

diagnostic biomarker proxies which have been used to interpret the palaeoenvironmental conditions in previous studies, and also used in this study, are summarized in Table 1.

3. Results

3.1. Biomarker C_{max} and homologue distributions

Core SL6 (supplementary data Figure S2 and table A2) is dominated by long chain *n*-alkanes with odd-over-even predominance and carbon chain maximums (C_{max}) at *n*-C_{29} and *n*-C_{31} (38% and 24%, respectively). At ca. 24.5 and between 12.7 and 9.2 kcal yr BP, C_{max} occurs at either *n*-C_{23} or *n*-C_{25}, whereas remaining parts of the core exhibit long chain *n*-alkane C_{max} values (>*n*-C_{25}). The *n*-alkanoic acid distributions show a predominant bi-modal distribution of C_{16} and mid-length chain monomers (C_{22}/C_{24}), with prevalence for even-over-odd arrangements and C_{max} of *n*-C_{22} (78%). Likewise, the *n*-alkanols also exhibit a general bi-modal distribution of mid-length and long chain monomers, but relative low even-over-odd predominance and dominant C_{max} of *n*-C_{22} (51%).

Table 1: Summary of biomarker proxies

Proxy	Acronym	Equation	Background	Indications	References
Carbon preference index (all)	CPI	$CPI_1 = [\Sigma(C_{21} - C_{29})\ odd + \Sigma(C_{23} - C_{31})\ odd]/\ 2\Sigma(C_{22} - C_{30})\ even$ $CPI_2 = [\Sigma(C_{20} - C_{30})\ even + \Sigma(C_{22} - C_{32})\ even]/2\Sigma(C_{21} - C_{31})\ odd$	Plants produce leaf wax with odd-over-even (*n*-alkane) or even-over-odd (*n*-alkanonic acid & *n*-alkanol) predominance. During diagenesis, this odd over even or even over odd characteristic diminishes.	↑ Better preserved or less labile OM source e.g. terrestrial vs submerged OM input; ↓ More degraded or more labile OM source	Rieley et al., 1991; Zhou et al.,2010, 2005; Andersson et al., 2012
Average chain length (all)	ACL	$ACL_1 = (\Sigma[Ci]\ x\ i) / \Sigma[Ci]$, for i = 23 – 33 where Ci = conc. of n–alkane containing i carbon atoms; $ACL_2 = (\Sigma[Ci]\ x\ i) / \Sigma[Ci]$, for I = 22 – 32 where Ci = conc. of n-alkanoic acid or n-alkanol containing i carbon atoms	Plants produce long chain leaf wax layers in response to drier and warmer conditions. Changes in ACL trends can be used to elucidate climatic conditions during photosynthesis.	↑ Longer average chain lengths in leaf wax layers e.g. hotter and drier conditions; ↓ shorter average chain lengths e.g. during cooler and wetter conditions	Gagosian and Peltzer, 1986; Schefuß et al., 2003; Zhou et al., 2005; Carr et al., 2014
Aquatic plant (*n*-alkanes only)	P_{aq}	$P_{aq} = \frac{C_{23} + C_{25}}{C_{23} + C_{25} + C_{29} + C_{31}}$	Aquatic plant leaf waxes are dominated by mid-chain alkanes (*n*-C_{23} & C_{25}). P_{aq} is used to elucidate relative amounts of aquatic vs. higher plant input.	↑ more aquatic plant OM input e.g. during higher water levels; ↓ More terrestrial plant OM input e.g. during low water levels	Cranwell, 1984; Ficken et al., 2000; Zhou et al., 2010, 2005; Andersson et al., 2011
Terrestrial plant (*n*-alkanes only)	P_{wax}	$P_{wax} = \frac{C_{27} + C_{29} + C_{31}}{C_{23} + C_{25} + C_{27} + C_{29} + C_{31}}$	Emergent and terrestrial plant leaf waxes have long-chain alkanes (*n*-C_{27}, C_{29} and C_{31}). P_{wax} indicates variation in terrestrial plant input in relation to bulk plant input.	↑ higher proportions of terrestrial plant OM input during low water levels; ↓ less terrestrial plant OM input during high water levels	Eglinton and Hamilton, 1967; Rieley et al., 1991; Zheng et al. 2007; Andersson et al., 2011
saturated vs. unsaturated (*n*-alkanoic acids only)	$Sat/unsat_{FA}$ $18:1/18:0_{FA}$ $16:1/180_{FA}$	Various ratios	Unsaturated short chain n-alkanoic acids are more susceptible to microbial reworking and the sat/unsat alkanoic acid ratios indicate microbial decomposition.	↑ higher proportions of saturated vs unsaturated n-alkanoic acids e.g. higher microbial reworking i.e. higher temperatures; ↓ less microbial reworking i.e. lower temperatures	Meyers & Kawka, 1984; Zhou et al., 2005

3.2. TOC and biomarker concentrations

As reported in Baker et al. (2014), the bulk TOC concentration (Figure 2, supplementary data Table A2) fluctuates between a maximum of 50.9% (ca. 3.4 kcal yr BP) and minimum of 4.5% (ca. 30.6 kcal yr BP), with no noticeable trend up core. Besides the relative high TOC values between ca. 45.7 and 41.1, 38.0, 23.1 and from ca. 14.8 kcal yr BP throughout the Holocene (with the

exception of at ca. 7.1 kcal yr BP), the core exhibits extreme low % TOC values at ca. 46.9, 30.6 and between 23.1 and 18.4 kcal yr BP, coinciding with the Heinrich 3 (H3) event and conclusion of the LGM.

The *n*-alkane concentration (supplementary data Figure S3 and Table A2) fluctuates between a maximum of 40.8 ng/mg TOC (ca. 16.7 kcal yr BP) and minimum of 2.4 ng/mg TOC (ca. 23.1 kcal yr BP), trending similarly to *n*-alkanoic acid concentrations. The *n*-alkanoic acid concentration exhibits a maximum of 200 (ca. 18.4 kcal yr BP) and minimum of 10.2 ng/mg TOC (ca. 14.8 kcal yr BP), trending similarly to the other biomarkers. The *n*-alkanol concentration shows a similar trend as *n*-alkanoic acids, with a maximum at ca. 18.4 kcal yr BP (36.2 ng/mg TOC) and minimum at ca. 27.4 kcal yr BP (0.1 ng/mg TOC).

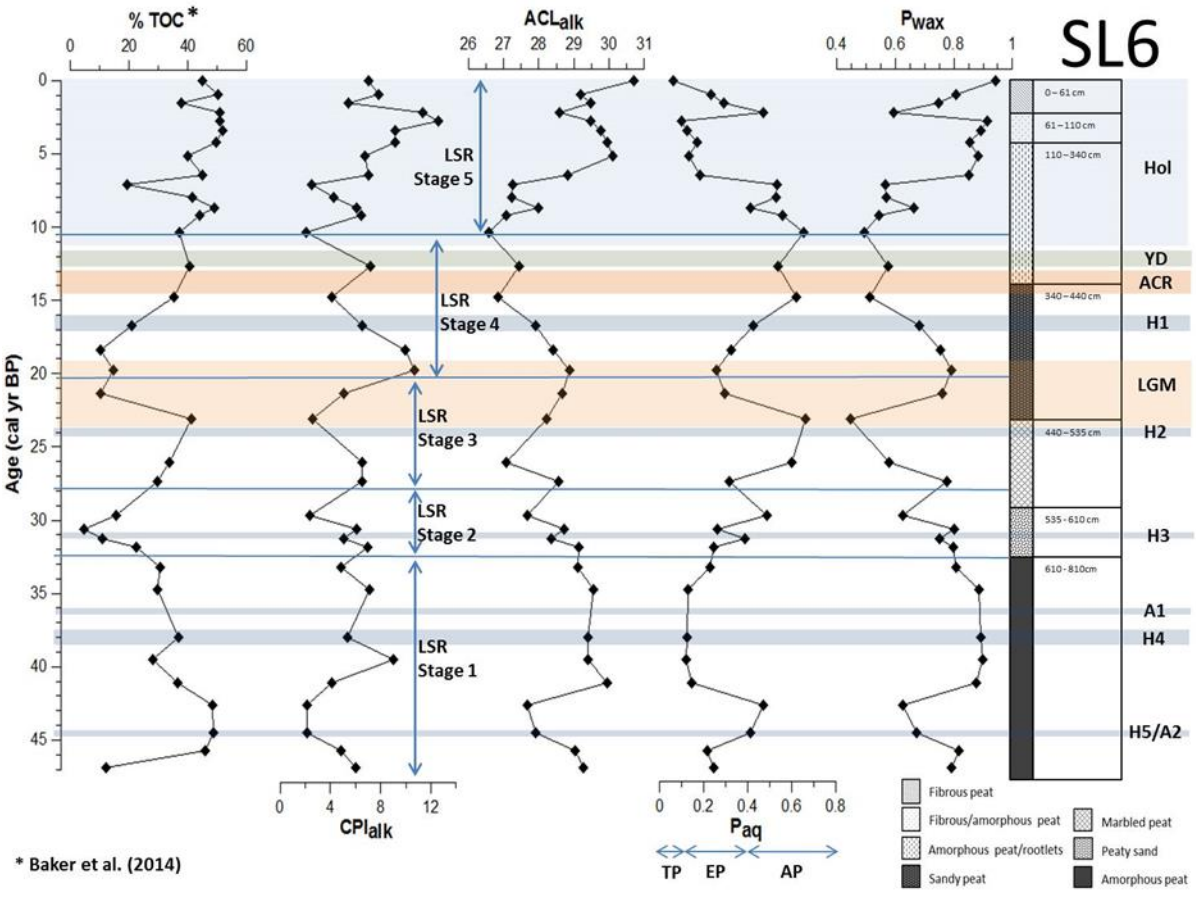

Figure 2: SL6 core %TOC plotted against *n*-alkane proxies, carbon preference index (CPI), average chain length (ACL), aquatic plant (P_{aq}) and terrestrial wax (P_{wax}) proxies. TP = terrestrial plants, EP = emergent plants and AP = aquatic plants. H1 – 5 = Heinrich events (dates from Hemming, 2004); A1 and A2 = Antarctic warming events (Blunier et al., 1998; Stocker, 2000); LGM = Last Glacial Maximum; ACR = Antarctic cold reversal (Stocker, 2000); YD = Younger Dryas; Hol = Holocene.

3.3. *n*-Alkane ratios

Core SL6 profile exhibits carbon preference index (CPI_{alk}; Figure 2, supplementary data Table A2) ranging between a minimum of 2.1 (ca. 42.6 kcal yr BP) and maximum of 12.6 (ca. 2.8 kcal yr BP), while the average chain length (ACL_{alk}) values range between a minimum of 26.6 (ca. 10.4 kcal yr BP) and maximum of 30.7 (present day); both display no notable up-core trends. The aquatic plant (P_{aq}) value ranges between 0.06 (present day) and 0.66 (ca. 23.1 kcal yr BP), while the terrestrial leaf wax (P_{wax}) proxy values range between a minimum of 0.45 (ca. 23.1 kcal yr BP) and a maximum of 0.94 (ca. 0 kcal yr BP), in an opposite trend compared to the P_{aq} values.

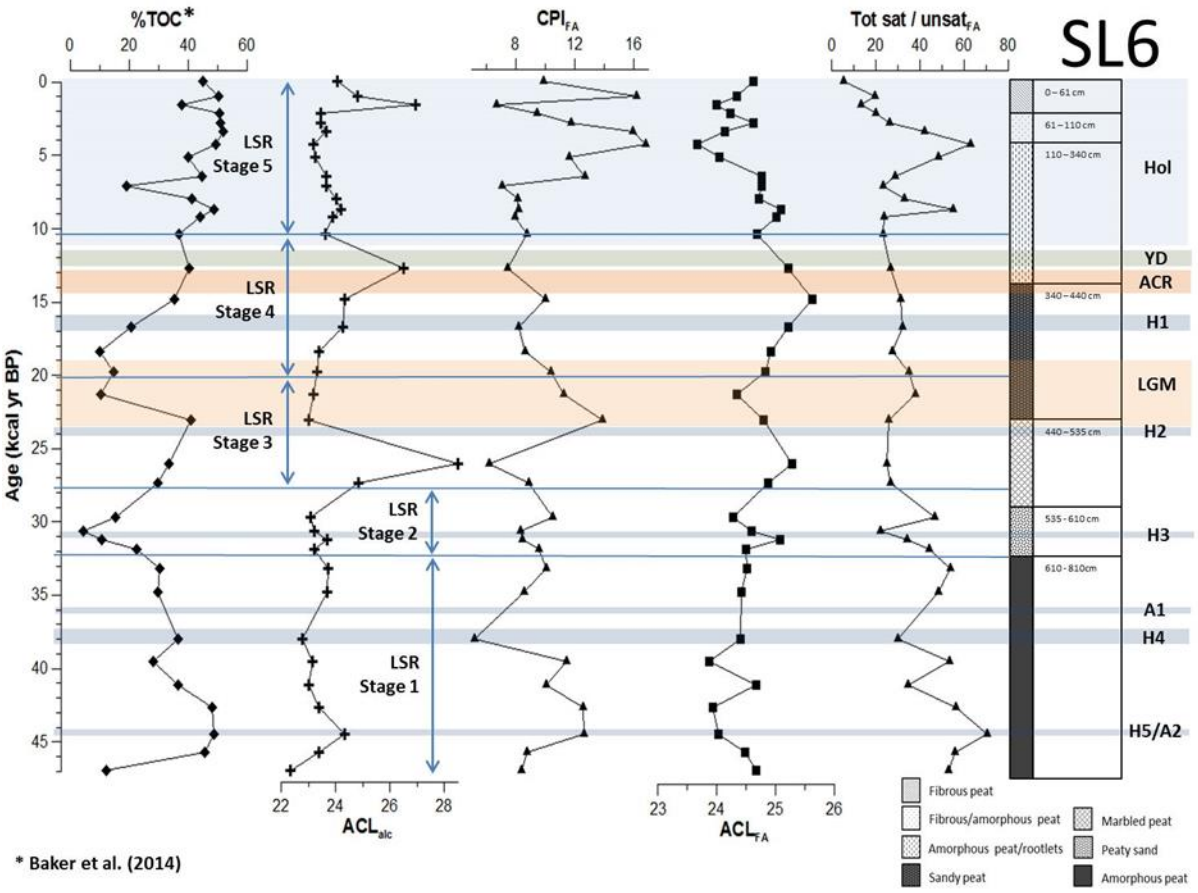

Figure 3: Core SL6 % TOC plotted against *n*-alkanol average chain length (ACL_{alc}), *n*-alkanoic acid carbon preference index (CPI_{FA}), average chain length (ACL_{FA}) and total concentration of saturated / unsaturated *n*-alkanoic acids ($sat/unsat_{FA}$). H1 – 5 = Heinrich events (dates from Hemming, 2004); A1 and A2 = Antarctic warming events (Blunier et al., 1998; Stocker, 2000); LGM = Last Glacial Maximum; ACR = Antarctic cold reversal (Stocker, 2000); YD = Younger Dryas; Hol = Holocene.

3.4. *n*-Alkanoic acid and *n*-alkanol ratios

The ratios between the unsaturated and saturated short chained (C_{16} and C_{18}; supplementary data Table A2) *n*-alkanoic acids trend towards zero within the top 76 cm and 157 cm, respectively with

only a few excursions to above average values for the $C_{18:1}/C_{18:0}$ between ca. 6.4 and 7.1 kcal yr BP, 10.4 and 30.6 kcal yr BP. The total saturated / unsaturated *n*-alkanoic acids ($sat/unsat_{FA}$) maximises at 70.5 (ca. 44.5 kcal yr BP; Figure 3, supplementary data Table A1) and minimizes at 5.1 (ca. 0 kcal yr BP), trending overall negatively with the $C_{16:1}/_{16:0}$ and $C_{18:1}/C_{18:0}$ ratios. The CPI values of the *n*-alkanoic acids (CPI_{FA}, Figure 3, supplementary data Table A2) fluctuate predominantly at below average values (<10) with the exception of between ca. 44.5 and 39.5, 23.1 and 19.8, 6.4 and 2.8 and 0.9 kcal yr BP, whereas the *n*-alkanoic acid average chain length (ACL_{FA}) fluctuates around the core average with a minimum of 23.6 (ca. 4.2 kcal yr BP) and maximum of 25.6 (ca. 14.8 kcal yr BP).

The CPI values for *n*-alkanols (CPI_{alc}; Figure 3, supplementary data Table A2) exhibit a low and narrow range of 0.25 (0.0 kcal yr BP) to 2.3 (ca. 26.1 kcal yr BP), whereas the *n*-alkanol ACL values (ACL_{alc}) fluctuates within a relatively narrow range averaging 23.9.

4. Discussion

4.1. Palaeoenvironment

In the tropics, peatlands are subject to consistently warm and often humid conditions. Although elevated temperatures facilitate microbial decomposition and rapid turnover of OM, these parameters also increases net primary production (NPP) due to longer growing seasons and associated higher local precipitation (Zheng et al. 2007). Because peat accumulates when NPP outstrips microbial decomposition (Chimner and Ewel, 2005), the overriding dominant control on (sub) tropical peat formation is the extent of waterlogging. Waterlogging enables anaerobic depositional conditions to prevail that ultimately retards the rate of decomposition and permits OM rich peat sediments to accumulate (Rieley et al., 1996). Even though air temperature and local precipitation determines the rate of NPP, microbial activity is additionally influenced by OM chemistry and reactivity, soil pH, redox conditions and accessibility to potential decomposers (Schmidt et al., 2011). The Mfabeni peatland began accumulating peat within an interdunal valley lined by a non-permeable clay layer after a palaeo-channel linking Lake St Lucia with the Mfabeni

basin was obstructed (Grundling et al., 2013). Once the basin was sealed, persistent groundwater input and local precipitation resulted in extended periods of waterlogging that allowed peat to accumulate. Consequently, the physical C accumulation parameters (linear sedimentation rates, mass accumulation rates and carbon accumulation rates) in core SL6 were used by Baker et al. (2014) to reconstruct changes in sedimentation regimes which they argued were ultimately controlled by climate.

Fluctuations in TOC concentrations in core SL6 is the measure of changes in OM production, deposition and subsequent preservation in the Mfabeni peat deposit (Baker et al., 2014; Zheng et al., 2007). The periods of relatively elevated TOC concentrations (ca. 45.7 - 41.1, 38.0, 23.1, from 14.8 kcal yr BP up to and including the majority of the Holocene; Figures 2 and 3) suggests that conditions were ideal for OM preservation, either as a consequence of high NPP (and high sedimentation rates) or waterlogged anoxic depositional conditions that retarded OM remineralisation, or a combination of both. Vegetation types also played a role in OM preservation. Long-chain *n*-alkanes emanating from epicuticular waxes of emergent and terrestrial plants (like grasses and sedges) are more resistant to microbial decomposition when compared to the mid- and short-chain *n*-alkanes from submerged macrophyte and algal sources, respectively (Meyers, 1997; Meyers and Ishiwatari, 1993). Alternatively, during periods of extremely low TOC concentrations (ca. 46.9, 30.6 and between 23.1 and 18.4 kcal yr BP; Figures 2 and 3), the dominant cause for low OM preservation would have been low peatland water levels and persistent aerobic microbial remineralisation and, to a less extent, declining NPP, both of which can be linked to the prevailing climatic conditions.

4.1.1. Organic matter sources

Since *n*-alkanes are more recalcitrant than other hydrocarbons, they are regarded as one of the more promising indicators of OM sources in sediments. The Mfabeni peat deposit is dominated by long chain n-alkanes (>*n*-$C_{23;}$ supplementary data Figure S2) suggesting that throughout the peatlands' ± 47 k years of depositional history, higher terrestrial plants have been the primary source of OM input. Although core SL6 *n*-alkane C_{max} values (supplementary data Table A2) are dominated by *n*-C_{29} (36%) and *n*-C_{31} (26%), which are indicative of both woody plants and

graminoids (Jaffé et al., 2001; Mead et al., 2005), at ca. 24.5, 14.8 to 9.2 and 8.0 to 7.0 kcal yr BP, the core displays C_{max} values of either *n*-C_{23} or *n*-$C_{25,}$ corresponding to dominant OM inputs from submerged macrophytes or mosses (Cranwell, 1984; Ficken et al., 2000; Mead et al., 2005; supplementary data Table A2). Both the *n*-alkanoic acids and *n*-alkanols exhibit bimodal distributions of either short and mid-chain or mid- and long chain homologues, respectively, reflecting the mixed origins of both primary plant and secondary microbial sources for these biomarkers (supplementary data Figure S2).

When comparing the trends in total concentrations of the three biomarkers analysed in this study (supplementary data Figure S3 and Table A3), the *n*-alkanes versus *n*-alkanoic acids (r=0.56, P=0.01, df=34) and *n*-alkanoic acids versus *n*-alkanols (r=0.41, P=0.01, df=34) show strong positive and significant correlations, implying they share a common primary plant source. However, since the homologue distributions of the *n*-alkanoic acids and *n*-alkanol biomarkers are comparatively different to the *n*-alkane distributions (supplementary data Figure S2), we can infer that these two relatively labile biomarkers have in part been diagenetically altered and their OM source signatures partially overprinted by secondary microbial biomarkers, similarly to the biomarker distributions observed in the Hani peat sequence (Zhou et al., 2010).

Several studies have used the P_{aq} (Ficken et al., 2000) and P_{wax} (Zheng et al., 2007) palaeohydrology proxies, in conjunction with other geochemical proxies, to explore shifts between dominant moss and vascular plant input into the northern hemisphere *Sphagnum* peatlands, and reconstruct past water levels (Andersson et al., 2011; Nichols et al., 2006; Zheng et al. 2007; Zhou et al., 2010, 2005). However, in sub-tropical peatlands, mosses are rare if not completely absent. Consistent with this, the Mfabeni palynology study by Finch and Hill (2008) showed little evidence of moss spores, which leads us to conclude that the mid-chain length *n*-alkanes reported in core SL6, are predominantly of submerged macrophyte origin. The interpretation of the P_{wax} proxy, on the other hand, could be complicated by the fact that emergent macrophytes (in particular sedges) thrive in seasonally inundated sub-tropical peatlands, and display homologue distributions similar to terrestrial plants (Ficken et al., 1998, 2000). Nevertheless, during exceptionally high water levels that facilitate proliferation of submerged plants, the oxic water / sediment interface layer is

reduced substantially resulting in a lack of adequate oxygen to support vascular plant roots (Nichols et al., 2009). As a consequence, submerged and emergent macrophytes are unlikely to occupy the same habitat at the same time. Consistent with this, core SL6 exhibits a significant negative correlation between P_{aq} and P_{wax} ($r = -0.98$; $P = 0.01$; $df = 37$; Figure 2), validating the antagonistic link between these two proxies, and their expediency for understanding past peatland hydrology. The majority of the P_{aq} values in core SL6 falls within the dominant emergent plant range (0.1-0.4; Ficken et al., 2000) with the exception of ca. 44.5 – 42.6, 29.7, 26.1 – 23.1, 16.7 – 7.1 and 2.2 kcal yr BP where a submerged / floating plant signature is exhibited (>0.4), and present day sediments indicating a dominant source of terrestrial OM input (<0.1).

Although Gagosian and Peltzer (1986) observed overall longer chain *n*-alkane wax lipids in vascular land plants growing in warm climates, compared to cold climate species, other authors (Andersson et al., 2011; Bush and McInerney, 2013; Schefuß et al., 2003; Zhou et al., 2010, 2005) have reported that ACL_{alk} values respond more strongly to changes in moisture. Core SL6 exhibits a significant negative relationship between $P_{aq,}$ and ACL_{alk} signals ($r= -0.83$; $P= 0.01$; $df = 37$; Figure 2), suggesting a causal link between peatland water levels and ACL_{alk} values. The relative abundance of different plant species can also impact the ACL_{alk} signal by producing distinct *n*-alkane distributions as a result of shifts in plant assemblages in response to changing peatland hydrology (Cranwell, 1974; Schwark et al., 2002). The contemporary local dominant *Poaceae* (grasses) and *Cyperaceae* (sedges) present in the peatland today is represented by ACL_{alk} and P_{wax} core maximums (30.8 and 0.94), and P_{aq} core minimum (0.06, supplementary Table A2; Figure 2) in surface sediments, which validates these proxies as an indicator of palaeovegetation assemblages. Excursions to elevated ACL_{alk} values (between ca. 41.1 and 33.2, 5.2 and 2.8, and 1.5 kcal yr BP to present), coincides with low P_{aq} values (Figure 2), most probably as a result of increased inputs of grasses in response to drier conditions (Cranwell, 1974). This is consistent with the high frequency of local *Poaceae* macrofossils documented in the Mfabeni palynology study (Finch and Hill, 2008) during the same periods.

CPI_{alk} values have often been used to infer palaeoenvironmental conditions that were either conducive or unfavourable for microbial decomposition in temperate, boreal and continental humid

peat deposits (Andersson et al., 2011; Routh et al., 2014; Xie et al., 2004; Zheng et al., 2007; Zhou et al., 2005, 2010). These authors attributed the high CPI values to cold conditions that retarded the rate of microbial alteration of *n*-alkanes. However, the typically moderate cooling experienced in African low latitude areas (Bard, et al., 1997) during the LGM, which Finch and Hill (2008) specifically attribute to the Mfabeni peatland's proximity to the ocean, resulted in a negligible temperature effect on the rate of microbial decomposition. Nonetheless, it is not only thermal dynamics that dictates the extent of degradation in sub-tropical peatlands, but also lability of OM and the amount of oxygen available during deposition. The CPI_{alk} profile (Figure 2) exhibits an opposite trend to TOC concentrations up until the Pleistocene-Holocene boundary ($r = -0.46$; $P = 0.01$, $df = 23$), after which both profiles trend positively ($r = 0.78$, $P = 0.01$, $df = 12$). The opposite trend exhibited during the Pleistocene implies that OM source bioreactivity, as opposed to depositional dynamics played the dominant role in peat accumulation in the Mfabeni peatland. Furthermore, the P_{aq} signal exhibits a significant negative relationship with CPI_{alk} ($r= -0.51$, $P=0.01$, $df=37$; Figure 2), which demonstrates that low CPI values are concordant with increases in mid-chain *n*-alkane submerged macrophyte input (e.g. from ca. 44.5 –41.2, 24.5 and 10.4 kcal yr BP; Figure 2). Since the degree of waterlogging is typically the driving factor for OM preservation in subtropical peats (Rieley et al., 1996), it can be postulated that during periods of elevated TOC concentrations, the extent of waterlogging could have been sufficient to support increased and/or dominant submerged macrophyte populations. This increase in in-situ aquatic plants would have in turn resulted in SOM with relatively lower CPI_{alk} signatures owing to the less recalcitrant mid-chain *n*-alkanes prevalent in submerged aquatic plants (Meyers, 1997; Meyers and Ishiwatari, 1993).

The reason for the switch to a positive trend between TOC and CPI_{alk} profiles during the Holocene is not easily explained, however, the dramatic adjustment in peat accumulation dynamics could offer some insights. The extreme shift in average C accumulation rates (see Baker et al., 2014: Figure 4 and details therein) from 12 g $C.m^{-2}.yr^{-1}$ during the Pleistocene to 32 $C.m^{-2}.yr^{-1}$ in the Holocene, suggests a sharp increase in both NPP and OM preservation in the Mfabeni peatland. This trend implies that peat accumulation occurred as a result of high sedimentation rates in the

basin. This observation is further supported by the overall increase in CPI_{alk} and decreasing P_{aq} values (Figure 2) recorded during the Holocene. All these trends indicate a dominant emergent and terrestrial higher plant OM source input towards the mid- and late Holocene, and supports the inference of a combined higher NPP and low OM decomposition due to high sedimentation rates, and a refractory OM source. The relatively minor differences between the LGM and Holocene average temperature in the Southern African sub-tropics, compared to higher latitudes (Bard et al., 1997; Chevalier and Chase, 2015; Finch and Hill, 2008), can arguably be the reason for both the CPI_{alk} and ACL_{alk} proxies exhibiting more dominant moisture variability, as opposed to temperature effects.

4.1.2. Microbial alteration

Since microbial decay of OM tends to be reduced during cool and dry climatic conditions (Kuder and Kruge, 1998), biomarkers that are more susceptible to microbial reworking have previously been employed to reconstruct palaeoenvironmental conditions, mostly in temperate peatlands and lake archives (Bai et al., 2009; Zheng et al., 2007; 2011a, 2011b; Zhou et al., 2005, 2010). The Mfabeni peatland experienced relatively minor variations in temperature during the last glacial and interglacial transition (Finch and Hill, 2008) and C accumulation was mainly controlled by waterlogging and, to a lesser extent, NPP. Consistent with this, the positive and significant relationship between total sat/$unsat_{FA}$ ratio and TOC concentration ($r=0.36$, $P=0.05$, $df=37$; Figure 3) suggests that when there was an increase in C preservation, there was a corresponding increase in microbial alteration of unsaturated *n*-alkanoic acids. This relationship implies that during times of high peatland water levels (and associated anaerobic induced low decomposition rates as a result of increased precipitation); temperatures were also been elevated. Although temperature variations in the Mfabeni peatland did not significantly affect local plant physiology (i.e. increased waxy coatings; ACL_{alk}), it seems to have had an effect on microbial decomposition. Chevalier and Chase (2015) analized 13 regional pollen sequences in the SRZ of South Africa and concluded that a positive relationship existed between temperature and rainfall in the north eastern parts of South Africa, at least during the Late Pleistocene. Additionally, since short chained unsaturated *n*-alkaonic acids (*n*-C_{16} and *n*-C_{18}) are up to 7 times more susceptible to microbial

alteration than their long chained saturated counterparts (Haddad et al., 1992), the rapidly decreasing $C_{16:1/16:0}$ and $C_{18:1/18:0}$ *n*-alkanoic acids (supplementary data Table A2) observed down core in the Mfabeni, reinforces the sat/unsat$_{FA}$ ratios as a reliable proxy for microbial reworking and palaeotemperature reconstructions in sub-tropical peatlands.

According to Zhou et al. (2010), high peat CPI$_{FA}$ values can indicate either elevated preservation of the original OM plant material or overprinting of secondary biomarker acids produced by microbes during diagenesis. Because *n*-alkanoic acids are highly susceptible to degradation (Meyers, 2003), it could be argued that high CPI$_{FA}$ values in core SL6 indicate intensive microbial reworking of primary plant acids into secondary microbial acids. To this degree, the positive and significant statistical correlation between CPI$_{FA}$ and sat/unsat$_{FA}$ data sets ($r = 0.32$, $P = 0.05$, $df = 37$; Figure 3) imply that during periods of increased microbial reworking of unsaturated *n*-alkanoic acids, and therefore higher ambient temperatures, the corresponding higher CPI$_{FA}$ values were as a result of an increase in post-depositional secondary microbial acids production, at the expense of the primary plant acids. Furthermore, both the ACL$_{alc}$ and ACL$_{FA}$ data sets trend negatively to sat/unsat$_{FA}$ data set ($r = -0.34$, $P = 0.05$, $df = 37$; $r = -0.41$, $P = 0.01$, $df = 37$, respectively; Figure 3). This reinforces the palaeoenvironmental link established above between lower plant wax ACL$_{alc}$ and ACL$_{FA}$ values during high peatland water levels and temperature induced increases in microbial reworking of *n*-alkanoic acids.

4.2. Palaeoenvironment reconstruction

By combining the palaeoenvironmental proxies in core SL6, we can surmise the climatic controls on peat forming processes within the Mfabeni peatland. To facilitate comparisons between the bulk geochemical (Baker et al., 2014) and molecular proxies, the palaeoreconstruction will be divided up into linear sedimentation rate (LSR) stages as outlined in Baker et al. (2014) namely, LSR stage 1 (ca. 47.0 –32.4 kcal yr BP); LSR stage 2 (ca. 32.1 –27.9 kcal yr BP); LSR stage 3 (ca. 27.6 –20.3 kcal yr BP); LSR Stage 4 (ca. 19.8 –10.4 kcal yr BP); LSR stage 5 (ca. 10.2 kcal yr BP – present).

LSR stage 1 (ca. 47.0 –32.4 kcal yr BP) is characterised by low to average CPI_{alk} values, predominantly above average ACL_{alk} values and emergent / terrestrial plant signal (low P_{aq} and high P_{wax} values), with the exception of between ca. 44.5 and 42.6 kcal yr BP (Figure 2). The $sat/unsat_{FA}$ and CPI_{FA} proxy signals (Figure 3) exhibits predominantly elevated values, suggesting increased microbial reworking and relatively elevated ambient air temperatures. The raised P_{aq} (and low P_{wax}) values between ca. 44.5 and 42.6 kcal yr BP correspond with elevated TOC concentrations (48.8%) and $sat/unsat_{FA}$ (70.5) core maximum, implying a period of extensive waterlogging and elevated temperatures, which provided an ideal habitat for the proliferation of submerged macrophytes. The simultaneous A2 warming event (ca. 44.5 kcal yr BP and Heinrich 5; H5) has been documented in the Antarctic ice cores (Blunier et al., 1998; Stocker, 2000), and coincides with a sharp increase in SST in a Mozambique Channel marine core (Figure 4; MD79257; $20^0$24' S; $26^0$20' E; Bard et al., 1997; Sonzogni et al., 1998), supporting the inference of a discernible increase in submerged aquatic macrophyte input in response to raised water levels.

The H4 event occurred at ca. 38 kcal yr BP, while the A1 warming event was recorded in Antarctic cores at ca. 37 kcal yr BP (Blunier et al., 1998; Stocker, 2000) coincidental with elevated Mozambique Channel MD79257 core SST data (Bard et al., 1997; Sonzogni et al., 1998), and arguably increased continental rainfall. However, core SL6 OM source biomarker proxies imply that water levels in the peatland during the A1 event were not elevated sufficiently to exclude emergent and terrestrial plants ($P_{aq} = 0.2$), but rather resulted in a switch to a seasonally inundated peatland, with increased contribution of sedges and grasses (Baker at al., 2014; Kotze and O'Connor, 2000), supported by elevated ACL_{alk} values during the second half of LSR stage 1. The $sat/unsat_{FA}$ and CPI_{FA} proxies (Figure 3) decreases in the lead up to the H4 event, but rebounds after the A1 warming event signifying a slight cooling during the H4 event, and return to elevated ambient temperatures.

LSR stage 2 (ca. 32.1 –27.9 kcal yr BP) exhibits parameters which imply an overall drier and cooler climate compared to LSR stage 1. The TOC signal decreases to the core minimum (4.5%; ca. 30.6 kcal yr BP; H3), coinciding with an increase in sandy peat deposition, low $sat/unsat_{FA}$ and CPI_{FA} values, suggesting cool and dry climatic conditions (Figures 2 and 3).

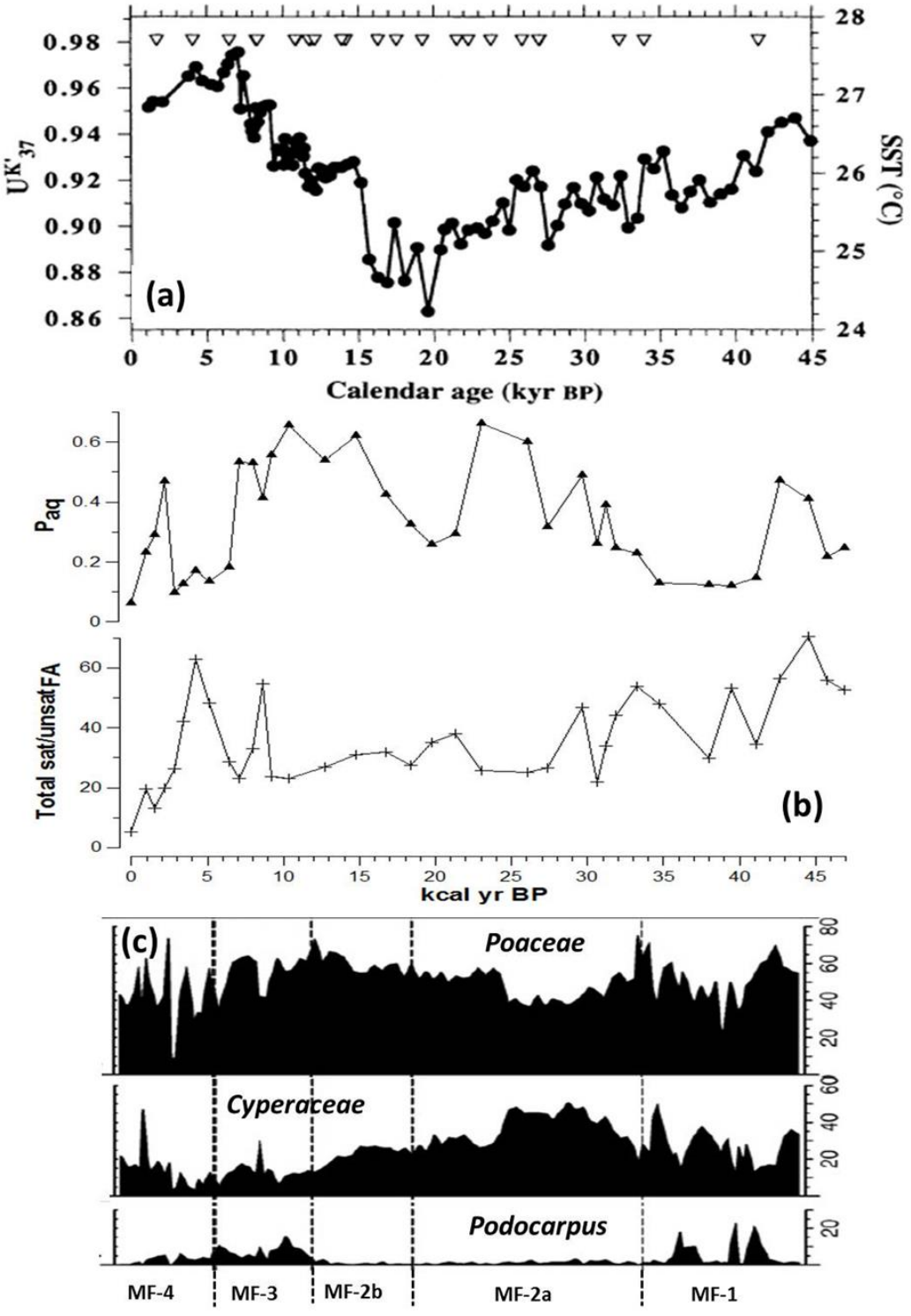

Figure 4: Comparison between proximal Indian Ocean SST reconstruction, Mfabeni peatland hydrology and temperature proxies and local Mfabeni plant frequencies. (a) Alkenone SST proxy from marine core MD79257 in the Mozambique Channel (20^{0}24' S; 26^{0}20' E; Bard et al., 1997). (b) *n*-Alkane (Paq) precipitation and *n*-alkanoic acid total sat/unsat (sat/unsatFA) temperature proxy trends from the Mfabeni peat core. (c) Pollen frequencies of 3 most abundant local species in the Mfabeni peatland - Poaceae (grasses), Cyperaceae (sedges) and Podocarpus (arboreal forest tree). Time zones MF-1: ~44,000 – 33,000 cal yr BP; MF-2a: ~33,000 – 17,500 cal yr BP; MF-2b: ~17,500 – 11,000 cal yr BP; MF-3: 11,000 – 5,000 cal yr BP; MF-4: ~5,000 – present (modified from Finch and Hill, 2008).

After ca. 30.6 kcal yr BP, the TOC signal increases steadily, coinciding with decreases in CPI_{alk}, ACL_{alk}, P_{wax} and increases in P_{aq} values signalling an increase in aquatic submerged plant input due to an increase in peatland water levels. The spike in $sat/unsat_{FA}$ and CPI_{FA} (Figure 3) values indicates simultaneous increase in ambient air temperature, corroborated by a spike in MD79257 marine core SST data (Bard et al., 1997; Sonzogni et al., 1998), regional speleothem (Talma and Vogel, 1992), lake (Partridge, 2002), and Vostok Antarctic ice core data (Stocker, 2000) at ca. 28 kcal yr BP.

LSR stage 3 (ca. 27.6 –20.3 kcal yr BP) displays two very distinctive climatic settings. Between ca. 27.6 and 23.1 kcal yr BP, the TOC values continue to increase, with average to low CPI_{alk}, fluctuating ACL_{alk}, decreasing P_{wax} and elevated P_{aq} values, indicating a period of increased waterlogging and dominance of local submerged aquatic plants. The elevated excursion of the palaeohydrology proxies, suggests an intensive period of waterlogging and a relative short (± 3000 yrs) period of submerged conditions in the Mfabeni peatland, while the $sat/unsat_{FA}$ proxy (Figure 3) displays below average values, thereby implying this period was subject to relatively moderate temperatures. Around 23.1 kcal yr BP, a sharp decline in TOC concentrations, coinciding with increased CPI_{alk}, P_{wax}, and a sharp decline in P_{aq} values, imply minimal waterlogging and a shift to cool and dry glacial conditions. The microbial reworking proxies trend negatively towards below average values (CPI_{FA} and $sat/unsat_{FA,}$ respectively; Figure 3), indicating a decline in ambient air temperatures. Similar regional climate adjustments to cooler and dry conditions were reported by Baker et al. (2014), Bard et al. (1997), Blunier et al. (1998), Finch and Hill (2008) and Holmgren et al. (2003) during the LGM.

LSR stage 4 (ca. 19.8 –10.4 kcal yr BP) sees a steady decrease in CPI_{alk}, ACL_{alk} and P_{wax} and recovery in P_{aq} values (Figure 2), accompanied by overall increasing TOC values, whereas the proxies for microbial reworking remain low throughout SLR stage 4 (CPI_{FA} and $sat/unsat_{FA}$; Figures 3). These trends suggest a slow increase in submerged macrophytes due to a gradual change from low glacial water levels to a shallow lacustrine environment leading up to ca. 15 kcal yr BP, but stagnant ambient air temperatures till the beginning of the Holocene. During the Antarctic cold reversal (ACR; ca. 14.5 – 12.9 kcal yr BP) the *n*-alkane signals briefly reverse their respective

trends suggesting an increase in emergent and terrestrial plant input in response to a brief period of dry conditions, thereafter, a recovery occurs at the onset of the YD (ca.12.8 kcal yr BP). While our findings are in agreement with the Antarctic ice cores (Stocker, 2000) and regional stalagmite records (Holmgren et al., 2003; Talma and Vogel, 1992), they are in conflict with other terrestrial climate records stemming from the African tropics (Schefuß et al., 2005; Talbot et al., 2007), regional inland escarpment peatland (Norström et al., 2009), Eastern escarpment Wonderkrater spring mound (Truc et al., 2013) and the winter rainfall area in the south Western Cape (Chase et al., 2011). These archives recorded a deglaciation reversal during the YD period, as opposed to the ACR. In further support of our findings, recent investigations by Schefuß et al. (2011) observed increased continental summer rainfall output in the Zambezi catchment area (marine core GeoB9307-3, 18^0 33.9' S, 37^0 22.8' E) during the H1 and YD events. Similarly, the Mozambique Channel core MD79257 ($20^0$24 S; $26^0$20 E) SST archive recorded a sharp temperature increase after ca. 15 kyr BP (Figure 4; Bard et al., 1997; Sonzogni et al., 1998), with a reversal during the ACR, and a pause in the increasing SST corresponding to the YD event, before continuing on a positive trend into the Holocene.

LSR stage 5 (ca. 10.2 kcal yr BP – present) spans the Holocene and is characterised by overall elevated C accumulation rates compared to the preceding glacial period (Baker et al., 2014). Finch and Hill (2008) observed high frequency of arboreal *Podocarpus* species during the early Holocene, and rapid increase in swamp forest pollen and a predominant local *Pteridophyta* signal during the Holocene Altithermal (~ 8 – 6 kcal yr BP), followed by a decline in *Podocarpus* and increases in *Poaceae* and *Cyperaceae* species towards the end of mid-Holocene (Figure 4). They used these pollen sequences to infer an initial moist and cool local climate, and then shift to warm and moist conditions during the Holocene Altithermal, followed by a cooler and drier climate towards the end of the mid-Holocene. The first half of LSR stage 5 exhibits fluctuating CPI_{alk}, ACL_{alk} and predominant submerged macrophyte signals, accompanied by a steady decline of the CPI_{FA} proxy until ca. 7.1 kcal yr BP (Figure 3), coinciding with the lowest Holocene TOC concentration (19.2%). The East coast palynology record in Lake Eteza similarly recorded a drying

event between ca. 8 and 7 kcal yr BP (Neumann et al., 2010), coinciding with a drop in SST in the Mozambique Channel after ca. 8 kcal yr BP (Bard et al., 1997; Sonzogni et al., 1998).

The P_{aq} and P_{wax} values switch to a predominant emergent plant signal after ca. 7.1 kcal yr BP, concordant with a rebound in TOC (Figure 2) and increase in microbial activity proxies (CPI_{FA} and $sat/unsat_{FA}$; Figure 3). The δD *n*-C_{31} alkane, terrestrial leaf wax input and SST proxies in marine core GeoB9307-3 (Schefuß et al., 2011) and SST of marine core MD79257 (Figure 4; Bard et al., 1997; Sonzogni et al., 1998) reveal an increase in ocean temperatures and continental rainfall output between ca.5.5 and 4 kcal yr BP. Similarly, Neumann et al. (2010, 2008) interpreted the palynology profile in Lake Sibaya and Lake Eteza, on the northern KwaZulu Natal coast to symbolize a moist and warm mid-Holocene. We propose that due to changes in the Holocene C accumulation dynamics (compared to the glacial period; Baker et al., 2014), higher Holocene NPP resulted in increased C preservation without the obligatory permanent waterlogging required for high OM preservation in the late Pleistocene. This change in environmental and deposition dynamics resulted in moderate precipitation (i.e. seasonal as opposed to permanent inundation or shallow lake levels) conducive for vascular plant growth in the Mfabeni peatland while maintaining relatively high C preservation. This would explain the terrestrial and emergent plant (low P_{aq} and high P_{wax}) signal being concordant with elevated TOC values in the mid- to late Holocene period.

The late-Holocene is characterised by an elevated CPI_{alk} profile, which steadily increases until ca. 2.2 kcal yr BP, concordant with predominant emergent plant signals, elevated TOC values and declining CPI_{FA} and $sat/unsat_{FA}$ ratios. Finch and Hill (2008) observed peripheral swamp forest taxa maximum in the beginning of the late Holocene, which they concluded was a response to warm and moist conditions and the steady decline in arboreal pollen attributed to increased anthropogenic agricultural practices (Figure 4). After ca. 3 kcal yr BP, they proposed the establishment of open savannah / woodland vegetation as a result of a drying trend. Similarly, Neumann et al. (2010) observed a drying trend in the proximal Lake Eteza after ca. 3.6 kcal yr BP. The Mfabeni record, however, suggests an increase in emergent sedges and terrestrial grasses (corresponding to elevated TOC) between ca. 4.4 and 2.2 kcal yr BP, arguably in response to increased moisture availability, coeval with tropical Indian Ocean GeoB937-3 marine core

precipitation δD and SST proxies (Schefuß et al., 2011). At ca. 2.2 kcal yr BP, an abrupt increase in P_{aq} values occurs, corresponding to decreases in ACL_{alk} and P_{wax} values, inferring an increase in water levels and aquatic plant input. Although Talma and Vogel (1992) recorded a late Holocene constant temperature range, varying only within +1 and -2^{0}C, a discernable escalation in ambient air temperatures was observed at ca. 2.5 k cal yr BP in a Cango Cave speleothem archive. We surmise, due to the elevated TOC values and submerged plant signature observed in core SL6, shallow lacustrine conditions occurred after the recorded transition to open savannah vegetation by Finch and Hill (2008). Consistent with this, Walther and Neumann (2011) recorded a definitive change to a savannah environment only after ca. 2 kcal yr BP in two proximal coastal plain sediments, namely Lake Sibaya and Kosi Bay, citing dry conditions on the northern KwaZulu Natal coast as the cause, which has persisted till today.

Climate variability during the late Pleistocene in the southern subtropics of Africa was influenced by the mean latitudinal position of the ITCZ, either as result of southward displacement during high latitude Northern Hemisphere cooling events (Johnson et al., 2002; Schefuß et al., 2011) or northward displacement in response to direct insolation forcing (Castañeda et al., 2009; Johnson et al., 2002). However, due to the close correlation between the Mozambique Channel marine records (Bard et al., 1997; Schefuß et al., 2011; Sonzogni et al., 1998) and palaeoenvironmental proxies in the Mfabeni peatland, the primary forcing mechanism on the northern KwaZulu Natal coastal palaeoenvironment appears to have been the evaporation and advection of moisture from the adjacent Indian Ocean, as established by Truc et al. (2013) for the wider South Eastern African region. The overriding climatic control of the Indian Ocean SST on this area could go some way towards explaining the general anti-phase inter-hemispheric trends exhibited in the Mfabeni record, which lends support to the theory that the northern and southern hemispheres exhibited opposite climatic responses to the possible switching on/ off of the global oceanic thermohaline circulation system during the late Pleistocene (Bard et al., 1997; Blunier et al, 1998; Stocker 2000). However, this theory can only be fully tested once further high resolution climate archive investigations are undertaken.

5. Conclusions

Biomarker distributions were analysed in a ca. 47 kyr old continuous peat sequence to elucidate the late Pleistocene and Holocene palaeoenvironment and reconstruct the climate on the northern KwaZulu Natal coast of South Africa. The peat sequence is dominated by higher terrestrial plant input, with the exception of increased submerged macrophyte input during periods of shallow lacustrine conditions (ca. 44.5 to 42.6; 29.7; 26.0 to 23.1; 16.7 to 7.0 and 2.2 kcal yr BP) representing discernible increases in precipitation. The statistical negative relationship between P_{aq} and ACL_{alk}, CPI_{alk} proxies, suggests strong effects of moisture availability, as opposed to temperature fluctuations on local plant physiology. This is arguably due to relatively moderate glacial cooling, but prominent precipitation fluctuations in the Mfabeni peatland. Nonetheless, by employing temperature sensitive $sat/unsat_{FA}$ and CPI_{FA} proxies, we were able to disentangle temperature and precipitation fluctuations on a local scale, and observed a general positive trend between increased temperature and moisture availability throughout the core. We report high variability in moisture availability but subdued temperatures during the late Pleistocene. In contrast, the Holocene is characterised by elevated ambient air temperatures and precipitation in comparison to the preceding glacial period, with the exception of a millennial scale cooling event at ca. 7.1 kcal yr BP.

The close association between the Mozambique Channel marine records and the Mfabeni palaeoproxies implies the dominant control on the SE African climate to have been the adjacent Indian Ocean SST, as opposed to the changes in the ITCZ latitudinal positioning since the late Pleistocene. However, there is a need for further high resolution studies of marine and terrestrial archives to firmly establish the climate forcing mechanism of adjacent ocean SST on past continental precipitation and growing season temperatures in the region.

6. Acknowledgments

Alistair Clulow assisted with field access and site identification. A Russian peat corer was loaned to the project by Piet-Louis Grundling. iSimangaliso Authority and Ezemvelo KZN Wildlife granted

park access and sampling permits. We thank an anonymous reviewer and Phil Meyers whose suggestions were very helpful in improving the manuscript. The project was supported through a bilateral funding agreement by the Swedish Research Link-South Africa program (Grant 348-2009-6500). Student support was supplied by the Department of Science and Technology, National Research Foundation and InKaba yeAfrica (AEON). This is an Inkaba ye Africa publication no. 121 and AEON publication no. 141.

7. References

Al-Mutlaq, K.F., Standley, L.J., Simoneit, B.R.T., 2008. Composition and sources of extractable organic matter from a sediment core in Lake Kivu, East African rift valley. Applied Geochemistry. 23, 1023–1040.

Anderson, J.A.R., Muller, J., 1975. Palynological study of a Holocene peat and a Miocene coal deposit from NW Borneo. Review of Palaeobotany and Palynology. 19 (4), 291-317.

Andersson, R. a., Kuhry, P., Meyers, P., Zebühr, Y., Crill, P., Mörth, M., 2011. Impacts of paleohydrological changes on *n*-alkane biomarker compositions of a Holocene peat sequence in the eastern European Russian Arctic. Organic Geochemistry. 42, 1065–1075.

Andersson, R. A., Meyers, P. a., 2012. Effect of climate change on delivery and degradation of lipid biomarkers in a Holocene peat sequence in the Eastern European Russian Arctic. Organic Geochemistry. 53, 63–72.

Baker, A., Routh, J., Blaauw, M., Roychoudhury, a. N., 2014. Geochemical records of palaeoenvironmental controls on peat forming processes in the Mfabeni peatland, Kwazulu Natal, South Africa since the Late Pleistocene. Palaeogeography, Palaeoclimatology, Palaeoecology. 395, 95–106.

Bai, Y., Fang, X., Nie, J., Wang, Y., Wu, F., 2009. A preliminary reconstruction of the paleoecological and paleoclimatic history of the Chinese Loess Plateau from the application of biomarkers. Palaeogeography, Palaeoclimatology, Palaeoecology. 271, 161–169.

Bard, E., Rostek, F., Sonzogni, C., 1997. Interhemispheric synchrony of the last deglaciation inferred from alkenone palaeothermometry. Nature. 385, 707-710.

Bate, G.C., Taylor, R.H., 2008. Sediment salt-load in the St Lucia Estuary during the severe drought of 2002-2006. Environmental Geology. 55, 1089–1098.

Bendle, J., Kawamura, K., Yamazaki, K., Niwai, T., 2007. Latitudinal distribution of terrestrial lipid biomarkers and *n*-alkane compound-specific stable carbon isotope ratios in the atmosphere over the western Pacific and Southern Ocean. Geochimica et Cosmochimica Acta. 71, 5934–5955.

Bendle, J. A., Kawamura, K., Yamazaki, K., 2006. Seasonal changes in stable carbon isotopic composition of *n*-alkanes in the marine aerosols from the western North Pacific: Implications for the source and atmospheric transport. Geochimica et Cosmochimica Acta .70, 13–26.

Blaauw, M., Christeny, J.A., 2011. Flexible paleoclimate age-depth models using an autoregressive gamma process. Bayesian Analysis. 6, 457–474.

Blunier, T., Chappellaz, J., Schwander, J., DaÈllenbach, A., Stauffer, B., Stocker, T. F., Raynaud, D., Jouzel, J., Clausen, H. B., Hammer, C. U., Johnsen, S. J., 1998. Asynchrony of Antarctic and Greenland climate change during the last glacial period. Nature 394, 739–743. DOI:10.1038/29447.Botha, G., Porat, N., 2007. Soil chronosequence development in dunes on the southeast African coastal plain, Maputaland, South Africa. Quaternary International. 162-163, 111–132.

Botha, G., Porat, N., 2007. Soil chronosequence development in dunes on the southeast African coastal plain, Maputaland, South Africa. Quaternary International 162-163, 111-132

Bush, R.T., McInerney, F. A., 2013. Leaf wax *n*-alkane distributions in and across modern plants: Implications for paleoecology and chemotaxonomy. Geochimica et Cosmochimica Acta .117, 161–179.

Carr, A.S., Boom, A., Grimes, H.L., Chase, B.M., Meadows, M.E., Harris, A., 2014. Leaf wax *n*-alkane distributions in arid zone South African flora: Environmental controls, chemotaxonomy and palaeoecological implications. Organic Geochemistry. 67, 72–84.

Castañeda, I.S., Werne, J.P., Johnson, T.C., Filley, T.R., 2009. Late Quaternary vegetation history of southeast Africa: The molecular isotopic record from Lake Malawi. Palaeogeography, Palaeoclimatology, Palaeoecology. 275, 100–112.

Chase, B.M., Meadows, M.E., 2007. Late Quaternary dynamics of southern Africa's winter rainfall zone. Earth-Science Reviews. 84, 103–138.

Chase, B.M., Thomas, D.S.G., 2007. Multiphase late Quaternary aeolian sediment accumulation in western South Africa: Timing and relationship to palaeoclimatic changes inferred from the marine record. Quaternary International. 166, 29–41.

Chase, B.M., Meadows, M.E., Carr, A.S., Reimer, P.J., 2010. Evidence for progressive Holocene aridification in southern Africa recorded in Namibian hyrax middens: Implications for African Monsoon dynamics and the "African Humid Period". Quaternary Research. 74, 36–45.

Chase, B.M., Quick, L.J., Meadows, M.E., Scott, L., Thomas, D.S.G., Reimer, P.J., 2011. Late glacial interhemispheric climate dynamics revealed in South African hyrax middens. Geology. 39, 19–22.

Chase, B.M., Scott, L., Meadows, M.E., Gil-Romera, G., Boom, A., Carr, A.S., Reimer, P.J., Truc, L., Valsecchi, V., Quick, L.J., 2012. Rock hyrax middens: A palaeoenvironmental archive for southern African drylands. Quaternary Science Reviews. 56, 107–125.

Chevalier, M., Chase, B.M., 2015. Southeast African records reveal a coherent shift from high- to low-latitude forcing mechanisms along the east African margin across last glacial–interglacial transition. Quaternary Science Review. 125, 117–130.

Chimner, R. A., Ewel, K.C., 2005. A tropical freshwater wetland: II. Production, decomposition, and peat formation. Wetlands Ecology and Management. 13, 671–684.

Clulow, A. D., Everson, C.S., Mengistu, M.G., Jarmain, C., Jewitt, G.P.W., Price, J.S., Grundling, P.L., 2012. Measurement and modelling of evaporation from a coastal wetland in Maputaland, South Africa. Hydrology and Earth System Sciences. 16, 3233–3247.

Cranwell, P.A., House, T.F., 1984. Lipid geochemistry of sediments from Upton Broad, a small productive lake. Organic Geochemistry. 7, 25–37.

Cranwell, P. A., 1974. Monocarboxylic acids in lake sediments: Indicators, derived from terrestrial and aquatic biota, of paleoenvironmental trophic levels. Chemical Geology. 14, 1–14.

Dommain, R., Couwenberg, J., Glaser, P.H., Joosten, H., Suryadiputra, I.N.N., 2014. Carbon storage and release in Indonesian peatlands since the last deglaciation. Quaternary Science Reviews. 97, 1–32.

Dommain, R., Couwenberg, J., Joosten, H., 2011. Development and carbon sequestration of tropical peat domes in south-east Asia: Links to post-glacial sea-level changes and Holocene climate variability. Quaternary Science Reviews. 30, 999–1010.

Eglinton, G., Hamilton, R.J., 1967. Leaf Epicuticular Waxes. Science. 156, 1322–1335.

Ficken, K.J., Farrimond, P., 1995. Sedimentary lipid geochemistry of Framvaren: impacts of a changing environment. Marine Chemistry. 51, 31–43.

Ficken, K.J., Barber, K.E., Eglinton, G., 1998. Lipid biomarker, δ13C and plant macrofossil stratigraphy of a Scottish montane peat bog over the last two millennia. Organic Geochemistry. 28, 217–237.

Ficken, K.J., Li, B., Swain, D.L., Eglinton, G., 2000. An *n*-alkane proxy for the sedimentary input of submerged / floating freshwater aquatic macrophytes. Organic Geochemistry. 31, 745–749.

Finch, J.M. 2005. Late Quaternary palaeoenvironments of the Mfabeni peatland, Northern Kwazulu-Natal: Master's thesis. MSc thesis. University of KwaZulu-Natal, Pietermaritzburg.

Finch, J.M., Hill, T.R., 2008. A late Quaternary pollen sequence from Mfabeni Peatland, South Africa: Reconstructing forest history in Maputaland. Quaternary Research. 70, 442–450.

Gagosian, R.B., Peltzer, E.T., 1986. The importance of atmospheric input of terrestrial material to deep sea sediments. Organic Geochemistry. 10, 661–669.

Grundling, P.L. 2001. The quaternary peat deposits of maputaland, northern kwazulu-natal, south africa: Categorisation, chronology and utilisation. MSc thesis. University of Johannesburg.

Grundling, P.L., Grootjans, A. P., Price, J.S., Ellery, W.N., 2013. Development and persistence of an African mire: How the oldest South African fen has survived in a marginal climate. Catena. 110, 176–183.

Haddad, R.I., Martens, C.S., Farrington, J.W., 1992. Quantifying early diagenesis of fatty acids in a rapidly accumulating coastal marine sediment. Organic Geochemistry. 19, 205–216.

Hemming, S.R., 2004. Heinrich events: Massive late Pleistocene ditritus layers of the North Atlanitc and their global cliamate imprint. Reviews of Geophysics. 42.

Hillaire-Marcel, C., de Vernal, A., 2007. Introduction Methods in Late Cenozoic Paleoceanography: Introduction. Dev. Marine Geology. 1, 1–15.

Holmgren, K., Lee-Thorp, J. A., Cooper, G.R.J., Lundblad, K., Partridge, T.C., Scott, L., Sithaldeen, R., Talma, A. S., Tyson, P.D., 2003. Persistent millennial-scale climatic variability over the past 25,000 years in Southern Africa. Quaternary Science Reviews. 22, 2311–2326.

Holzkämper, S., Holmgren, K., Lee-Thorp, J., Talma, S., Mangini, A., Partridge, T., 2009. Late Pleistocene stalagmite growth in Wolkberg Cave, South Africa. Earth and Planetary Science Letters. 282, 212–221.

Hu, J., Peng, P., Jia, G., Fang, D., Zhang, G., Fu, J., Wang, P., 2002. Biological markers and their carbon isotopes as an approach to the paleoenvironmental reconstruction of Nansha area , South China Sea , during the last 30 ka. Organic Geochemistry. 33, 1197–1204.

Huang, Y., Street-Perrott, A.F., Perrott, A.R., Metzger, P., Eglinton, G., 1999. Glacial – interglacial environmental changes inferred from molecular and compound-specific δ13C analyses of sediments from Sacred Lake , Mt . Kenya. Geochimica et Cosmochimica Acta. 63, 1383–1404.

Ishiwatari, R., Yamamoto, S., Uemura, H., 2005. Lipid and lignin/cutin compounds in Lake Baikal sediments over the last 37 kyr: implications for glacial–interglacial palaeoenvironmental change. Organic Geochemistry. 36, 327–347.

Jaffe, R., Mead, R., Hernandez, M.E., Peralba, M.C., Ja, R., Diguida, O.A., 2001. Origin and transport of sedimentary organic matter in two subtropical estuaries: a comparative, biomarker-based study. Organic Geochemistry. 32, 507–526.

Johnson, T.C., Brown, E.T., McManus, J., Barry, S., Barker, P., Gasse, F., 2002. A high-resolution paleoclimate record spanning the past 25,000 years in southern East Africa. Science. 296, 113–132.

Kotze, D.C., O'Connor, T.G., 2000. Vegetation Variation within and among Palustrine Wetlands along an Altitudinal Gradient in KwaZulu-Natal , South Africa. Plant Ecology. 146, 77–96.

Kristen, I., Wilkes, H., Vieth, A., Zink, K.-G., Plessen, B., Thorpe, J., Partridge, T.C., Oberhänsli, H., 2010. Biomarker and stable carbon isotope analyses of sedimentary organic matter from Lake Tswaing: evidence for deglacial wetness and early Holocene drought from South Africa. Journal of Paleolimnology. 44, 143–160.

Kuder, T., Kruge, M.A., 1998. Preservation of biomolecules in sub-fossil plants from raised peat bogs - a potential paleoenvironmental proxy. Organic Geochemistry. 29, 1355–1368.

Kurnianto, S., Warren, M., Talbot, J., Kauffman, B., Murdiyarso, D., Frolking, S., 2014. Carbon accumulation of tropical peatlands over millennia: A modeling approach. Global Change Biology. 431–444.

Lee-Thorp, J.A., Holmgren, K., Lauritzen, S.E., Linge, H., Moberg, A., Partridge, T.C., Stevenson, C., Tyson, P.D., 2001. Rapid climate shifts in the southern African interior throughout the mid to late Holocene. Geophysical Research Letters. 28, 4507–4510.

McCormac, F.G., Hogg, A.G., Higham, T.F.G., Lynch-Stieglitz, J., Broecker, W.S., Baillie, M.G.L., Palmer, J., Xiong, L., Pilcher, J.R., Brown, D., Hoper, S.T., 1998. Temporal variation in the interhemispheric 14C offset. Geophysical Research Letters. 25, 1321–1324.

Mead, R., Xu, Y., Chong, J., Jaffé, R., 2005. Sediment and soil organic matter source assessment as revealed by the molecular distribution and carbon isotopic composition of *n*-alkanes. Organic Geochemistry. 36, 363–370.

Meadows, M., Baxter, A., Parkington, J., 1996. Late Holocene environments at Verlorenvlei, Western Cape Province, South Africa. Quaternary International. 33, 81–95.

Meadows, M.E., Baxter, A.J., 1999. Late Quaternary palaeoenvironments of the southwestern Cape, South Africa: A regional synthesis. Quaternary International. 57-58, 193–206.

Meadows, M., 2001. The role of Quaternary environmental change in the evolution of landscapes: case studies from southern Africa. Catena. 42, 39–57.

Meyers, P. A., 1997. Organic geochemical proxies of paleoceanographic, paleolimnologic, and paleoclimatic processes. Organic Geochemistry. 27, 213–250.

Meyers, P. A., 2003. Applications of organic geochemistry to paleolimnological reconstructions: A summary of examples from the Laurentian Great Lakes. Organic Geochemistry. 34, 261–289.

Meyers, P. A., Ishiwatari, R., 1993. Lacustrine organic geochemistry—an overview of indicators of organic matter sources and diagenesis in lake sediments. Organic Geochemistry. 20, 867–900.

Meyers, P.A., Kawka, O.E., 1984. Geolipid, pollen and diatom stratigraphy in postglacial lacustrine sediments. Organic Geochemistry. 6, 727–732.

Mucina, L., Adams, J.B., Knevel, I.C., Rutherford, M.C., Powrie, L.W., Bolton, J.J., van der Merwe, J.H., Anderson, R.J., Bornman, T.G., le Roux, A., Janssen, J.A.M., 2006. Coastal vegetation of South Africa, in: Mucina, L., Rutherford, M.C. (Eds.), The Vegetation of South Africa, Lesotho and Swaziland. South African National Biodiversity Institute, Pretoria, pp. 658–696.

Nash, D.J., Meadows, M.E., 2012. Africa, in: Metcalfe, S.E., Nash, D.J. (Eds.), Quaternary Environmental Change in the Tropics. John Wiley and Sons, Ltd., UK, pp. 79–150.

Neumann, F.H., Stager, J.C., Scott, L., Venter, H.J.T., Weyhenmeyer, C., 2008. Holocene vegetation and climate records from Lake Sibaya, KwaZulu-Natal (South Africa). Review of Palaeobotany and Palynology. 152, 113–128.

Neumann, F.H., Scott, L., Bousman, C.B., van As, L., 2010. A Holocene sequence of vegetation change at Lake Eteza, coastal KwaZulu-Natal, South Africa. Review of Palaeobotany and Palynology. 162, 39–53.

Nichols, J.E., Booth, R.K., Jackson, S.T., Pendall, E.G., Huang, Y., 2006. Paleohydrologic reconstruction based on *n*-alkane distributions in ombrotrophic peat. Organic Geochemistry. 37, 1505–1513.

Nichols, J.E., Walcott, M., Bradley, R., Pilcher, J., Huang, Y., 2009. Quantitative assessment of precipitation seasonality and summer surface wetness using ombrotrophic sediments from an Arctic Norwegian peatland. Quaternary Research. 72, 443–451.

Norström, E., Scott, L., Partridge, T.C., Risberg, J., Holmgren, K., 2009. Reconstruction of environmental and climate changes at Braamhoek wetland, eastern escarpment South Africa, during the last 16,000 years with emphasis on the Pleistocene-Holocene transition. Palaeogeography, Palaeoclimatology, Palaeoecology. 271, 240–258.

Ogura, K., Machihara, T., Takada, H., 1990. Diagenesis of biomarkers in Biwa Lake sediments over 1 million years. Organic Geochemistry. 16, 805–813.

Page, S.E., Rieley, J.O., Banks, C.J., 2011. Global and regional importance of the tropical peatland carbon pool. Global Change Biology. 17, 798–818.

Pancost, R.D., Boot, C.S., 2004. The palaeoclimatic utility of terrestrial biomarkers in marine sediments. Marine Chemistry. 92, 239–261.

Partridge, T.C., 2002. Were Heinrich events forced from the southern hemisphere? South African Journal of Science. 98, 43–46.

Peters, K.E., Walters, C.C., Moldowan, J.M., 2004. The Biomarker Guide: Volume 1, Biomarkers and Isotopes in the Environment and Human History. Cambridge University Press.

Porat, N., Botha, G., 2008. The luminescence chronology of dune development on the Maputaland coastal plain, southeast Africa. Quaternary Science Reviews. 27, 1024–1046.

Preston-Whyte, R.A., Tyson, P.D., 1998. The atmosphere and weather of southern Africa. Oxford University Press, South Africa.

Ranjan, R.K., Routh, J., Val Klump, J., Ramanathan, A.L., 2015. Sediment biomarker profiles trace organic matter input in the Pichavaram mangrove complex, Southeastern India. Marine Chemistry. 171, 44-57.

Rieley, J.O., Ahmad-Shah, A.A., Brady, M.A., 1996. The Extent and Nature of Tropical Peat Swamps - Tropical Lowland Peatlands of Southeast Asia, in: Integrated Planning and Management of Tropical Lowland Peatlands Workshop.

Rieley, G., Collier, R.J., Jones, D.M., Eglinton, G., Eakin, P.A., Fallick, A.E., 1991. Sources of sedimentary lipids deduced from stable carbon-isotope analyses of individual compounds. Nature. 352, 425–427.

Routh, J., Hugelius, G., Kuhry, P., Filley, T., Tillman, P.K., Becher, M., Crill, P., 2014. Multi-proxy study of soil organic matter dynamics in permafrost peat deposits reveal vulnerability to climate change in the European Russian Arctic. Chemical Geology. 368, 104–117.

Schefuß, E., Ratmeyer, V., Stuut, J.B.W., Jansen, J.H.F., Sinninghe Damsté, J.S., 2003. Carbon isotope analyses of *n*-alkanes in dust from the lower atmosphere over the central eastern Atlantic. Geochimica et Cosmochimica Acta. 67, 1757–1767.

Schefuß, E., Schouten, S., Schneider, R.R., 2005. Climatic controls on central African hydrology during the past 20,000 years. Nature. 437, 1003–1006.

Schefuß, E., Kuhlmann, H., Mollenhauer, G., Prange, M., Pätzold, J., 2011. Forcing of wet phases in southeast Africa over the past 17,000 years. Nature. 480, 509–512.

Schmidt, M.W.I., Torn, M.S., Abiven, S., Dittmar, T., Guggenberger, G., Janssens, I. A., Kleber, M., Kögel-Knabner, I., Lehmann, J., Manning, D. A. C., Nannipieri, P., Rasse, D.P., Weiner, S., Trumbore, S.E., 2011. Persistence of soil organic matter as an ecosystem property. Nature. 478, 49–56.

Schwark, L., Zink, K., Lechterbeck, J., 2002. Reconstruction of postglacial to early Holocene vegetation history in terrestrial Central Europe via cuticular lipid biomarkers and pollen records from lake sediments. Geology. 30, 463–466.

Scott, L., Holmgren, K., Partridge, T.C., 2008. Reconciliation of vegetation and climatic interpretations of pollen profiles and other regional records from the last 60 thousand years in

the Savanna Biome of Southern Africa. Palaeogeography, Palaeoclimatology, Palaeoecology. 257, 198–206.

Smuts, W.J., 1992. Peatlands of the Natal Mire Complex - goemorphology and characterization. South African Journal of Science. 88, 474–83.

Sonzogni, C., Bard, E., Rostek, F., 1998. Tropical sea-surface temperatures during the last glacial period: A view based on alkenones in Indian Ocean sediments. Quaternary Science Reviews. 17, 1185–1201.

Staub, J.R., Esterle, J.S., 1994. Peat-accumulating depositional systems of Sarawak, East Malaysia. Sedimentary Geology. 89 (1-2), 91-106.

Stocker, T.F., 2000. Past and future reorganizations in the climate system. Quaternary Science Reviews. 19, 301–319.

Stokes, S., Thomas, D.S.G., Washington, R., 1997. Multiple episodes of aridity in southern Africa since the last interglacial period. Nature. 388, 154–158.

Strack, M., Waddington, J.M., Turetsky, M., Roulet, N.T., Byrne, K. A., 2008. Northern peatlands, greenhouse gas exchange and climate change, in: Strack, M. (Ed.), Peatlands and Climate Change. International Peat Society, Jyväskylä, Finland, pp. 44–69.

Talbot, M.R., Filippi, M.L., Jensen, N.B., Tiercelin, J.J., 2007. An abrupt change in the African monsoon at the end of the Younger Dryas. Geochemistry, Geophysics, Geosystems. 8, 1–16.

Talma, A.S., Vogel, J.C., 1992. Late Quaternary paleotemperatures derived from a speleothem from Cango Caves, Cape Province, South Africa. Quaternary Research. 37, 203–213.

Taylor, R., Kelbe, B., Haldorsen, S., Botha, G. A., Wejden, B., Været, L., Simonsen, M.B., 2006a. Groundwater-dependent ecology of the shoreline of the subtropical Lake St Lucia estuary. Environmental Geology. 49, 586–600.

Taylor, R., Adams, J.B., Haldorsen, S., 2006b. Primary habitats of the St Lucia Estuarine System, South Africa, and their responses to mouth management. African Journal of Aquatic Science. 31, 31–41.

Truc, L., Chevalier, M., Favier, C., Cheddadi, R., Meadows, M.E., Scott, L., Carr, A.S., Smith, G.F., Chase, B.M., 2013. Quantification of climate change for the last 20,000years from Wonderkrater, South Africa: Implications for the long-term dynamics of the Intertropical Convergence Zone. Palaeogeography, Palaeoclimatology, Palaeoecology. 386, 575–587.

Tyson, P.D., Preston-Whyte, R.A., 2000. The Weather and Climate of Southern Africa, 2nd ed. Oxford University Press Incorporated, Cape Town, South Africa.

Valsecchi, V., Chase, B.M., Slingsby, J. A., Carr, A.S., Quick, L.J., Meadows, M.E., Cheddadi, R., Reimer, P.J., 2013. A high resolution 15,600-year pollen and microcharcoal record from the Cederberg Mountains, South Africa. Palaeogeography, Palaeoclimatology, Palaeoecology. 387, 6–16.

Venter, C.E., 2003. Vegetation ecology of Mfabeni peat swamp, St Lucia, KwaZulu-Natal. MSc thesis. Botany Department, University of Pretoria. http://repository.up.ac.za/handle/2263/24480.

Vrdoljak, S.M., Hart, R.C., 2007. Groundwater Seeps as Potentially Important Refugia for Freshwater Fishes on the Eastern Shores of Lake St Lucia, KwaZulu-Natal, South Africa. African Journal of Aquatic Science. 32, 125–132.

Wakeham, S.G., Peterson, M.L., Hedges, J.I., Lee, C., 2002. Lipid biomarker fluxes in the Arabian Sea , with a comparison to the equatorial Pacific Ocean. Deep. Res. II 49, 2265–2301.

Walther, S.C., Neumann, F.H., 2011. Sedimentology, isotopes and palynology of late Holocene cores from Lake Sibaya and the Kosi Bay system (KwaZulu-Natal, South Africa). South African Geographical Journal. 93, 133–153.

Wang, Y., Zhu, L., Wang, J., Ju, J., Lin, X., 2012. The spatial distribution and sedimentary processes of organic matter in surface sediments of Nam Co, Central Tibetan Plateau. Chinese Science Bulletin. 57, 4753–4764.

Xie, S., Nott, C.J., Avsejs, L. A., Maddy, D., Chambers, F.M., Evershed, R.P., 2004. Molecular and isotopic stratigraphy in an ombrotrophic mire for paleoclimate reconstruction. Geochimica et Cosmochimica Acta. 68, 2849–2862.

Zheng, Y., Zhou, W., Meyers, P. A., Xie, S., 2007. Lipid biomarkers in the Zoigê-Hongyuan peat deposit: Indicators of Holocene climate changes in West China. Organic Geochemistry. 38, 1927–1940.

Zheng, Y., Zhou, W., Meyers, P.A., 2011a. Proxy value of *n*-alkan-2-ones in the Hongyuan peat sequence to reconstruct Holocene climate changes on the eastern margin of the Tibetan Plateau. Chemical Geology. 288, 97–104.

Zheng, Y., Zhou, W., Liu, X., Zhang, C.L., 2011b. *n*-Alkan-2-one distributions in a northeastern China peat core spanning the last 16kyr. Organic Geochemistry. 42, 25–30.

Zhou, W., Xie, S., Meyers, P. A., Zheng, Y., 2005. Reconstruction of late glacial and Holocene climate evolution in southern China from geolipids and pollen in the Dingnan peat sequence. Organic Geochemistry. 36, 1272–1284.

Zhou, W., Zheng, Y., Meyers, P. A., Jull, a. J.T., Xie, S., 2010. Postglacial climate-change record in biomarker lipid compositions of the Hani peat sequence, Northeastern China. Earth and Planetary Science Letters. 294, 37–46.

Supplementary data

Table A1: Chronology of Mfabeni peatland core SL6 with uncalibrated AMS ^{14}C dates, corresponding percentage total organic carbon (TOC) and bulk stable carbon isotope values (from Baker et al., 2014).

Sample code	Depth (cm)	Material	uncalibrated date	% C	$\delta^{13}C_{TOC}$
SL6 10-11	10	Peat	109 ± 0.35 pMC	45.1	-21.8
SL6 109-110	109	Peat	3240 ± 30 BP	51.9	-16.8
SL6 209-210	209	Peat	6170 ± 30 BP	19.2	-24.5
SL6 309-310	309	Peat	9270 ± 70 BP	37.1	-21.5
SL6 405-406	405	Peat	16940 ± 80 BP	14.7	-19.1
SL6 510-511	510	Peat	22800 ± 130 BP	29.6	-18.6
SL6 609-610	609	Peat	27600 ± 190 BP	22.5	-19.0
SL6 709-710	709	Peat	>48000 BP	28.1	-17.6
SL6 805-806	805	Peat	49000 ± 2200 BP	12.2	-20.1

Table A2: Biomarker concentrations, distributions and molecular proxy values for core SL6 extracted from the Mfabeni peatland.

			n-Alkanes						*n*-Alkanols				*n*-Alkanoic Acids						
Depth	Age		Tot conc.						Tot conc.				Tot conc.						Total Sat /
(cm)	k cal BP	%TOC	ng/mg TOC	C_{max}	CPI_1	ACL_1	P_{aq}	P_{wax}	ng/mg TOC	C_{max}	CPI_2	ACL_2	ng/mg TOC	C_{max}	CPI_2	ACL_2	C16:1/C16:0	C18:1/C18:0	Unsat conc.
8	0.0	45.1	10.4	31	7.0	31	0.06	0.94	8.1	25	0.3	24	50.7	16	9.9	25	0.130	0.375	5.1
41	0.9	50.3	6.0	31	7.8	30	0.23	0.81	0.3	23	0.3	25	66.6	22	16.2	24	0.029	0.127	19.4
57	1.5	37.8	7.3	31	5.5	30	0.29	0.75	0.2	32	1.7	27	37.0	22	6.7	24	0.021	0.167	13.2
76	2.2	50.8	6.5	25	11.4	29	0.47	0.60	17.8	23	0.5	23	51.6	22	9.4	24	0.008	0.091	19.8
92	2.8	51.0	6.4	29	12.6	30	0.10	0.92	12.1	23	0.5	23	49.8	24	11.8	25	0.004	0.047	26.4
108	3.4	51.9	12.0	31	9.2	30	0.13	0.89	11.9	23	0.4	24	84.5	22	15.9	24	0.009	0.044	42.2
134	4.2	49.6	14.8	33	9.2	30	0.17	0.86	19.0	22	0.8	23	67.1	22	16.9	24	0.003	0.013	62.9
157	5.1	40.0	32.6	31	6.8	30	0.13	0.88	4.6	23	0.7	23	154.6	22	11.7	24	0.004	0.007	48.1
191	6.4	44.8	6.6	29	7.1	29	0.18	0.85	4.7	31	0.7	24	42.5	22	12.7	25	0.004	0.061	28.8
209	7.1	19.2	10.3	25	2.5	28	0.53	0.57	29.6	23	0.8	24	84.3	16	7.1	25	0.004	0.070	23.2
237	8.0	41.3	8.6	25	4.3	28	0.53	0.57	23.3	22	0.7	24	49.3	22	8.1	25	0.001	0.041	33.0
257	8.7	49.0	6.7	29	6.1	29	0.41	0.66	6.1	31	0.5	24	64.9	22	8.2	25	0.001	0.030	54.8
273	9.2	44.0	5.1	25	6.5	28	0.56	0.54	3.3	24	1.7	24	40.9	26	8.0	25	0.001	0.047	23.7
309	10.4	37.1	25.1	23	2.1	28	0.65	0.49	0.6	23	0.5	24	22.9	24	8.8	25	0.003	0.094	23.0
335	12.7	40.6	4.5	25	7.2	29	0.54	0.57	11.1	22	0.6	26	33.4	26	7.5	25	0.000	0.039	26.7
355	14.8	35.3	3.6	23	4.1	28	0.62	0.51	0.5	31	0.5	24	10.2	22	10.0	26	0.000	0.016	31.0
375	16.7	20.7	40.8	27	6.5	29	0.42	0.68	13.1	31	0.5	24	111.2	22	8.2	25	0.002	0.020	32.0
390	18.4	10.1	32.4	29	10.0	29	0.33	0.75	36.2	22	0.7	23	200.1	22	8.6	25	0.002	0.026	27.5
404	19.8	14.7	27.6	29	10.7	29	0.26	0.79	35.9	22	0.8	23	132.9	22	10.4	25	0.000	0.016	35.0
424	21.3	10.3	28.1	29	5.0	29	0.29	0.76	4.7	22	1.1	23	132.5	22	11.3	24	0.002	0.029	37.9
450	23.1	41.1	2.4	33	2.6	30	0.66	0.45	3.9	23	0.8	23	12.2	22	13.9	25	0.001	0.048	25.6
492	26.1	33.5	21.4	27	6.5	28	0.60	0.58	1.2	17	2.3	28	12.6	26	6.2	25	0.000	0.017	25.0
510	27.4	29.6	27.1	27	6.5	29	0.32	0.78	0.1	22	1.6	25	42.8	22	8.9	25	0.000	0.033	26.5
559	29.7	15.5	19.8	27	2.4	28	0.49	0.63	6.3	22	1.7	23	37.6	22	10.5	24	0.000	0.006	46.7
580	30.6	4.5	32.1	29	6.1	29	0.26	0.80	11.7	22	1.9	23	107.8	22	8.3	25	0.000	0.108	22.0
595	31.2	10.7	25.1	29	5.0	29	0.39	0.75	2.8	22	1.3	24	60.4	22	8.4	25	0.000	0.020	33.9
609	31.9	22.5	6.5	31	6.9	30	0.25	0.80	2.3	22	1.1	23	38.5	22	9.6	24	0.003	0.012	44.0
630	33.2	30.4	17.4	29	4.9	30	0.23	0.81	3.0	22	1.1	24	70.1	22	10.1	25	0.001	0.009	53.9
649	34.8	29.7	22.4	29	7.1	30	0.13	0.89	4.5	22	0.9	24	111.7	22	8.6	24	0.002	0.022	48.1
690	38.0	36.6	4.3	31	5.4	30	0.12	0.89	15.0	22	1.7	23	57.4	22	5.2	24	0.001	0.031	29.8
709	39.5	28.1	23.4	29	9.0	30	0.12	0.90	4.4	20	1.7	23	105.4	22	11.5	24	0.005	0.011	53.1
730	41.1	36.6	11.8	31	4.2	30	0.15	0.87	4.1	22	1.0	23	86.3	22	10.1	25	0.001	0.006	34.4
749	42.6	48.3	4.4	29	2.2	29	0.47	0.63	2.7	22	1.0	23	35.9	22	12.6	24	0.002	0.038	56.3
773	44.5	48.8	14.2	29	2.2	29	0.41	0.67	0.5	22	1.1	24	56.1	22	12.6	24	0.001	0.016	70.5
789	45.7	45.8	3.5	29	4.9	29	0.22	0.82	1.6	22	1.1	23	46.7	22	8.8	24	0.000	0.027	55.7
804	46.9	12.2	10.3	31	6.0	30	0.25	0.79	1.7	22	1.3	22	192.9	22	8.4	25	0.001	0.019	52.7

* Paq values < 0.1 = dominant terrestrial plant input, 0.1 - 0.4 = emergent macrophytes and, 0.4 - 1 = submerged macrophyte input (Ficken et al., 2000).

$$P_{wax} = \frac{C_{27} + C_{29} + C_{31}}{C_{23} + C_{25} + C_{27} + C_{29} + C_{31}}$$

$CPI_1 = [\Sigma(C_{21} – C_{29})\ \text{odd} + \Sigma(C_{23} – C_{31})\ \text{odd}]/\ 2\Sigma(C_{22} – C_{30})\ \text{even}$

$CPI_2 = [\Sigma(C_{20} – C_{30})\ \text{even} + \Sigma(C_{22} – C_{32})\ \text{even}]/2\Sigma(C_{21} – C_{31})\ \text{odd}$

$$P_{aq} = \frac{C_{23} + C_{25}}{C_{23} + C_{25} + C_{29} + C_{31}}$$

ACL_1 = (Σ[Ci] x i) / Σ[Ci], for i = 23 – 33 where Ci = concentration of *n*–alkane containing i carbon atoms

ACL_2 = (Σ[Ci] x i) / Σ[Ci], for I = 22 – 32 where Ci = concentration of *n*-alkanoic acid or *n*-alkanol containing i carbon atoms

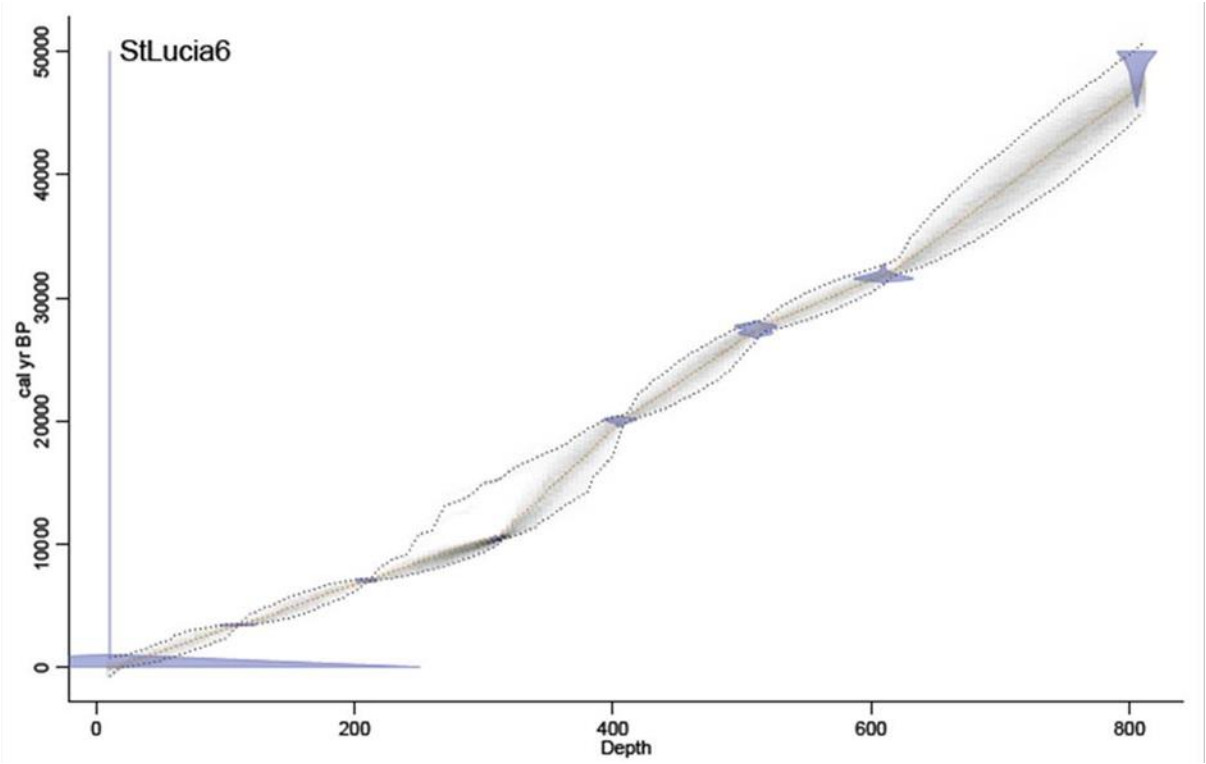

Figure S1: Core SL6 age-depth model with uncertainty ranges (from Baker et al., 2014).

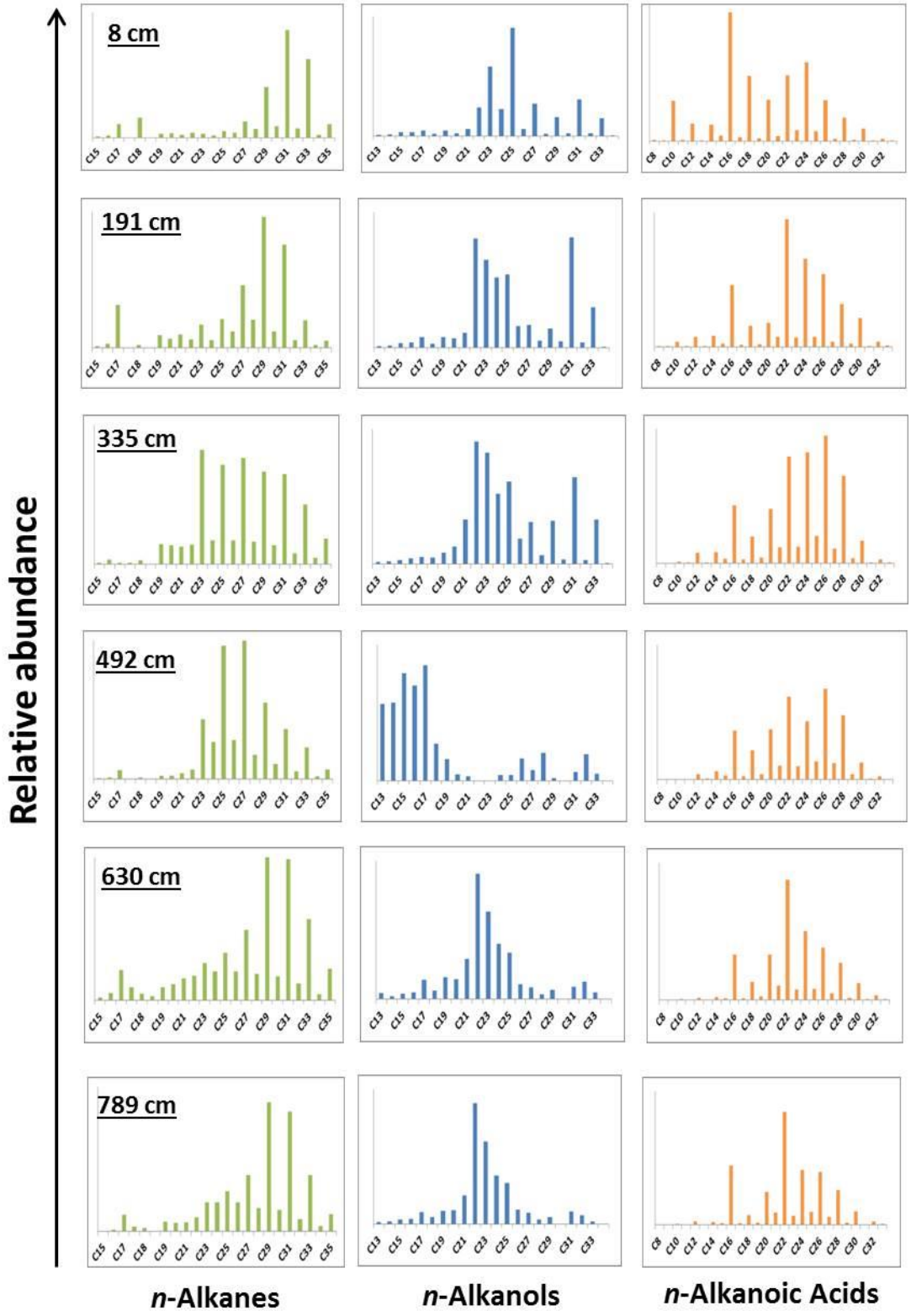

Figure S2: **Homologue distributions of *n*-alkanes, *n*-alkanols and *n*-alkanoic acids at specific depth intervals throughout Mfabeni peat core SL6.**

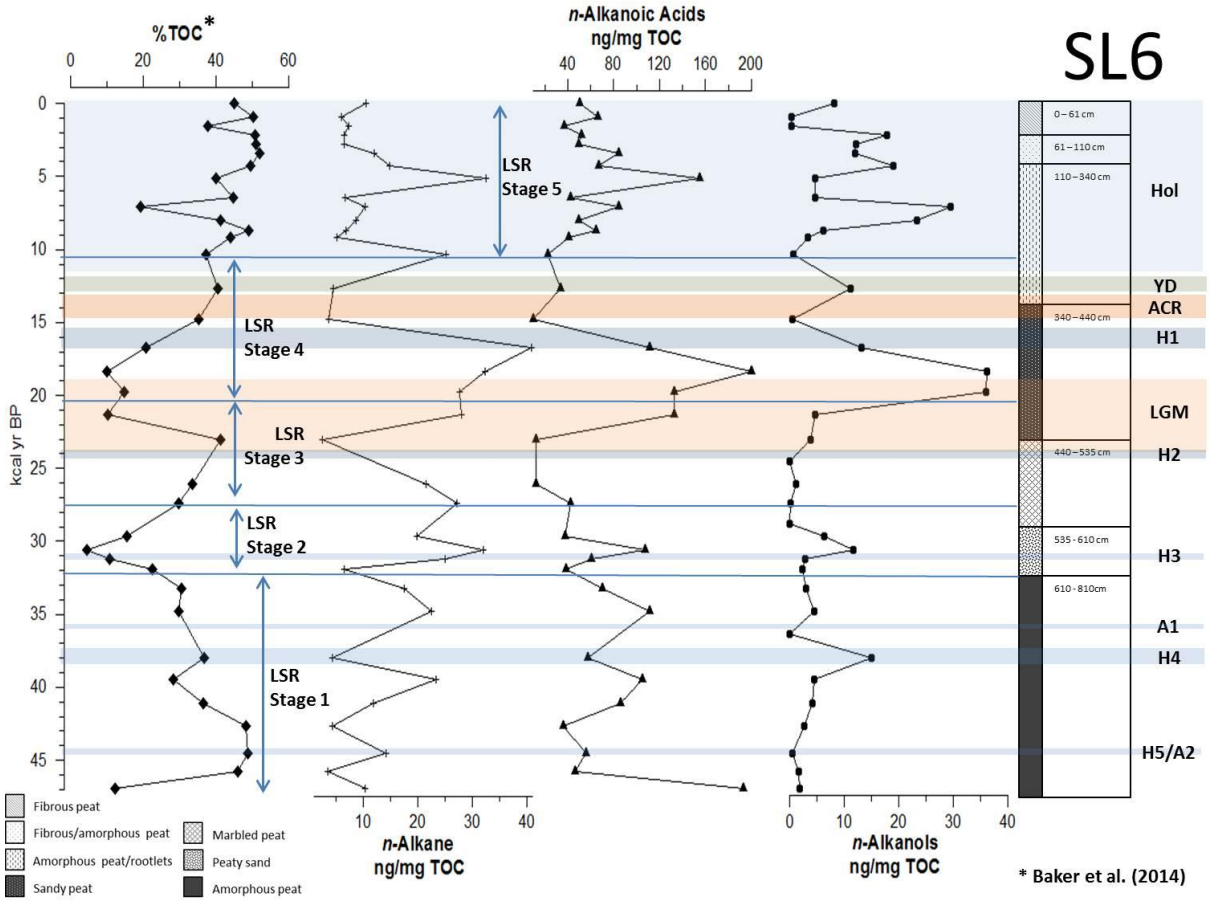

<u>Figure S3:</u> Biomarker concentrations in relation to % total organic carbon (TOC) in core SL6. H1 – 5 = Heinrich events (dates from Hemming, 2004); A1 and A2 = Antarctic warming events (Blunier et al., 1998; Stocker, 2000); LGM = Last Glacial Maximum; ACR = Antarctic cold reversal (Stocker, 2000); YD = Younger Dryas; Hol = Holocene.

Chapter 4:

Carbon isotope records of climatic variability in Mfabeni peatland (South Africa) since the late Pleistocene

A presentation of a prepared research paper

This research manuscript has been prepared for submission to the *Journal of Quaternary Science*.

The Biomarker samples were extracted and separated into *n*-alkane fraction by myself under the guidance of Dr Routh. The separation of individual *n*-alkanes and analysis of the leaf wax *n*-alkane C isotopes was carried out by Dr Pedentchouk. I was responsible for the data processing, generation of all the figures and data tables, concept design and write up of the article. The manuscript was improved with feedback and comments from Dr Pedentchouk. Dr Routh assisting with overall editing and Prof Roychoudhury assisted in the final editing of the manuscript.

Carbon isotope records of climatic variability in Mfabeni peatland (South Africa) since the late Pleistocene

Andrea BAKER[1*], Nikolai PEDENTCHOUK[2], Joyanto ROUTH[3], Alakendra N. ROYCHOUDHURY[1]

[1]Department of Earth Sciences, Stellenbosch University, Stellenbosch, South Africa

[2]School of Environmental Sciences, University of East Anglia, Norwich, UK

[3]Department of Thematic Studies – Environmental Change, Linköping University, Linköping, Sweden

Abstract

Southern Africa is exposed to tropical, sub-tropical and temperate climates, with varying altitudes and seasonal rainfall zones. Contemporary regional C3 and C4 terrestrial plant distributions, primarily *Poaceae* (grasses) and *Cyperaceae* (sedges), display a definitive geographical pattern dictated by the different growing season rainfall and temperature zones. Even though soil carbon isotope records have proven to be robust proxies for reconstructing palaeoenvironments elsewhere, the Southern Africa region has an overall semi-arid climate and steep escarpment topography which has generally prevented preservation of continuous sedimentary archives. As a result, there are major gaps in our understanding of past climate driven environmental fluctuations in the region, most particularly during the last glacial period. The Mfabeni peatland, with the basal age of ca. 47 thousand years calibrated before present (kcal yr BP), is a notable exception and is one of the oldest continuous coastal peat archives in this part of Africa and provides a rare opportunity to conduct high-resolution palaeoecological research since the late Pleistocene. Molecular leaf wax $\delta^{13}C$ isotopes ($\delta^{13}C_{wax}$) were analysed in a 810 cm long core, and along with

previously published bulk geochemical data ($\delta^{13}C_{bulk}$, total organic carbon), palynological and stratigraphic studies, used to reconstruct the late Pleistocene and Holocene palaeoenvironment. Due to the strong and significant correlation observed between $\delta^{13}C_{bulk}$ and $\delta^{13}C_{wax}$ data sets, we established that the high-resolution $\delta^{13}C_{bulk}$ signal characterises the proportional contributions of C3 and C4 terrestrial plant assemblages, which correlated strongly with the palynology and stratigraphic records throughout the depositional history of the peatland. We found evidence for environmental shifts for some of the well-established climatic events since the Late Pleistocene (namely Heinrich 4, Last Glacial Maximum, deglacial and Holocene periods), which are consistent with adjacent Indian Ocean sea surface temperature records. However, the other shorter events (namely, Heinrich 5, 3, 2, 1, Antarctic cold reversal and Younger Dryas) showed rather muted responses in our core, in all probability due to local hydrological overprinting of the Mfabeni record.

1. Introduction

There has been much scientific debate regarding the mechanisms by which the C4 photosynthetic pathway evolved, most notably in grasslands, and which environmental drivers facilitated this carbon (C) fixing mechanism. Cerling et al. (1997) proposed global C4 grasslands expansion began in the late Miocene as a result of a better adaption to lower atmospheric CO_2 and higher growing season temperatures compared to C3 grasses. Approximately 85% of all terrestrial plant species use the C3 photosynthetic pathway to fix carbon (Ehleringer et al., 1997), whereas the C4 pathway is restricted to the Dicotyledonae and Monocotyledonae clades, with the greatest diversity found within the widespread monocots group, that is dominated by the *Poaceae* (grasses) and *Cyperaceae* (sedges) families (Ehleringer et al., 1997). The different biochemical pathways employed during photosynthesis causes a variation in degrees of $^{13}C/^{12}C$ fractionation, resulting in characteristic bulk $\delta^{13}C$ values ranging from -22‰ to -30‰ for C3 and -10‰ to -14‰ for C4 plants (Vogel et al., 1978). However, the bulk $\delta^{13}C$ signal encompasses many different inorganic and organic inputs of C into sediments, which can complicate reconstructions. Long chain *n*-alkane compounds (> C_{25}) are exclusively produced in the leaf waxes of higher plants (Eglinton and Hamilton, 1967) and are generally accepted to be the most recalcitrant of all the hydrocarbons

found in sediments (Meyers, 1997). Compound specific C isotope ($\delta^{13}C_{wax}$) values of these long chained *n*-alkane compounds is primarily controlled by the C fixation pathways employed during photosynthesis, and to a lesser degree, changes in temperature, moisture and inorganic C source (Chikaraishi and Naraoka, 2003; Hayes et al., 1990). Hence, observed changes in peat $\delta^{13}C_{wax}$ trends can best be explained by the changes in relative abundance between C3 and C4 plant input, and thereupon a direct link can be made to the representational proportion of C3 and C4 plants that were present at the time of peat formation.

Southern Africa is situated at the junction between tropical, sub-tropical and temperate climate systems, with varying topography / altitudes, and three distinctive growing season rainfall zones, namely winter rainfall (WRZ), all year rainfall (ARZ) and summer rainfall (SRZ) zones (Figure 1). As a consequence, the region is an ideal location for research into C3 and C4 plant distributions and their physiological adaptations to various palaeoenvironments and palaeoclimates (Scott, 2002). Due to the steep escarpment topography and predominant semi-arid climate of the region, continuous palaeoclimate archives are rarely preserved. Consequently, there is a gap in our understanding of past climate driven environmental fluctuations throughout the region, most especially variations under glacial and interglacial conditions.

Although C3 plant species are found throughout Southern Africa, the C3 and C4 plant distributions of the *Poaceae* (grasses) family within South Africa have been shown to occur in distinct geographical areas, determined largely by growing season temperatures. Vogel et al. (1978) found that C4 grasses predominate in the SRZ, whereas C3 grasses are more prevalent in the WRZ and high altitude regions of the eastern escarpment of South Africa. On the other hand, Stock et al. (2004) showed that temperature variations did not fully account for the C3 and C4 *Cyperaceae* (sedges) family distributions in South Africa, but seem to be more closely related to annual rainfall. They suggest that the C4 sedges evolved under wetland conditions, but are generally more abundantly represented in warm and wet tropical areas (Rommerskirchen et al., 2006), although not in such high proportions as in the case for the *Poaceae* family (up to 95% in SRZ; Vogel et al., 1978).

The Mfabeni peatland, with its basal ^{14}C age of ca. 47 thousand years calibrated before present (kcal yr BP) is proving to be an exceptional continuous and relatively ancient record with Grundling et al. (2013) proposing it to be the oldest known peatland archive in the Southern African region. This archive provides a unique opportunity to conduct high resolution glacial and interglacial palaeoecological research in the SRZ on the north eastern KwaZulu Natal coastal plain.

The aim of our study is to reconstruct the late Pleistocene and Holocene depositional environment and to explore the climatic controls governing peat formation in the Mfabeni peatland under glacial and interglacial conditions. We show compound specific $\delta^{13}C_{wax}$, bulk $\delta^{13}C$ and total organic carbon (TOC) records, integrated with information from proximal stratigraphic and palynological studies undertaken in the peatland, to reconstruct peatland hydrology, sedimentation regimes and proportional inputs of C3/C4 plants. We use these diagnostic palaeoenvironmental indicators to compare the Mfabeni archive with other regional climate records, and investigate if a robust climate signal is preserved in the peat deposit.

2. Methods

2.1. Site description

The UNESCO World Heritage iSimangaliso Wetland Park is situated on the northern coastline of Kwazulu-Natal province, South Africa (Figure 1). The shallow, but extensive 350 km^2 St Lucia Lake dominates the park and forms part of the largest estuarine wetland system on the African continent (Vrdoljak and Hart, 2007). The Mfabeni fen lies on the eastern shores of Lake St Lucia, within an interdunal basin (Botha and Porat, 2007) measuring ca. 10 x 3 km (Clulow et al., 2012), and up to 11 m in depth (Grundling et al., 2013). The fen's hydrology is influenced primarily by the unconfined Maputaland aquifer (Grundling et al., 2013; Taylor et al., 2006a) and local precipitation. The site falls within a sub-tropical climate, which experiences mainly austral summer rainfall of between 900 and 1200 mm/yr (Taylor et al., 2006b), which is driven by sea surface temperatures (SST) anomalies in the adjacent southwest Indian Ocean (Jury et al., 1993; Reason and Mulenga, 1999).

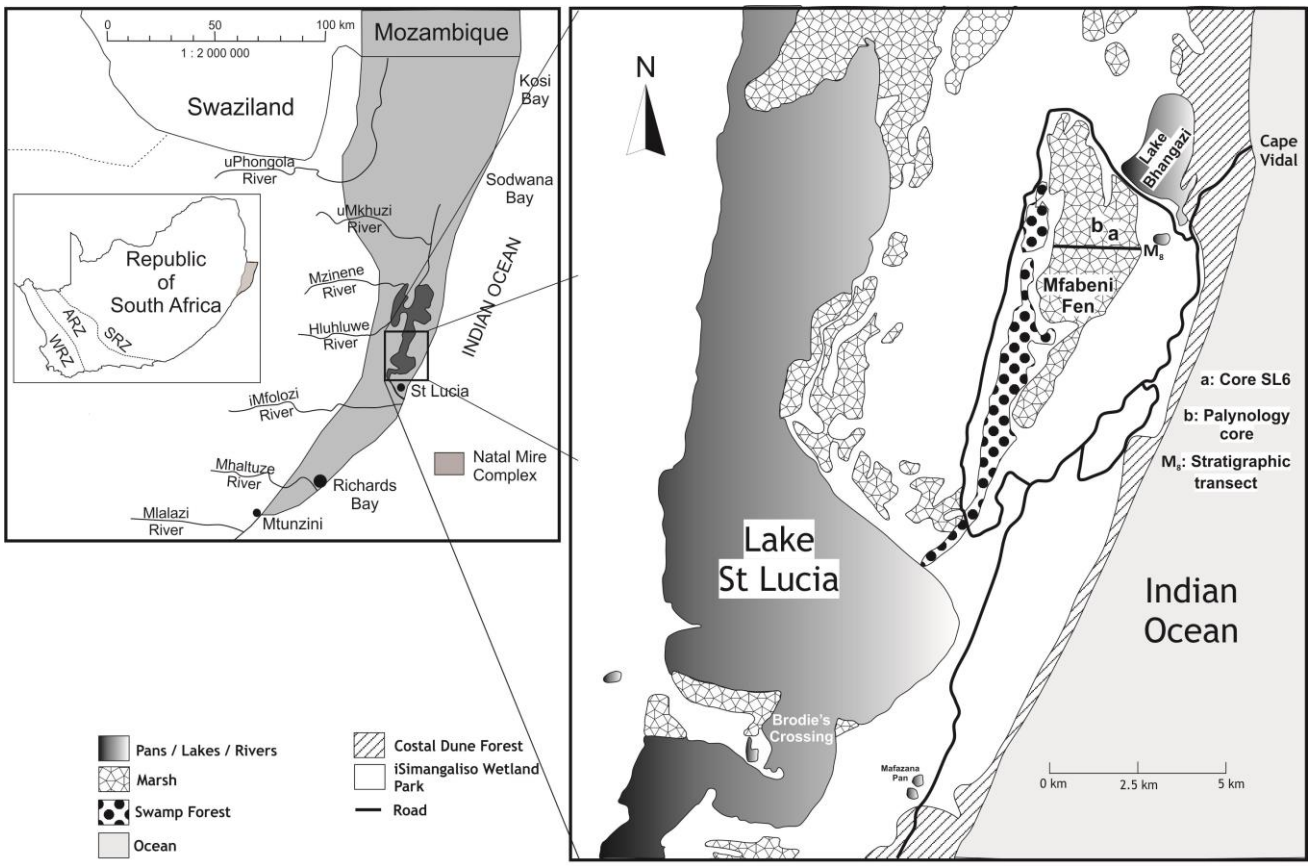

Figure 1: Location of core SL6 (a) in the Mfabeni peatland, iSimangaliso Wetland Park, northern Kwazulu-Natal, South Africa. Location of palynology core (b; Finch and Hill, 2008) and most proximal and deepest stratigraphic transect (M_8; Grundling et al. 2013) included for orientation. WRZ = winter rainfall zone; ARZ = all-year rainfall zone; SRZ = summer rainfall zone.

However, distinctive cyclical drying events with a roughly decadal periodicity (Tyson and Preston-Whyte, 2000) have been identified in the contemporary rainfall records from this region (Bate and Taylor, 2008). The Mfabeni fen forms part of the greater Natal Mire Complex (NMC; Figure 1) that extends from southern Mozambique to Richards Bay, Kwazulu-Natal. It was formed by valley infilling within the KwaMbonanbi formation coastal dune depression (Smuts, 1992), as a result of sustained, but varying groundwater input from the Maputaland aquifer and aggregational blockage of a palaeochannel linking the southern part of the peatland basin with Lake St Lucia (Grundling et al., 2013). The iSimangaliso wetland park vegetation is broadly made up of Maputaland wooded grassland, coastal belt and sub-tropical freshwater wetland and northern coastal forests (Mucina et al., 2006), whereas the fen itself is dominated by herbaceous reed sedges and grasses (Finch and Hill, 2008).

2.2. Sampling techniques

Core SL6 was extracted from the deepest part of the Mfabeni fen (28°9' 0.76"S; 32°31' 30.29"E) to a depth of 810 cm in consecutive coring events using a Russian peat corer (5 cm diameter x 50 cm length core chamber). The individual core samples were logged in the field, and later described and sectioned into 1-2 cm intervals in the laboratory, after which the sediments were freeze-dried in preparation for geochemical analysis.

2.3. Radiocarbon dating / age model

^{14}C dating and age-depth modelling was prepared as per methods listed in Baker et al. (2014, and references therein). Nine evenly spaced samples were chemically pre-treated and measured on a Compact Carbon AMS and conventional ^{14}C ages were calculated using a correction factor for isotopic fractionation. Ages were then calibrated using the IntCal09 calibration curve with a 40 ±20 ^{14}C year southern hemisphere offset (McCormac et al., 1998), while post-bomb ages were calibrated using the southern hemisphere post-bomb curve. Comprehensive core ages were extrapolated within the Bayesian framework, using the age-depth Bacon modelling software.

2.4. Bulk stable C isotope analyses

Bulk stable C and Nitrogen (N) isotope analyses were prepared as per method listed in Baker et al. (2014 and references therein). The peat samples were analysed on a Thermo Scientific Flash 2000 organic elemental analyser, coupled to a Thermo Scientific Delta V Plus isotope ratio mass spectrometer (detection limit 5µg), whereas the sand dominated samples were combusted on a Thermo Finnigan Flash EA 1112 series elemental analyser, coupled to a Thermo electron Delta Plus XP isotope ratio mass spectrometer (detection limit 15 µg). The precision for both analytical systems was 0.05 and 0.08‰ for N and C, respectively. N isotopic composition is expressed relative to atmospheric N, whereas C is expressed relative to Pee-Dee Belemnite formation.

2.5. Compound specific *n*-alkane leaf wax isotope analyses

Stable carbon isotope measurements of *n*-alkanes were done using a Delta V Advantage isotope ratio mass spectrometer interfaced with a GC-Isolink Trace Ultra GC Combustion system (Thermo Scientific). Individual *n*-alkanes were separated using a DB-5 capillary column (30 m × 0.32 mm ×

0.25 µm). Helium was used as a carrier gas at a flow rate of 1.2 ml/min. The GC oven was programmed from 50 °C (1 min) at 20 °C/min to 150 °C and further at 8 °C/min to 320 °C and held for 10 min isothermally. The saturate hydrocarbon fraction containing *n*-alkanes was injected using programmable temperature vaporization (PTV) injector in splitless mode at 280 °C. Combustion of *n*-alkanes to CO_2 was done at 1030 °C. Carbon isotope compositions of *n*-alkanes are reported based on duplicate analyses of well-resolved peaks. The absolute difference between duplicate *n*-alkane $\delta^{13}C$ measurements was 0.5‰ or better. The $\delta^{13}C$ for C_{29}/C_{31} represents a weighted average of individual $\delta^{13}C$ values for each compound:-

$(\delta^{13}C_{29} \times C_{29}\text{peak area} + \delta^{13}C_{31} \times C_{31}\text{peak area})/(C_{29}\text{ peak area} + C_{31}\text{ peak area})$

3. Results

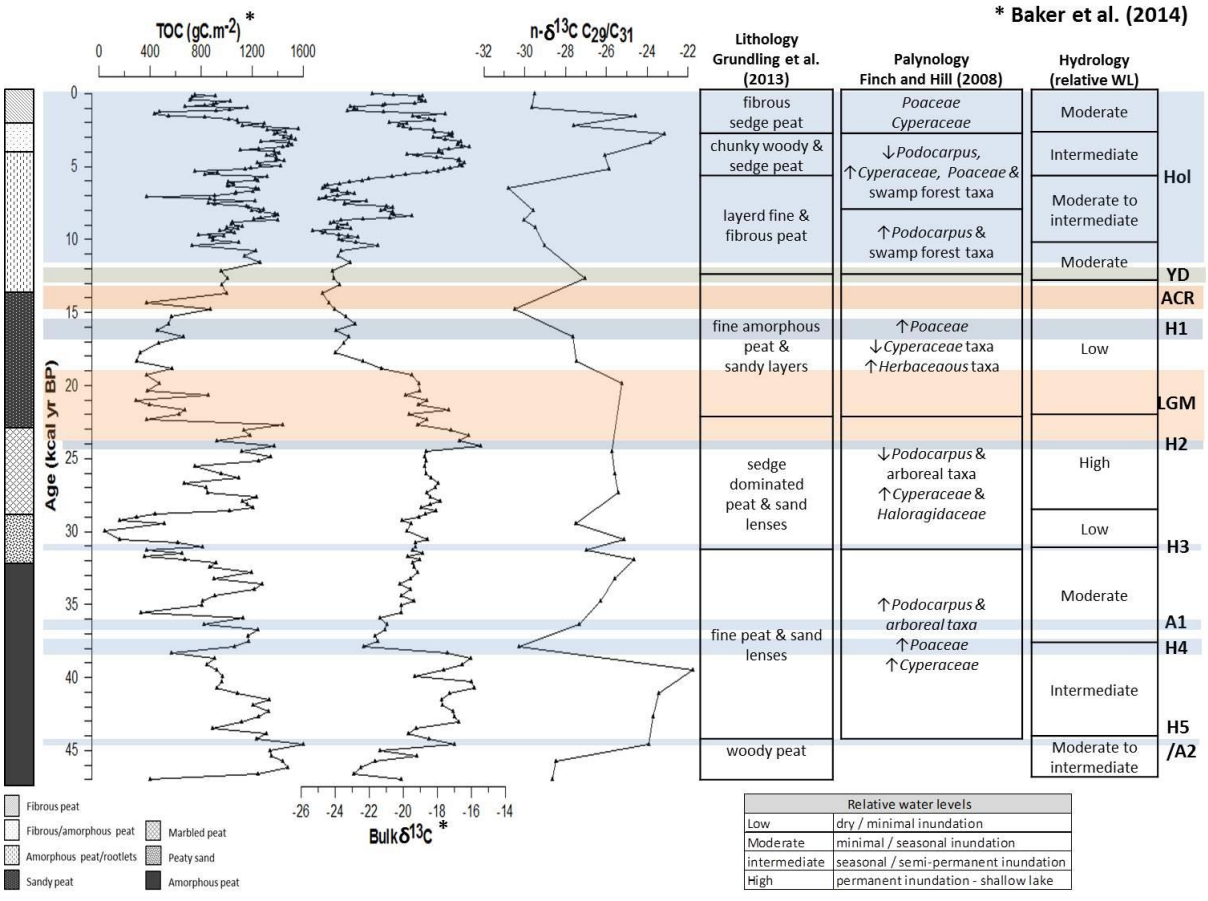

Figure 2: Core SL6 TOC (n=198) , bulk carbon (n=198) and leaf wax (n=35) isotope profiles in comparison with peatland development chronology by Grundling et al. (2013), palynology record by Finch and Hill (2008) and local hydrology interpretation of the Mfabeni peatland. Core SL6 TOC and bulk C isotopic data modified from Baker et al. (2014). H1 – 5 = Heinrich events; A1 and A2 = Antarctic warming events; LGM = Last Glacial Maximum; ACR = Antarctic cold reversal; YD = Younger Dryas; Hol = Holocene.

3.1. Leaf wax $\delta^{13}C$ signatures ($\delta^{13}C_{wax}$)

The leaf wax compound specific C isotope ($\delta^{13}C_{wax}$) values range between -30.8 and -21.8‰ and display a strong statistical correlation with the bulk $\delta^{13}C$ profile (r = 0.87, P=0.01, df = 35, Figure 2, Table 1). The $\delta^{13}C_{wax}$ profile exhibits elevated $\delta^{13}C$ values from 44.5 to 39.5 kcal yr BP and 4.2 to 2.8 kcal yr BP, whereas depleted values were observed at 38.0, 18.4 to 6.5, 2.7 and 1 kcal yr BP to present, with core average values for the remaining sections of the core. The $\delta^{13}C_{wax}$ values are depleted by -8.5 and -3.0‰ with respect to the equivalent bulk $\delta^{13}C$ (Table 1).

Depth (cm)	Age kcal yr BP	TOC gC.m^{-2}	Bulk $\delta^{13}C$	CSIA $\delta^{13}C29/C31$
8	-0.02	n/a	-21.8	-29.5
42	0.98	1163	-22.9	-29.7
57	1.54	540	-19.5	-24.6
75	2.17	1121	-20.3	-27.6
93	2.81	1370	-17.3	-23.2
108	3.39	1491	-16.8	-23.8
135	4.26	1311	-19.2	-26.1
158	5.14	1146	-17.6	-25.9
192	6.46	1227	-24.8	-30.8
209	7.08	371	-24.5	n/a
237	7.99	1194	-21.3	-29.6
258	8.69	1401	-23.7	-30.0
273	9.17	1001	-23.9	-29.5
310	10.40	729	-21.5	-29.1
335	12.64	1005	-24.1	-27.1
355	14.79	871	-24.0	-30.5
375	16.67	657	-23.2	-27.6
390	18.32	295	-22.4	-27.5
405	19.83	469	-19.1	-25.3
424	21.34	393	-19.1	n/a
450	23.06	1131	-17.2	n/a
470	24.50	1118	-18.7	-25.7
490	26.07	955	-18.7	-25.6
510	27.33	850	-18.6	-25.4
539	28.77	434	-18.7	n/a
555	29.46	510	-19.5	-27.5
580	30.58	157	-18.6	-25.2
595	31.24	371	-19.5	-27.0
610	31.90	671	-19.0	-24.6
630	33.21	900	-19.6	-25.6
650	34.76	810	-19.3	-26.3
670	36.33	821	-21.0	-27.3
690	37.92	1063	-22.3	-30.3
710	39.52	922	-17.6	-21.8
730	41.10	1080	-17.3	-23.4
750	42.68	1251	-17.0	-23.7
775	44.61	1602	-17.0	-23.9
790	45.78	1441	-21.7	-28.5
805	46.97	396	-20.1	-28.7

Table 1: TOC, bulk and compound specific leaf wax isotopic values for peat samples that underwent biomarker extraction in core SL6. n/a = data not available due to sample contamination or age model restrictions.

3.2. Bulk $\delta^{13}C$ signatures ($\delta^{13}C_{bulk}$)

As reported in Baker et al. (2014), $\delta^{13}C$ bulk signal fluctuates between a maximum of -15.5‰ (ca. 24.2 kcal yr BP) and minimum of -25.3 (ca. 9.4 kcal yr BP), with no discernible overall trend (Figure 2). With the exception of the base interval, the $\delta^{13}C$ signal becomes enriched in ^{13}C up core from ca. 46.6 to ca. 38.3 kcal yr BP before becoming depleted in ^{13}C at ca. 37.9 kcal yr BP. Thereafter, the $\delta^{13}C$ signal increases steadily to the core maximum value at ca. 24.2 kcal yr BP, and then declines again to the core minimum at ca. 9.4 kcal yr BP. For the remaining part of the upper core, the $\delta^{13}C$ signal becomes enriched in ^{13}C through a succession of fluctuating cycles displaying pronounced enrichment shifts in ^{13}C of 4.5‰ (ca. 8.8 to 8.4 kcal yr BP), 8.2‰ (ca. 6.5 to 4.7 kcal yr BP) and 4.5‰ (ca. 1.2 to 0.15 kcal yr BP).

3.3. Total Organic Carbon (TOC)

As reported in Baker et al. (2014), the sediment TOC of core SL6, fluctuates between a minimum of 9.65 g C.m-2 (ca. 30.4 kcal yr BP) and a maximum of 1600 g C.m-2 (ca. 44.6 kcal yr BP) with a

total core average of 981 g C.m-2 (Figure 2). TOC increases up core to the maximum at ca. 44.6 kcal yr BP, after which a steady overall decline occurs to the core minimum at c 30.4 kcal yr BP. TOC values then steadily increase again to 1131 g C.m-2 at ca. 23.1 kcal yr BP, followed by a sharp decline and continued below average TOC values are exhibited until ca. 12.6 kcal yr BP. Thereafter, TOC increases in the lead up to and during the Holocene which shows overall elevated TOC values with sharp millennial scale declines at ca. 7.08 and 1.54 kcal yr BP.

4. Discussion

The C3 and C4 photosynthetic pathways employed by higher plants gives rise to characteristic leaf wax $\delta^{13}C$ signatures, which to a large extent, get preserved in peat deposits (Cranwell, 1981). However, lipid biomarkers make up only a small percentage of TOC preserved in sediments (Meyers, 1997). As a consequence, multi-proxy bulk geochemical data should be considered in conjunction with compound specific C isotopic values to help delineate physical peat forming processes and organic matter (OM) sources at time of sedimentation. Tropical and sub-tropical peatlands occur in warm and moist environments, conditions that are favourable for OM remineralisation (Kuder et al., 1998). Since peat accumulates when net primary production (NPP) outstrips microbial decomposition (Chimner and Ewel, 2005), the overriding control on peat formation in the tropics is the extent of waterlogging, and to a lesser degree, NPP, which generates anaerobic conditions and results in peat formation (Rieley et al., 1996). In this context, the OM rich Mfabeni fen deposit is ideally suited for palaeoenvironmental study as it is a relatively ancient continuous peat deposit that is a well preserved record of an autochthonous depositional regime subject only to local precipitation and groundwater recharger (Baker et al., 2014; Grundling et al., 2013). Grundling et al. (2013) argued that the Mfabeni fen's geomorphological and consistent groundwater recharge was the overriding factors for the uninterrupted peat accumulation since its inception and this could have buffered the fen against climatic disturbances. Consistent with this, the biomarker study done by Baker et al., (in review) showed definitive periods of high water levels that facilitated a dominant submerged macrophyte input in the Mfabeni (ca. 44.5 – 42.6, 29.7, 26.1 – 23.1, 16.7 – 7.1 and 2.2 kcal yr BP), highlighting the control that local hydrology had on the plant

type assemblages within the peatland. However, hydrological studies of the eastern shores of the St Lucia estuarine system (Taylor et al., 2006a) have found that regional and temporal variations in rainfall are the driving factors controlling the local hydrological regime. The highest contemporary rainfall (> 1200 mm/yr) occurs on the coastal dune barrier that is the main recharge area of the Maputaland aquifer, with approximately 20% of total rainfall falling on the dunes ending up as recharge in the aquifer (Kelbe and Rowlins, 1993).

A significant and strong statistical correlation exists between the $\delta^{13}C_{bulk}$ and $\delta^{13}C_{wax}$ trends in core SL6 ($r=0.87$, $P=0.01$, $df=35$), which suggests that the dominant control on $\delta^{13}C_{bulk}$ values is the relative contributions of C3 and C4 plant types into the peat record. There is a lack of research on the effects of growing season temperatures and moisture availability on the $\delta^{13}C_{wax}$ signal of contemporary plants in the region. However, based on the strong statistical correlation between the bulk and leaf wax $\delta^{13}C$ signals in core SL6, we make the assumption that the $\delta^{13}C_{bulk}$ values of core SL6 is an accurate historical record of the proportional inputs of C3 and C4 vegetation into the peatland. Furthermore, Baker et al. (2014) showed by comparing elemental C and N trends with depth, and the lack of consistent statistical correlations between $\delta^{13}C_{TOC}$, $\delta^{15}N$ and atomic C/N, that core SL6 exhibits a high degree of preservation, which advocates for minor post-depositional isotopic C fractionation in the Mfabeni peatland.

4.1. Plant assemblage and chronology reconstruction

To assist in delineating the late Pleistocene and Holocene palaeoenvironmental origins of the relatively dramatic shifts in leaf wax and bulk C isotopic signature in the Mfabeni fen, a comparison exercise was undertaken with similarly age constrained proximal stratigraphy (Grundling et al., 2013) and palynology studies (Finch and Hill, 2008). The palynology research was conducted on a single core extracted from the deepest part of the fen in close proximity to core SL6, while the stratigraphic investigation was based on several cores drilled along eight east-west transects, spaced between 800 to 1600 m apart from north to south (see figure 1 for core locations and most proximal transect).

When we compare the three different Mfabeni records (Figure 2), they correlate strongly in respect to boundary and transition ages where major deviations in plant assemblages and peat chronology are recorded. Since the average *n*-alkane C isotopic composition of C3 plants has been estimated to be ca. -36‰ and plants using the C4 photosynthetic pathway ca. -21.5‰ (Collister et al., 1994), the fluctuations in the C_{29} and C_{31} leaf wax C isotope values can be used to indicate changes in proportional contribution to the soil organic matter of these two groups of plant types. By comparing the $\delta^{13}C_{wax}$ data with the stratigraphic and palynology records, we have reconstructed the palaeoenvironment changes in Southern Africa since ca. 47 kcal yr BP.

4.1.1. Before the Last Glacial Maximum (LGM)

From ca. 47.0 to 44.5 kcal yr BP (Figure 2), the molecular isotope signal suggests a high proportion of C3 plant input into the sediments in conjunction with the stratigraphy study recording a riparian / swamp forest dominated environment (Grundling et al., 2013) with increasing TOC values. These parameters indicate the intrusion of C3 swamp forest / arboreal vegetation into the peatland, implying moderate water levels during this period. At ca. 44.5 kcal yr BP, the leaf wax C isotope signal becomes ^{13}C-enriched, suggesting a shift to higher proportions of C4 plant input, coincidental with a switch to a shallow lake environment (Grundling et al., 2013) in the area where core SL6 was extracted. The palynology study records dominant local grass and sedge taxa (Finch and Hill, 2008) correlating with core SL6 TOC maximum (Baker et al., 2014). A sustained elevated water level could feasibly have pushed the C3 forests to the periphery, and facilitated C4 sedges and grasses to colonise the peatland basin, resulting in higher TOC and molecular $\delta^{13}C$ values. Similarly, the stable isotope record in the Lobatse II cave in the semi-arid SRZ of Botswana, displayed a strong C4 signature between ca. 46 and 43 kyr BP, which Holmgren et al. (1995) proposed was as a result of C4 grass proliferation in response to a drier climate, rather, due to a reduction of winter rainfall.

The trend towards higher $\delta^{13}C_{wax}$ values continues until ca. 38 kcal yr BP, coeval with slowly decreasing TOC. Following this, a sharp decrease in $\delta^{13}C_{wax}$ signal occurs more than likely as a result of declining water levels in the peatland and the re-encroachment of the abundant C3 arboreal forests into the basin (*Podocarpus, Anacardiaceae* and *Celastraceae;* Finch and Hill,

2008). A similar sharp decrease in $\delta^{13}C_{wax}$ values was recorded ca. 37 ka in a Sadwala Cave stalagmite, situated in the SRZ transition between the Highveld and Lowveld habitats, which Green et al. (2015) attributed to the expansion of closed C3 forest environments at the site. Thereafter, the Mfabeni $\delta^{13}C_{wax}$ values steadily increase and stabilise to above average values for the next ca. 10 kcal yr BP, with the exception of excursions to below average values at ca. 31.2 and 29.5 kcal yr BP (Figure 2 and Table 1). Both events are accompanied by low TOC values suggesting a reduced water table with a mixed C3 arboreal forest and C4 sedge palynological signal. The fluctuating $\delta^{13}C_{wax}$ signal between ca. 31.9 and 28.7 kcal yr BP (accompanied by low, but unstable TOC signal, sedge dominated peat and a slow increase in sedge populations at the expense of arboreal forests) could be due to the interplay between encroaching and receding C3 forests into the sedge dominated peatland in response to fluctuating water levels during this period. After ca. 28 kcal yr BP, the TOC values steadily increase, while the $\delta^{13}C_{wax}$ signal stabilizes at above average values implying a permanently established C4 sedge fen type environment accompanied by the first appearance of aquatic plant taxa in the palynology record (Finch and Hill, 2008). These parameters, along with a peak in the $\delta^{13}C_{bulk}$ values, advocate sufficiently elevated water table levels in the peatland to support both submerged (Baker et al., in review) and emergent plant types to the exclusion of arboreal forests up until ca. 23 kcal yr BP.

4.1.2. The Last Glacial Maximum and deglacial

A sharp decline in TOC, decrease in $\delta^{13}C_{wax}$ values and an abrupt change to a grass dominated environment recorded in both the stratigraphic and palynology records occurs after ca. 23 kcal yr BP. These trends continue up till ca. 14.8 kcal yr BP, with the exception of a gradual increase in TOC values after ca. 18.3 kcal yr BP. Both Grundling et al. (2013) and Finch and Hill (2008) interpreted the strong grassland stratigraphic and palynology signal to signify drying conditions in the peatland that facilitated the expansion of grasses to the exclusion of sedges and swamp forests in and around the Mfabeni basin. The sharp excursion in core SL6 $\delta^{13}C_{wax}$ signal to more negative values suggests a large increase in C3 plant input into the sediments during this same period, inferring a change to more temperate C3 grasses during the LGM and late glaciation. Scott (2002), Rommerskirchen et al. (2006) and Dupont et al. (2011) concluded that there is very little

evidence for increased C4 grasses during the LGM in sub-tropical Southern Africa, and that C3 grasses more than likely dominated the region during this period. This is in direct contrast to records studied in the tropical regions of Africa where there is strong evidence for C4 plant expansion during the LGM (Castañeda et al., 2009; Sinninghe Damsté et al., 2011). Furthermore, McLean and Scott (1999) undertook a phytolith investigation in the Tswaing Crater, situated on the SRZ escarpment of South Africa, and observed that *Festucoid* C3 grasses were dominant during the LGM. An increase of 3.4‰ to more positive leaf wax $\delta^{13}C$ values occurs at ca. 12.6 kcal yr BP, coeval with increased TOC and continued high frequency of grassland taxa. These parameters indicate a switch to predominant C4 grasses and sedge populations in the peatland, more than likely in response to increasing water levels during the transition from glacial to interglacial conditions.

4.1.3. Holocene

At the start of the Holocene (ca. 11.5 kcal yr BP), the $\delta^{13}C_{wax}$ data set once again becomes more negative, continuing on the declining trend until the beginning of the mid-Holocene (ca. 6.5 kcal yr BP), corresponding to rapid increases in arboreal and a peak in swamp forest taxa (Finch and Hill, 2008), and overall increased TOC values. Lee-Thorp and Beaumont (1995) similarly observed deviations to higher C3 plant signatures in tooth enamel samples of grazers found in Equus Cave, which is located in the sub-tropical SRZ, during the early Holocene (ca. 12 – 9.5 kyr BP). These parameters infer a switch from overall low water levels of the glacial and deglacial periods to increased ground water inundation and direct precipitation in the Mfabeni, conditions conducive for the intrusion of C3 swamp forests into the peatland which resulted in the depleted $\delta^{13}C_{wax}$ signal. Included in this period is an intense, but short excursion to low TOC values (ca. 7.1 kcal yr BP), signifying a drying period (Baker et al. 2014) before a recovery of TOC values (and water levels) at ca. 6.5 kcal yr BP, after which the TOC signal remains elevated till ca. 1.5 kcal yr BP. The ensuing elevated water levels are accompanied by a switch to more enriched $\delta^{13}C_{wax}$ values and a marked increase in sedge and grass taxa at the expense of arboreal forest pollens. Scott et al. (2003) also observed a relatively large enrichment in ^{13}C in the peat $\delta^{13}C_{bulk}$ values between ca. 5 and 3 kyr BP from the Wonderkrater thermal spring located in the sub-tropical SRZ of the Limpopo province.

The Mfabeni stratigraphic study recorded chunky and fibrous peat, remnants of swamp forest OM input during this period according to Grundling et al. (2013). However, our core SL6 peat texture and the palynology record, indicates an open sedge fen environment, with reduced input from arboreal and swamp forests. This discrepancy could arguably be put down to dating discrepancies and different age models employed by the various investigations. This period of more positive $\delta^{13}C_{wax}$ and elevated TOC values corresponds to a decline in arboreal pollen and a marked increase in sedge and grass taxa, suggesting the increased basin water levels pushed back C3 forests and allowed for C4 sedges to flourish in the peatland. After ca. 2.9 kcal yr BP till present, all three parameters start an overall declining but fluctuating trend, representing a general drying trend interspersed with elevated water levels that resulted in the periodic incursion, and subsequent retreat, of peripheral swamp forests into the sedge and grassland dominated peatland, as is prevalent in the plant distribution found in and around the peatland today.

4.2. Palaeoclimate reconstruction

As previously discussed, the strong and significant correlation between core SL6 $\delta^{13}C_{wax}$ and $\delta^{13}C_{bulk}$ signals suggests that the dominant control on soil $\delta^{13}C$ values, is the relative contribution of terrestrial C3 and C4 plant types into the Mfabeni sediments. The comparatively low resolution of the molecular C isotope sampling ($\delta^{13}C_{wax}$ n = 35) does not lend the data set to high resolution climate reconstructions, however, the bulk C isotopic sampling resolution is higher ($\delta^{13}C_{bulk}$ n = 198) providing us the opportunity to correlate the geochemical signal in core SL6 with other climate proxies. To facilitate this investigation, we overlaid the TOC, $\delta^{13}C_{wax}$ and $\delta^{13}C_{bulk}$ data sets with established northern and southern Hemisphere climatic events, along with interpretations of bulk geochemical (Baker et al., 2014), stratigraphy (Grundling et al., 2013) and palynology (Finch and Hill, 2008) investigations in the Mfabeni deposit (Figure 2).

When reviewing the data sets collectively, there appears to be definitive geochemical perturbations, either at the onset, during or termination of H4, LGM, deglaciation and Holocene periods (Figure 2). The H5/A2 events (ca. 44.5 kcal y BP) is marked by the transition from moderate to intermediate water levels and an overall gradual switch from C3 riparian / swamp

forest to C4 sedge and grass dominated vegetation, coeval with a peak in core %TOC values. This infers an increase in local precipitation and a switch to seasonal/ semi-permanently inundated hydrology in the basin that was conducive for the propagation of water loving sedges to the exclusion of arboreal forests. SST analysed in a proximal Mozambique Channel marine core (MD79257; $20^0$24' S; $26^0$20' E; Bard et al., 1997) exhibited a sharp increase during the same A2 warming event, which would be expected to cause increased continental precipitation over eastern and southern Africa (Goddard and Graham, 1999; Dupont et al., 2011).

At the onset of the H4 event, a sharp depletion is observed for both the bulk (-4.9‰) and molecular C isotope (-8.5‰) values, coeval with a switch back to moderate water levels and high frequencies of C3 arboreal forest taxa. These parameters suggest a reduction in local precipitation and temperatures, allowing for the intrusion of arboreal forests into the peatland, supported by a reduction of bacterial activity biomarker proxies (*n*-alkanoic acid carbon preference index; CPI_{FA} and *n*-alkanoic acid saturated vs unsaturated concentrations; $sat/unsat_{FA}$) in the Mfabeni (Baker et al. in review) during the same period. At ca. 28.0 kcal yr BP, a sharp recovery in TOC values occurs, concordant with gradually increasing bulk and molecular $\delta^{13}C$ signals and a peak in TOC and $\delta^{13}C_{bulk}$ at ca. 22.7 and ca. 24.2 kcal yr BP (H2), respectively. This period is interpreted to represent a shallow lake environment with predominant C4 sedge and aquatic plant assemblages (biomarker aquatic plant proxy; P_{aq}; Baker et al. in review). This relatively large increase in local precipitation is corroborated by the Mozambique Channel marine core (MD79257) SST spike (Bard et al., 1997), an increase in ambient temperatures recorded in ARZ Cango Cave speleothem (Talma and Vogel, 1992) and peak in lake levels of the SRZ Tswaing impact crater lake at around ca. 28 kcal yr BP.

At the peak of LGM, the Mfabeni record exhibits a dramatic shift to dry and cooler conditions (Figure 2, ca. 22.7 kcal yr BP) inferred by the abrupt decline in TOC values, change to sandy peat and therefore low water levels, and a transition to more dominant C3 grasslands, which persisted until ca. 15.0 kcal yr BP. This interpretation is further supported by several biomarker proxies investigated in the Mfabeni peatland (Baker et al. in review), where a definite switch from aquatic to terrestrial plant input (P_{aq} and leaf wax proxy; P_{wax}) and a decrease in temperature sensitive

microbial decomposition rates (CPI_{FA} and $sat/unsat_{FA}$) occurred after 23.1 kcal yr BP. Several supplementary Southern African regional climate archives likewise recorded a dry and cool climate during the LGM. Most notably, the Mozambique marine core MD79257, which returned its lowest SST value at ca. 20 kcal yr BP (Bard et al., 1997), and a palynology study on marine core MD96-2048 situated ~ 120 km south of Limpopo River mouth (Dupont et al., 2011), inferring lower regional temperatures and moderately less rainfall. Additionally, a SRZ Cold Air Cave stalagmite in the Makapansgat Valley exhibited lower temperatures between ca. 23 and 21 kyr (Holmgren et al., 2003), and the proximal Wonderkrater fossil pollen sequence recorded both 6 ± 2 °C cooler LGM temperatures and ca. 50% less precipitation than the Holocene period (Truc et al., 2013) during the LGM. These cooler and drier glacial conditions could arguably have been the cause for a shift to C3 grass dominance in the Mfabeni, which tend to have an advantage over C4 grasses at lower growing season temperatures (Sage et al., 1999; Kotze and O' Conner, 2000), and appear to have dominated the sub-tropical and WRZ of Southern African during the LGM (Scott, 2002; Rommerskirchen et al., 2006; Dupont et al., 2011). These conditions persist with TOC fluctuating at below average core levels, the $\delta^{13}C_{bulk}$ signal becoming increasingly more negative and dry grassland palynology signature continuing until ca. 15 kcal yr BP. Thereafter, even though the TOC profile steadily increases after the onset of the Antarctic cold reversal (ACR) event, the $\delta^{13}C_{bulk}$ signal remains relatively low until the onset of the early Holocene.

The early Holocene (ca. 10.5 – 7.1 kcal yr BP) is depicted in core SL6 by overall elevated TOC values compared to the preceding deglacial period (Baker et al., 2014), albeit for a brief millennial scale excursion to low TOC level at ca. 7.1 kcal yr BP, and fluctuating but predominant C3 arboreal and swamp forest molecular and bulk $\delta^{13}C$ signatures. The Mfabeni biomarker investigation (Baker et al. in review) showed that the early Holocene (ca. 10.5 – 7.1 kcal yr BP) was a period of relatively cool (low microbial activity; CPI_{FA}) and wet (high P_{aq}) conditions, conducive for the proliferation of submerged macrophytes in and arboreal swamp forests (Finch and Hill, 2008) around the basin. This interpretation is supported by the Wonderkrater palynology sequence (Truc et al., 2013) and stable isotope speleothem record in the Cold Air Cave (Holmgren et al., 2003).

The Holocene maximum was terminated in the Mfabeni by a short dry event at ca. 7.1 kcal yr BP (low TOC; Baker et al., 2014), corroborated by the proximal lake Eteza palynology record (Neumann et al., 2010) and drop in Mozambique channel SST (Bard et al., 1997). After ca. 6.5 kcal yr BP, both the $\delta^{13}C_{wax}$ and $\delta^{13}C_{bulk}$ values abruptly increased and remain elevated until ca. 2.2 kcal yr BP. These isotopic trends are accompanied by increasing elevated TOC values, a switch to intermediate water levels and sedge dominated peat (Figure 2). During this period, the palynological investigation (Finch and Hill, 2008) recorded a marked increase in sedge and grasslands populations, inferring increased ambient temperatures and moisture content supported by the Mfabeni biomarker proxies (Baker et al., in review), δD and SST records in the adjacent Indian Ocean GeoB937-3 marine core (Schefuß et al., 2011). Thereafter, an overall decreasing, albeit fluctuating, trend in all three parameters, corresponding to a return to moderate peatland water levels and oscillating quantities of C3 peripheral arboreal pollen into the C4 graminoid dominated peatland in response to fluctuations in basin water levels. We interpret these trends to signify an overall drying trend with cyclical fluctuations in precipitation, corroborated by similar general drying conditions recorded in proximal Lake Sibaya and Kosi Bay after ca. 2 kcal yr BP (Walther and Neumann, 2011). The Mfabeni Holocene peat archive supports other investigations findings that the Holocene was not as stable as previously perceived both regionally (Bard et al., 1997; Schefuß et al., 2011; Baker et al., 2014) and globally (Mayewski et al., 2004).

Our research has shown that the high resolution bulk C isotopic trends in core SL6, which has a strong and significant correlation with the molecular leaf wax C isotopes, reveals perturbations during several of the established climate events since the late Pleistocene, namely the H4, LGM, deglaciation and Holocene period. However, some of the shorter, and possibly less intense, climatic events do not exhibit significant shifts in stable C isotope values. This implies that local hydrological overprinting blurred the climatic $\delta^{13}C_{bulk}$ signal for the more muted events in the Mfabeni peatland, by either attenuating the perturbations or resulting in changes in plant assemblages that did not significantly affect the $^{13}C/^{12}C$ fractionation ratio.

5. Conclusions

n-Alkane $\delta^{13}C$ record was analysed in the Mfabeni peat core and, along with published bulk geochemical data ($\delta^{13}C_{bulk}$, TOC) from the same core, compared to palynological data and stratigraphic investigations. These data sets were then used to reconstruct the late Pleistocene and Holocene environment variability and to investigate if a climate signal is preserved in the peat archive. The $\delta^{13}C_{wax}$ data set established large variability in the proportional contributions of C3 and C4 terrestrial plants throughout the sedimentary history of the Mfabeni peatland and correlated strongly with the palynology and stratigraphic records and other regional bulk C isotopic investigations. Due to the strong and significant correlation observed between $\delta^{13}C_{bulk}$ and $\delta^{13}C_{wax}$ data sets, we concluded that the $\delta^{13}C_{bulk}$ signal represents the proportional contributions of C3 and C4 terrestrial plant assemblages, which allowed us to substitute the high resolution $\delta^{13}C_{bulk}$ for the $\delta^{13}C_{wax}$ data set to explore if a climate signal was preserved in the Mfabeni deposit. We found evidence for palaeoenvironmental shifts during some of the well-established climatic events since the late Pleistocene (H4, LGM, deglacial period and Holocene). This is consistent with other regional climate records, most notably, the adjacent Indian Ocean SST records. However, due to the rather muted response of core SL6 $\delta^{13}C_{bulk}$ record with regard to the other shorter climatic events (H5/A2, A1, H3, H2, H1, ACR, and YD), we conclude that the local hydrology of the fen overprinted the signal for climatic events that were less pronounced and / or ephemeral events. Future work in this area would benefit from higher resolution leaf wax $\delta^{13}C$ analysis to definitively resolve the blurred palaeoenvironmental signals during the more ephemeral climatic events and provide a better understanding of palaeoecological variability in Southern Africa. Nonetheless, the Mfabeni peatland has proven to be an important archive of environment and climate variability during the late Pleistocene and Holocene, and a valuable contributor to our understanding of the mechanisms that drove environmental fluctuations in southern Africa during the last glacial and interglacial periods.

6. Acknowledgments

Alistair Clulow assisted with field access and site identification. A Russian peat corer was loaned to the project by Piet-Louis Grundling. iSimangaliso Authority and Ezemvelo KZN Wildlife granted park access and sampling permits. The project was supported through a bilateral funding agreement by the Swedish Research Link-South Africa program (Grant 348-2009-6500). Student support was supplied by the Department of Science and Technology, National Research Foundation and InKaba yeAfrica (AEON). This is an Inkaba ye Africa publication no. 160 and AEON publication no. 153.

7. References

Baker, A., Routh, J., Blaauw, M., Roychoudhury, A.N., 2014. Geochemical records of palaeoenvironmental controls on peat forming processes in the Mfabeni peatland, KwaZulu Natal, South Africa since the Late Pleistocene. Palaeogeography, Palaeoclimatology, Palaeoecology. 395, 95–106.

Baker, A., Routh, J., Roychoudhury, A.N., in review. Biomarker records of palaeoenvironmental variations in subtropical southern Africa since the late Pleistocene: evidence from a costal peatland. Palaeogeography, Palaeoclimatology, Palaeoecology.

Bard, E., Rostek, F., Sonzogni, C., 1997. Interhemispheric synchrony of the last deglaciation inferred from alkenone palaeothermometry. Nature. 385, 707-710.

Bate, G.C., Taylor, R.H., 2008. Sediment salt-load in the St Lucia Estuary during the severe drought of 2002-2006. Environmental Geology. 55, 1089–1098.

Botha, G., Porat, N., 2007. Soil chronosequence development in dunes on the southeast African coastal plain, Maputaland, South Africa. Quaternary International. 162-163, 111–132.

Castañeda, I.S., Werne, J.P., Johnson, T.C., Filley, T.R., 2009. Late Quaternary vegetation history of southeast Africa: The molecular isotopic record from Lake Malawi. Palaeogeography, Palaeoclimatology, Palaeoecology. 275, 100–112.

Cerling, T.E., Harris, J.M., Macfadden, B.J., Leakey, M.G., Quade, J., Eisenmann, V., Ehleringer, J.R., 1997. Global vegetation change through the Miocene / Pliocene boundary. Nature. 389, 153–158.

Chikaraishi, Y., Naraoka, H., 2003. Compound-specific δD–δ13C analyses of *n*-alkanes extracted from terrestrial and aquatic plants. Phytochemistry 63, 361–371.

Chimner, R. A., Ewel, K.C., 2005. A tropical freshwater wetland: II. Production, decomposition, and peat formation. Wetlands Ecology and Management. 13, 671–684.

Clulow, a. D., Everson, C.S., Mengistu, M.G., Jarmain, C., Jewitt, G.P.W., Price, J.S., Grundling, P.L., 2012. Measurement and modelling of evaporation from a coastal wetland in Maputaland, South Africa. Hydrology and Earth System Sciences.16, 3233–3247.

Collister, J.W., Rieley, G., Stern, B., Eglinton, G., Fry, B., 1994. Compound-specific ~3C analyses of leaf lipids from plants with differing carbon dioxide metabolisms. Organic Geochemitry. 21, 619–627.

Cranwell, P.A., 1981. Diagenesis of free and bound lipids in terrestrial detritus deposited in a lacustrine sediment. Organic Geochemistry. 3, 79–89.

Dupont, L.M., Caley, T., Kim, J.-H., Castañeda, I., Malaizé, B., Giraudeau, J., 2011. Glacial-interglacial vegetation dynamics in South Eastern Africa coupled to sea surface temperature variations in the Western Indian Ocean. Climate of the Past. 7, 1209–1224.

Ehleringer J.R., Cerling, T.E., Helliker, B.R., 1997. C4 Photosynthesis, atmospheric CO2 and climate. Oecologia. 112, 285 – 299.

Eglinton, G., Hamilton, R.J., 1967. Leaf Epicuticular Waxes. Science. 156, 1322–1335.

Finch, J.M., Hill, T.R., 2008. A late Quaternary pollen sequence from Mfabeni Peatland, South Africa: Reconstructing forest history in Maputaland. Quaternary Research. 70, 442–450.

Goddard, L., Graham, N.E., 1999. Importance of the Indian Ocean for simulating rainfall anomalies over eastern and southern Africa. Journal of Geophysical Research. 104, 190 - 199.

Green, H., Pickering, R., Drysdale, R., Johnson, B.C., Hellstrom, J., Wallace, M., 2015. Evidence for global teleconnections in a late Pleistocene speleothem record of water balance and vegetation change at Sudwala Cave, South Africa. Quaternary Science Reviews. 110, 114–130.

Grundling, P.L., Grootjans, A. P., Price, J.S., Ellery, W.N., 2013. Development and persistence of an African mire: How the oldest South African fen has survived in a marginal climate. Catena. 110, 176–183.

Hayes, J.M., Freeman, K.H., Popp, B.N., Hoham, C.H., 1990. Compound-specific isotopic analyses: a novel tool for reconstruction of ancient biogeochemical processes. Organic Geochemistry. 16, 1115–1128.

Holmgren, K., Karlén, W., Shaw, P. a, 1995. Paleoclimatic Significance of the Stable Isotopic Composition and Petrology of a Late Pleistocene Stalagmite from Botswana. Quaternary Research. 43, 320-328.

Holmgren, K., Lee-Thorp, J. a., Cooper, G.R.J., Lundblad, K., Partridge, T.C., Scott, L., Sithaldeen, R., Talma, a. S., Tyson, P.D., 2003. Persistent millennial-scale climatic variability over the past 25,000 years in Southern Africa. Quaternary Science Reviews. 22, 2311–2326.

Jury, M.R., Valentine, H.R., Lutjeharms, J.R.E., 1993. Influence of the Agulhas Current on Summer Rainfall along the Southeast Coast of South Africa. Journal of Applied Meteorology and Climatology. 32, 1282–1287.

Kelbe, B., Rawlins, B., 1993. Geohydrology of the eastern shores of St Lucia, in: Taylor, R.H. (Ed.), Proceedings of the Workshop on Water Requirements for Lake St Lucia. Department of Environmental Affairs, Pretoria, South Africa, pp. 32–38.

Kotze, D.C., O' Connor, T.G., 2000. Vegetation Variation within and among Palustrine Wetlands along an Altitudinal Gradient in KwaZulu-Natal , South Africa. Plant Ecology. 146, 77–96.

Kuder, T., Kruge, M.A., Shearer, J.C., Miller, S.L., 1998. Environmental and botanical controls on peatification — a comparative study of two New Zealand restiad bogs using Py-GC/MS , petrography and fungal analysis. The International Journal of Coal Geology. 37, 3–27.

Lee-Thorp, J. a, Beaumont, P.B., 1995. Vegetation and Seasonality Shifts during the Late Quaternary Deduced from 13C/12C Ratios of Grazers at Equus Cave, South Africa. Quaternary Research. 43, 426-432.

Mayewski, P. a., Rohling, E.E., Stager, J.C., Karlén, W., Maasch, K. a., Meeker, L.D., Meyerson, E. a., Gasse, F., van Kreveld, S., Holmgren, K., Lee-Thorp, J., Rosqvist, G., Rack, F., Staubwasser, M., Schneider, R.R., Steig, E.J., 2004. Holocene climate variability. Quaternary Research. 62, 243–255.

McCormac, F.G., Hogg, A.G., Higham, T.F.G., Lynch-Stieglitz, J., Broecker, W.S., Baillie, M.G.L., Palmer, J., Xiong, L., Pilcher, J.R., Brown, D., Hoper, S.T., 1998. Temporal variation in the interhemispheric 14C offset. Geophysical Research Letters. 25, 1321–1324.

McLean, B., Scott, L., 1999. Phytoliths in sediments of the Pretoria Saltpan (Tswaing Crater) and their potential as indicators of the environmental history at the site. Pretoria, South Africa.

Meyers, P. A., 1997. Organic geochemical proxies of paleoceanographic, paleolimnologic, and paleoclimatic processes. Organic Geochemistry. 27, 213–250.

Mucina, L., Adams, J.B., Knevel, I.C., Rutherford, M.C., Powrie, L.W., Bolton, J.J., van der Merwe, J.H., Anderson, R.J., Bornman, T.G., le Roux, A., Janssen, J.A.M., 2006. Coastal vegetation of South Africa, in: Mucina, L., Rutherford, M.C. (Eds.), The Vegetation of South Africa, Lesotho and Swaziland. South African National Biodiversity Institute, Pretoria, pp. 658–696.

Neumann, F.H., Scott, L., Bousman, C.B., van As, L., 2010. A Holocene sequence of vegetation change at Lake Eteza, coastal KwaZulu-Natal, South Africa. Review of Palaeobotany and Palynology. 162, 39–53.

Reason, C.J.C., Mulenga, H., 1999. Relationships between South African rainfall and SST anomalies in the southwest Indian Ocean. International Journal of Climatology. 19, 1651–1673.

Rieley, J.O., Ahmad-Shah, A.A., Brady, M.A., 1996. The Extent and Nature of Tropical Peat Swamps - Tropical Lowland Peatlands of Southeast Asia, in: Integrated Planning and Management of Tropical Lowland Peatlands Workshop - Tropical Lowland Peatlands of Southeast Asia.

Rommerskirchen, F., Eglinton, G., Dupont, L., Rullkötter, J., 2006. Glacial/interglacial changes in southern Africa: Compound specific δ13C land plant biomarker and pollen records from southeast Atlantic continental margin sediments. Geochemistry, Geophysics, Geosystems 7 (8).

Sage, R.F., Wedin, D.A., Li, M., 1999. The biogeography of C4 photosynthesis: patterns and controlling factors, in: Sage, R.F., Monson, R.K. (Eds.), C4 Plant Biology. Academic Press, San Diego, pp. 313–373.

Schefuß, E., Kuhlmann, H., Mollenhauer, G., Prange, M., Pätzold, J., 2011. Forcing of wet phases in southeast Africa over the past 17,000 years. Nature. 480, 509–512.

Scott, L., 2002. Grassland development under glacial and interglacial conditions in southern Africa: Review of pollen, phytolith and isotope evidence. Palaeogeography, Palaeoclimatology, Palaeoecology. 177, 47–57.

Scott, L., Holmgren, K., Talma, a. S., Woodborne, S., Vogel, J.C., 2003. Age interpretation of the Wonderkrater spring sediments and vegetation change in the Savanna Biome, Limpopo province, South Africa. South African Journal of Science. 99, 484-488.

Sinninghe Damsté, J.S., Verschuren, D., Ossebaar, J., Blokker, J., van Houten, R., van der Meer, M.T.J., Plessen, B., Schouten, S., 2011. A 25,000-year record of climate-induced changes

in lowland vegetation of eastern equatorial Africa revealed by the stable carbon-isotopic composition of fossil plant leaf waxes. Earth and Planetary Science Letters. 302, 236–246.

Smuts, W.J., 1992. Peatlands of the Natal Mire Complex - goemorphology and characterization. South African Journal of Science. 88, 474–83.

Stock, W.D., Chuba, D.K., Verboom, G. a., 2004. Distribution of South African C3 and C4 species of Cyperaceae in relation to climate and phylogeny. Austral Ecology. 29, 313–319.

Talma, A.S., Vogel, J.C., 1992. Late Quaternary paleotemperatures derived from a speleothem from Cango Caves, Cape Province, South Africa. Quaternary Research. 37, 203–213.

Taylor, R., Kelbe, B., Haldorsen, S., Botha, G. a., Wejden, B., Været, L., Simonsen, M.B., 2006a. Groundwater-dependent ecology of the shoreline of the subtropical Lake St Lucia estuary. Environmental Geology. 49, 586–600.

Taylor, R., Adams, J.B., Haldorsen, S., 2006b. Primary habitats of the St Lucia Estuarine System, South Africa, and their responses to mouth management. African Journal of Aquatic Science. 31, 31–41.

Truc, L., Chevalier, M., Favier, C., Cheddadi, R., Meadows, M.E., Scott, L., Carr, A.S., Smith, G.F., Chase, B.M., 2013. Quantification of climate change for the last 20,000years from Wonderkrater, South Africa: Implications for the long-term dynamics of the Intertropical Convergence Zone. Palaeogeography, Palaeoclimatology, Palaeoecology. 386, 575–587.

Tyson, P.D., Preston-Whyte, R.A., 2000. The Weather and Climate of Southern Africa, 2nd ed. Oxford University Press Incorporated, Cape Town, South Africa.

Vogel, J.C., Fuls, A., 1978. The geographical distribution of Kranz grasses in South Africa. South African Journal of Science. 58, 373 – 377.

Vrdoljak, S.M., Hart, R.C., 2007. Groundwater Seeps as Potentially Important Refugia for Freshwater Fishes on the Eastern Shores of Lake St Lucia, KwaZulu-Natal, South Africa. African Journal of Aquatic Science. Sci. 32, 125–132.

Walther, S.C., Neumann, F.H., 2011. Sedimentology, isotopes and palynology of late Holocene cores from Lake Sibaya and the Kosi Bay system (KwaZulu-Natal, South Africa). South African Geographical Journal. 93, 133–153.

Chapter 5

Synopsis

Climate change has become a very topical issue over the last decade and, although there are some detractors, climate research has shown that our planet is experiencing unprecedented atmospheric warming which is causing deviations in the global climate. The intensity and consequences of these changes are subject to intense debate and negotiations. Attempts are being made to model how these changes will affect biodiversity, food security and water resource challenges by considering all the cause and effect variables, parameters of which can be gauged from past non-anthropogenic climate fluctuations and the subsequent changes on the palaeoenvironment. This has put much impetus on palaeoenvironmental research globally, to reconstruct robust high resolution palaeoenvironmental records which can help us understand the cause and effect signals preserved in marine and terrestrial sediment archives.

The Southern African region has a dynamic climate which is influenced by the interhemispheric ITCZ (Stokes et al., 1997), and regional SST gradients between the Indian and Atlantic oceans (Tyson and Preston-Whyte, 2000). The manner in which these two mechanisms interacted under glacial and interglacial conditions and how this interplay affected the palaeoenvironment is still largely misunderstood due to continuous climate records being rare in Southern African (Chase and Meadows, 2007). This thesis addresses the shortfall in our understanding of climate driven palaeoenvironmental fluctuations on the south eastern sub-tropical coast of Africa, by using bulk geochemical proxies to reconstruct physical peat forming controls (chapter 2), plant biomarker indictors of palaeohydrology and microbial activity (chapter 3) and relative contributions of C3 and C4 plant assemblages (chapter 4) in the Mfabeni peatland since the late Pleistocene. In each chapter, we compare the specific palaeoenvironment indicators in the Mfabeni core to other regional archives of climate change (e.g. dunes, speleothems, marine sediments etc.) to substantiate our findings and inferred climatic drivers.

1.1. Climate summary

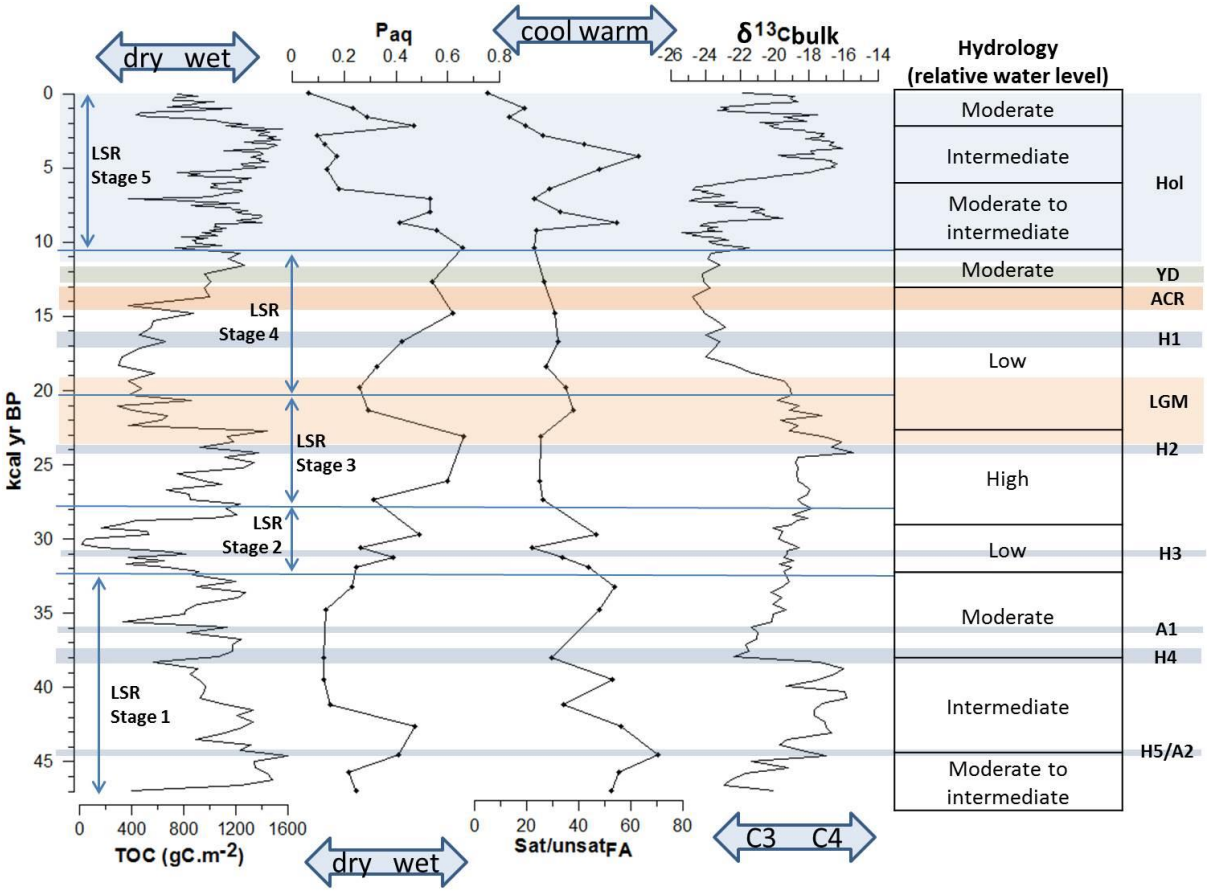

Figure 1: Summary of climate indictors discussed in chapters two, three and four. Total organic carbon (TOC), *n*-alkane aquatic plant hydrology proxy (P_{aq}), *n*-alkanoic acid total saturated / unsaturated temperature proxy (sat/unsat$_{FA}$) and proportional input of C3 and C4 plant OM ($\delta^{13}C_{bulk}$). Relative water levels: Low = dry/ minimal inundation; Moderate = minimal / seasonal inundation; intermediate = seasonal / semi-permanent inundation; High = permanent inundation / shallow lake. H1 – 5 = Heinrich events; A1 and A2 = Antarctic warming events; LGM = Last Glacial Maximum; ACR = Antarctic cold reversal; YD = Younger Dryas; Hol = Holocene.

By employing a combination of bulk geochemical, biomarker and isotope proxies (Figure 1), a summary of the climate reconstrution discussed in chapters 2 – 4 follows:-

LSR stage 1 (ca. 47 – 32.2 kcal yr BP): is characterised by increasing precipitation and temperatures resulting in peak water levels (H5/A2) that supported predominant C4 aquatic and emergent plants up until c. 38 kcal BP (H4) where a drop in precipitation and temperatures resulted in lower water levels allowing C3 aboreal trees to dominate the OM input in the peatland.

LSR stage 2 (ca. 32.2 to 27.6 kcal yr BP): displays initially a distinct drop in water levels and precipitation, coeval with an initial drop in temperatures and mixed C3 arboreal forest and C4 sedge palynological signal. At c. 28 kcal yr BP, a sudden increase in precipitation and

temperatures and dominant aquatic plants, signals a return to high water levels and increasing C4 sedge input.

LSR stage 3 (ca. 27.6 – 20.3 kcal yr BP): starts off with elevated precipitation, stable temperatures and dominant aquatic plant input suggesting high water levels and peak in C4 sedge and aquatic plant input (H2). After ca. 23.1 kcal yr BP, there is a dramatic shift to dry low water level conditions and a dominance of C3 grasslands during the height of the LGM.

LSR stage 4 (ca. 20.3 – 10.4 kcal yr BP): a continuation of glacial conditions persists up until c. 15 kcal yr BP represented by low water levels, subdued temperatures and C3 grassland vegetation. Thereafter, water levels increase supported by the change to dominant C3 aquatic plant input and sharp increase in TOC, corresponding with the beginning of the African Humid period. A slight reversal to glacial conditions occurred during the ACR, thereafter water levels and precipitation recover during the YD and into the Holocene.

LSR stage 5 (c. 10.4 kcal yr BP – present): the Holocene is characterised by overall elevated temperatures and precipitation in comparison to the previous glacial period, interspersed with abrupt millennial-scale cooling / dry events. This is proposed by overall elevated but fluctuating TOC, occilations in aquatic – emergent / terrestrial plant input, sat/unsat$_{FA}$ proxies and distinct interchanges between C3 and C4 plant assemblages.

The control on peat accumulation switched from OM bioreactivity during the Late Pleistocene, to a sedimentation control in the Holocene as a result of the differences in the overall glacial and interglacial climatic conditions. The Mfabeni peatland showed a strong correlation with Mozambique Channel marine SST records (Bard et al., 1997; Schefuß et al., 2011; Sonzogni et al., 1998), suggesting the primary forcing mechanism on the northern KwaZulu Natal coastal palaeoenvironment to be the evaporation and advection of moisture from the adjacent Indian Ocean. The peat archive also suggested a general anti-phase realationship with the main Northern Hemisphere cold climate events, however, this is only an observation as interhemispheric teleconections can only be established when several archives from both hemispheres are directly compared.

Simon et al. (2015) used geochemical modelling to ascertain the hydrological variability in the KwaZulu Natal (KZN) province of a 270,000 year old marine record retrieved from the southwest Indian Ocean ~160 km off the KZN coast. Their model showed that when the perihelion occurred close to the austral summer solstice, the high summer precession caused higher sea surface temperatures, but more especially higher land temperatures. This resulted in lower air pressure on land compared to surface pressures over the adjacent Indian Ocean which caused stronger easterly moisture laden surface winds to flow towards the south eastern Southern African coastline. Due to increased net precipitation only being partly owed to increased local evaporation on land, they suggested that continental precipitation originated mainly from outside the area. Therefore, the moisture transport system, comprising of specific humidity and horizontal winds, resulted in the transport of moist and tropical air masses from the Indian Ocean to move over the KZN region and increase rainfall during periods of maximum insolation. Additionally, by comparing speleothem $\delta^{18}O$ records from eastern China, they were able to suggest an anti-phase relationship between the Northern and Southern Hemisphere rainfall systems, which they attributed to the tropical mean circulation responding to Northern Hemisphere cooling and producing a southward shift of the sub-tropical anticyclones. This in turn, brought more moist easterly flow from the SW Indian Ocean and hence, more precipitation to the eastern part of Southern Africa during Northern Hemisphere cooling events.

Chevalier and Chase (2015) showed that SST in the Mozambique Channel and adjacent continental temperature variability generally trended positively. They also observed that the temperature difference between the LGM and Holocene period increased the further the archives were from the coast, more than likely as a result of the ocean's resistance to temperature changes. They conclude that the main driver of precipitation in the area was the fluctuations in SST for the Late Pleistocene, and local insolation during the Holocene. However, the Mfabeni climate proxies recorded close correlation with Indian Ocean SST throughout the Late Pleistocene and Holocene, which Simon et al. (2015) concluded was driven by insolation shifts during orbital precession cycles.

1.2. Major contributions

The Mfabeni archive has proven to be an invaluable continuous record of glacial and interglacial palaeoenvironmental fluctuations on the south eastern coast of Africa. We established the peatland to be a pristine archive that accurately recorded the palaeoenvironmental conditions throughout its depositional history and confirmed the peatland to be one of the oldest continuous coastal peat records on the continent (Grundling et al. 2013).

The hydrologic regime reconstruction, which is the dominant control on peat accumulation and plant assemblages within the peat deposit, showed substantial fluctuations during both glacial and interglacial periods. Although the overall dominant OM source into the peatland was terrestrial plants, there were definitive periods of dominant submerged macrophyte input, suggesting sufficiently elevated water levels that supported aquatic plant proliferation. By employing temperature sensitive proxies of different biomarkers we were able to disentangle temperature and precipitation fluctuations on a local scale. A general positive trend was observed between temperature and moisture availability throughout the depositional history of the peatland. We also concluded that local plant physiology was strongly affected by moisture availability, as opposed to temperature variations, arguably due to the relatively moderate cooling experienced during the LGM in Southern Africa compared to the higher latitudes (Bard et al., 1997; Finch and Hill, 2008).

The strong and significant correlation between $\delta^{13}C_{bulk}$ and $\delta^{13}C_{wax}$ values proposes that the soil C isotope signal was predominantly influenced by the proportional contributions of C3 and C4 plant OM input. The $\delta^{13}C_{wax}$ data set established large variability in the relative input of C3 and C4 plants into the Mfabeni peatland, with not only interchanges between plant clades but even recorded photosynthetic pathway switches within the *Poaceae* (grasses) and *Cyperaceae* (sedges) families in response to environmental conditions. These plant assemblage shifts were observed during some of the well-established climatic events (H4, LGM, deglacial and Holocene periods) while other shorter climatic events exhibited a muted response. We concluded that the local hydrologic conditions in the Mfabeni fen could have buffered the effects shorter climatic events had

on the $\delta^{13}C_{bulk}$ signal by either attenuating the perturbations or resulting in changes in plant assemblages that did not significantly affect the soil $^{13}C/^{12}C$ fractionation ratio.

Within a regional context, the Mfabeni record displays a close association with marine SST archives extracted from the adjacent Indian Ocean. We therefore infer the primary climate forcing mechanism on the northern KwaZulu Natal coast, since the Late Pleistocene, to be the evaporative potential of the Indian Ocean, governed by changes in water mass surface temperatures, as established by Truc et al. (2013) and Simon et al. (2015) for the wider south eastern African region. Interhemispherically, the Mfabeni archive suggests a general anti-phase link between Southern Africa and the Northern Hemisphere, which supports the theory that the two hemispheres displayed opposite climatic responses since the late Pleistocene, possibly in response to the switching on/off of the global oceanic thermohaline circulation system (Bard et al., 1997; Blunier et al., 1998; Simon et al., 2015; Stocker 2000).

1.3. Recommendations and future work

By undertaking various geochemical reconstructions of the palaeoenvironment on the eastern coast of Southern Africa since the Late Pleistocene, this thesis has contributed substantially to the scientific understanding of climate driven environmental fluctuations during the last glacial and interglacial periods and given insights into the mechanisms that drove the palaeoclimate of the region. However, this project has identified a number of shortcomings that can be addressed through future research:-

1. Due to the prohibitively high cost and time requirements for geochemical analysis, most notably ^{14}C dating, biomarker extraction and leaf wax C isotope analysis, only a small subsection of peat samples were extracted and analysed, requiring extrapolations to develop the age-depth model and stable C isotope profile for high resolution investigations. Future research would benefit from higher resolution sample analysis to ensure more robust investigations of the palaeoenvironment in the region which will assist in resolving the blurred signals during the more ephemeral climatic events.

2. The only way to fully understand past climate and environmental fluctuations in the region is to increase the number of archives under investigation, not only in number but through a variety of archives over a widespread area that encompasses different time scales in all the major climatic zones of the region. This is a serious challenge for palaeoscientists as the predominant semi-arid climate of the region is not conducive for the preservation of climate records. Nonetheless, researches are increasingly turning to unorthodox archives, such as *Hyrax* middens to compliment the more traditional lake, marine and peat sediment and spelothems climate archives, which are limited in the region. Therefore, additional high resolution multi-proxy and multi-archive regional studies are required to conclusively elucidate environmental responses to past climatic shifts in Southern Africa.

References

Bard, E., Rostek, F., Sonzogni, C., 1997. Interhemispheric synchrony of the last deglaciation inferred from alkenone palaeothermometry. Nature. 385, 707-710.

Blunier, T., Chappellaz, J., Schwander, J., DaÈllenbach, A., Stauffer, B., Stocker, T. F., Raynaud, D., Jouzel, J., Clausen, H. B., Hammer, C. U., Johnsen, S. J., 1998. Asynchrony of Antarctic and Greenland climate change during the last glacial period. Nature 394, 739–743. DOI:10.1038/29447.Botha, G., Porat, N., 2007. Soil chronosequence development in dunes on the southeast African coastal plain, Maputaland, South Africa. Quaternary International. 162-163, 111–132

Chase, B.M., Meadows, M.E., 2007. Late Quaternary dynamics of southern Africa's winter rainfall zone. Earth Science Reviews. 84 (3-4), 103-138.

Chevalier, M., Chase, B.M., 2015. Southeast African records reveal a coherent shift from high- to low-latitude forcing mechanisms along the east African margin across last glacial–interglacial transition. Quaternary Science Reviews. 125, 117–130.

Finch, J.M., Hill, T.R., 2008. A late Quaternary pollen sequence from Mfabeni Peatland, South Africa: Reconstructing forest history in Maputaland. Quaternary Research. 70, 442–450.

Grundling, P.L., Grootjans, A. P., Price, J.S., Ellery, W.N., 2013. Development and persistence of an African mire: How the oldest South African fen has survived in a marginal climate. Catena. 110, 176–183.

Schefuß, E., Kuhlmann, H., Mollenhauer, G., Prange, M., Pätzold, J., 2011. Forcing of wet phases in southeast Africa over the past 17,000 years. Nature 480, 509–512.

Simon, M.H., Ziegler, M., Bosmans, J., Barker, S., Reason, C.J.C., Hall, I.R., 2015. Eastern South African hydroclimate over the past 270,000 years. Science Reports. 5, 18153.

Sonzogni, C., Bard, E., Rostek, F., 1998. Tropical sea-surface temperatures during the last glacial period: A view based on alkenones in Indian Ocean sediments. Quaternary Science Reviews. 17, 1185–1201.

Stocker, T.F., 2000. Past and future reorganizations in the climate system. Quaternary Science Reviews. 19, 301–319

Stokes, S., Thomas, D.S.G., Washington, R., 1997. Multiple episodes of aridity in southern Africa since the last interglacial period. Nature. 388 (6638), 154-158.

Truc, L., Chevalier, M., Favier, C., Cheddadi, R., Meadows, M.E., Scott, L., Carr, A.S., Smith, G.F., Chase, B.M., 2013. Quantification of climate change for the last 20,000years from Wonderkrater, South Africa: Implications for the long-term dynamics of the Intertropical Convergence Zone. Palaeogeography, Palaeoclimatology, Palaeoecology. 386, 575–587

Tyson, P.D., Preston-Whyte, R.A., 2000. The weather and climate of southern Africa, Oxford University Press Incorporated, Cape Town, South Africa.